



Agreement Number: AIES-2347

Rocky Mountain Water Supply Resilience and Vulnerability

Report Date: 31 May 2019

Project Leader: John Pomeroy

Lead Institution: University of Saskatchewan

Project Partners: Dr John Diiwu, Alberta Agriculture and Forestry

Dr. Masaki Hayashi, University of Calgary

Dr. Sean Carey, McMaster University

Dr. Richard Petrone, University of Waterloo

Dr. Cherie Westbrook, University of Saskatchewan

Dr. Warren Helgason, University of Saskatchewan

Project Duration: 1 May 2016 - 20 April 2019

Disclaimer

Alberta Innovates (“AI”) and Her Majesty the Queen in right of Alberta make no warranty, express or implied, nor assume any legal liability or responsibility for the accuracy, completeness, or usefulness of any information contained in this publication, nor that use thereof infringe on privately owned rights. The views and opinions of the author expressed herein do not necessarily reflect those of AI or Her Majesty the Queen in right of Alberta. The directors, officers, employees, agents and consultants of AI and the Government of Alberta are exempted, excluded and absolved from all liability for damage or injury, howsoever caused, to any person in connection with or arising out of the use by that person for any purpose of this publication or its content

Executive Summary

In the last few years Alberta has been impacted by severe mountain-derived flooding (2013) and drought (2015-2019) that have caused flood damages exceeding \$6 billion and drought damages to tourism, ecosystem health, and food and energy production (unestimated at this point). These water crises suggest that the reliability and safety of Alberta's mountain waters are at risk, and therefore risks associated with climate change and extreme weather need to be reassessed and the potential to manage mountain watersheds for water resiliency re-examined. To address this, the overarching research question for this project is: *Are the Canadian Rocky Mountains a reliable future source of streamflow?* Underlining this question are three sub-questions—that form the Objectives of this project:

- i) How do the physical characteristics (forest cover, soil type, geology, etc.) of mountain headwater basins influence runoff generation? How does this vary across the region?
- ii) Will the hydrological systems of the Rocky Mountains enhance or dampen the effects of climate change and extreme events on downstream streamflow and water resources?
- iii) Can forest manipulations impact the hydrological resiliency of these systems?

The project relied upon observations in the Canadian Rockies Hydrological Observatory (CRHO), which was operated during and by this study to provide an unprecedented range of mountain multiscale hydrological, meteorological, ecological, cryospheric and subsurface field data for improving our understanding of mountain hydrology and for driving and testing novel hydrological models. The co-location of modelling and process hydrology studies led to rapid uptake of new scientific information into models.

Mountain forest evapotranspiration was divided into evapotranspiration and tree transpiration in a sub-alpine forest and examined over wet and dry summers. The drier summer resulted in higher transpiration and evapotranspiration levels, with no recharge to groundwater from surface water inputs during the growing season. This means that successive years of summer droughts could impact successional growth of subalpine forests as juvenile trees rely on soil moisture which was low in a drought year. It was also noted that windblown snow trapped by vegetation is an important input to summer growth and water supply of sub-alpine forests, both at treeline and lower elevations and so variation in winter snowpacks has great importance for summer evapotranspiration from subalpine forests.

Storm runoff celerity was examined as a function of soils and topography. The results suggest that warmer winters will result in shallower winter snowpacks and colder soils due to reduced insulation from the winter snowpack – this will impact infiltration to frozen soils and possibly increase spring runoff celerity.

Snowmelt dynamics was studied through new observations such as using a combination of LiDAR measurements from UAVs and remote sensing from satellites to quantify snowpacks. UAV-borne

LiDAR can measure snow depth accurately even under forest canopies and so can be used to inform and evaluate snow models. An improved understanding of blowing snow and turbulence interactions has pointed the way for new alpine blowing snow model development that takes into account sweep and ejection motions of the atmosphere rather than relying solely on time-averaged wind flows. This will improve alpine-subalpine snow modelling accuracy. An improved understanding and ability to simulate water flow through heterogeneous snowpacks is providing the basis to reformulate operational hydrological models so that they are more accurate in simulating runoff timing during rain-on-snow floods.

Studies of wetlands in alpine, subalpine, and foothill locations highlight the differences in hydrological functions of wetland, such as evapotranspiration, contributing flow, recharging and transmitting flow, and how this relates to topographic position and hydrographic position. Not all wetlands have equal function and those in foothill locations can be particularly important, but changing, throughout the summer whereas high elevations wetlands have seasonal importance. Importantly - mountain wetlands supply crucial baseflow during drought conditions and beaver-dammed wetlands provide important reduction in flood streamflow peaks, even in the highest flow conditions on record such as the June, 2013 flood.

Groundwater storage, flow paths and hydraulic response time understanding was improved based on intensive field studies that characterized contributions to streamflow, baseflow and wetlands characterized. Complex systems of coarse sediments in mountain headwaters (talus slopes, moraines, rock glaciers) play an important role in temporary storage of glacier melt, snowmelt and rain. These results and others noted above have informed hydrological modelling in the Cold Regions Hydrological Modelling platform (CRHM).

High mountain hydrology outside of glacierized basins is dominated by snowmelt in the Canadian Rockies and so a full representation of snow redistribution by wind and gravity, snow interception and the impact of slope and aspect on energy availability for melt is crucial for accurate hydrological modelling. These are available in CRHM which works well in several mountain basins. Unfortunately, CRHM hydrological predictions driven with the Environment and Climate Change Canada GEM numerical weather model at 2.5 km have insufficient accuracy for reliable hydrological modelling of high mountain basins.

In glacierized basins, represented by Peyto Glacier Research Basin, new glacier components help CRHM to indicate an increase in runoff from the 1960s to recent years. This increasing trend suggest the glacier is still able to provide a significant contribution to streamflow and buffer low water years. However, the melt patterns are changing; snowmelt peak is now a month earlier than historical values and glacier melt extends further into the fall. Diagnosis of CRHM outputs shows that high flow years have 34% more annual streamflow than low flow years, the source of extra streamflow in high flow years is from: + 13% snowmelt, + 80% icemelt, + 280% firmelt, + 106% rainfall-runoff and visible changes in the transition season, with earlier spring melt and increased fall rainfall-runoff.

Climate change has been anticipated to impact the hydrology of Marmot Creek Research Basin which has shown itself hydrologically resilient to substantial climate changes since the 1960s. Using CRHM under a “business as usual” climate change scenario, the basin warms up by 4.7 °C and receives 16% more precipitation, which leads to a 40 mm decline in seasonal peak snowpack, 84 mm decrease in snowmelt volume, and 49 days shorter snowcover duration. This will lead to earlier runoff of from 12% to 27% in most ecozones, whereas the treeline ecozone has a small (3%) decrease in runoff volume due to decreased melt volumes from smaller snowdrifts. Higher streamflows will occur in spring and fall and lower streamflows in late summer. Marmot Creek annual streamflow discharge will increase by 18% and so loses its hydrological resilience.

Climate change and forest disturbances impacts for the Bow and Elbow rivers were investigated using CRHM, setup with almost 3000 hydrological response units above Calgary. CRHM was found to predict annual streamflows adequately for these rivers. The model was run with a business as usual climate scenario to produce a likely climate of the late 21st C for comparison to the early 21st C. It was then perturbed to simulate land cover disturbances from wildfire, pine beetle and forest harvesting for the recent and future climate of the basins. Annual streamflow volumetric changes for climate change were modest, with increases of 2% for the Bow River and 7% for the Elbow River at Calgary, with higher increases in low flow years. The low and moderate severity wildfire, forest harvesting and pine beetle scenarios had little impact on streamflow volumes. The largest impact was on the Elbow River at Calgary where the pine beetle with salvage logging scenario resulted in an 11% increase in streamflow volumes. The severe wildfire scenario increased streamflows at Calgary on the Bow by 34% and the Elbow by 59%. With the combination of severe wildfire and climate change, streamflows on the Bow and Elbow at Calgary are predicted to increase by 42% and 70% respectively. This combination of future basin conditions is considered likely over the next century and puts Calgary at considerable risk of damage from high flows that will contribute to these high annual water yields.

The investigators wish to acknowledge the students and researchers who have contributed to this report and particularly to Xing Fang and Lindsey Langs who made substantial contributions to the writing and presentation of this final report.

Table of Contents

Executive Summary.....	2
Final Technical and Modelling Report.....	6
1.1 Project Description.....	6
1.2 Experimental Approach and Results.....	10
1.3 Key Findings and Conclusions.....	83
1.4 Scientific Achievements.....	86
1.5 References.....	104
1.4 Appendices.....	108

Final Technical and Modelling Report

1.1 Project Description

In the last few years Alberta has been impacted by severe mountain-derived flooding (2013) and drought (2015-2019) that have caused flood damages exceeding \$6 billion and drought damages to tourism, ecosystem health, and food and energy production (unestimated at this point). These water crises suggest that the reliability and safety of Alberta's mountain waters are at risk, and therefore risks associated with climate change and extreme weather need to be reassessed and the potential to manage mountain watersheds for water resiliency re-examined. Mountain water supply in Alberta is strongly influenced by snowpack dynamics. Whereas floods are driven primarily by heavy rains, particularly when they occur on snow, low flows are controlled by release of water from snow- and rain-fed groundwater, lake/wetland and glacier stores (Pomeroy et al., 2015; Shook and Pomeroy, 2015; Marshall et al., 2011; Pazurkas and Hayashi, 2015; Buttle et al., 2016). Snow-controlled hydrological systems are particularly sensitive to climate warming and the trends in the last 50 years show an average winter warming of 2.5 °C in the Bow River headwaters (DeBeer et al. 2015). Snowpacks at lower elevations have declined by as much as 50% over this period in the Kananaskis Valley, yet streamflows have been at most mildly affected (Harder et al., 2015; Pomeroy et al., 2015; Whitfield and Pomeroy, 2016). Whilst observations of headwaters mountain streamflow show a remarkable resiliency and stability under recent climate change and mild experimental forest disturbance (Harder et al. 2015; Whitfield and Pomeroy, 2016), recent results from numerical simulations suggest considerable vulnerability potential for future down-stream water supplies (Pomeroy et al., 2012; 2016; Fang and Pomeroy, 2016; Rasouli et al., 2019).

Notable impacts are:

- i) Peak flow timing advancing by one month and late summer flows declining substantially in mountain streams subject to observed and anticipated climate warming;
- ii) Up to a 25% increase in peak flow from snowmelt due to deforestation of mountain headwaters; and
- iii) Up to a doubling of peak flows in a simulation of the 2013 flood when canopy removal is coupled with soil compaction.

Given the dependence of Alberta water users on the timing and magnitude of high and low streamflows and the vulnerability of floodplain communities to peak flows, the conditions that promote water supply resilience and the conditions that result in vulnerability bear further investigation at larger river basin scales.

Key to assessing water futures under climate change is a more thorough understanding of the hydrological importance of forests, soils, snow, glaciers, frozen ground, permafrost, groundwater, lakes, wetlands and strong seasonality. Much of the mountain headwater catchments are forest covered and subject to a variety of federal, provincial and private

management regimes. These forests are used for a wide range of purposes including environmental conservation, recreational, cultural, watershed source area protection and wood/fibre products. The forests also support hundreds of forest dependent communities. The potential for managing forests for water supply objectives has been a long term goal in Alberta (Golding and Swanson, 1986) and with recent advances in Alberta mountain forest disturbance hydrology (Ellis et al., 2013; Pomeroy et al., 2012) there is potential to model the impacts of precision- management of forested watersheds for multiple uses.

This project leverages the experience of a consortium of university and Alberta Agriculture and Forestry scientists to develop an improved quantification of forest and high mountain water supply resilience and vulnerability in the Canadian Rockies. This has been accomplished through the provision of benchmarks against which assessments can be made and future water risks and management strategies identified. It takes advantage of a unique opportunity to better quantify mountain hydrological resilience and vulnerability by coupling mountain research basin findings with advances in hydrological modelling. The project is determining how climate, headwater basin forest cover and topography control streamflow generation and how this varies across the Bow and Elbow river headwaters. It is also assessing whether these basins enhance or dampen the effects of climate change, floods and droughts on downstream streamflow, and how forest management can be used as a tool to promote water resource resiliency to climate change and extreme weather events.

The overarching research question for this project is: *Are the Canadian Rocky Mountains a reliable future source of streamflow?* At present, this knowledge gap makes the implementation of all water policies and infrastructure proposals in Alberta highly uncertain. Underlining this question are three sub-questions—that form the Objectives of this project:

- iv) How do the physical characteristics (forest cover, soil type, geology, etc.) of mountain headwater basins influence runoff generation? How does this vary across the region?
- v) Will the hydrological systems of the Rocky Mountains enhance or dampen the effects of climate change and extreme events on downstream streamflow and water resources?
- vi) Can forest manipulations impact the hydrological resiliency of these systems?

Answering these questions requires an improved physical understanding of all mountain hydrological processes that integrate across a range of spatial and temporal scales to control streamflow generation. One challenge is to accelerate the improvement in understanding snowmelt and glacier-melt processes in complex terrain, snowmelt runoff in disturbed forests, evapotranspiration and runoff processes over forested hillslopes, surface-groundwater interactions in mountain headwaters including mountain wetlands and streamflow generation processes by intensive and detailed hydrological process observations at study sites in the Canadian Rockies Hydrological Observatory (CRHO). New advances from this understanding are incorporated into the object-oriented, distributed Cold Regions Hydrological Modelling platform (CRHM). Advancing CRHM through code improvement and an ever-expanding library of C++ process modules is a moderate challenge, followed by testing of new model structures against

detailed observations at research basins such as Marmot Creek. Once the performance of new model structures was satisfactory, CRHM is then be used to simulate the hydrology of much larger areas and timeframes than the field experiments allow. By applying CRHM to the Bow River above Calgary and then modifying the climate and land cover for the model, virtual experiments are conducted that provide an unique opportunity to assess the range and probability of various water futures for this basin.

Three main tasks were developed to answer the main project questions, with a series of sub-tasks to highlight specific areas of interest.

Task 1: Basin Process Studies and Data Collection

- 1.1 Canadian Rockies Hydrological Observatory
- 1.2 Mountain forest evapotranspiration
- 1.3 Storm runoff celerity as a function of soils and topography
- 1.4 Snowmelt dynamics at forest edges
- 1.5 Wetland storage and drainage
- 1.6 Groundwater storage, flow paths and hydraulic response time

Task 2: Develop and Improve Hydrological Model Based on Process Studies

- 2.1 Cold Regions Hydrological Model (CRHM) setup on Upper Bow River Basin and testing at Fortress Mountain Basin and Marmot Creek
- 2.2 Evapotranspiration modelling in mountain terrain
- 2.3 CRHM Glacier development and testing
- 2.4 Canadian Hydrological Model (CHM) development

Task 3: Assemble Basin and Past/Future Climate Information for Modelling

- 3.1 Assemble basin information for modelling
- 3.2 Assemble climate information for modelling
- 3.3 Validation of numerical weather model results with archived climate data

The research questions and tasks framed process based investigations and modelling analysis for the understanding of Rocky Mountain water supply resilience and vulnerability for the duration of this study.

1.2 Experimental Approach and Results

Literature Review

Water supplies from runoff in the eastward flowing Canadian Rockies drainages have been declining (St. Jacques et al., 2010) and are predicted to drop further just as increasing demand is projected due to rising population and greater consumption from downstream agriculture and industry (Mannix et al., 2010). The Canadian Rockies are typical of many cold regions mountain ranges in that they have substantial snow accumulation in the winter and melt in spring and summer, providing water for drier regions downstream during times of important agricultural and human consumption demand.

Mountain hydrological cycling in this region is sensitive to climate variations. It is suggested that the rising number of winter days with air temperature above the freezing point (Lapp et al., 2005) and decreases in spring snowcover extent (Brown and Robinson, 2011) are resulting in earlier spring runoff (Stewart et al., 2004) and lower annual streamflows (St. Jacques et al., 2010). These climate changes have been associated with increasing rates of forest disturbance due to wildfire (Fauria and Johnson, 2006), insect infestation (Aukema et al., 2008), and disease (Woods et al., 2005). The hydrological cycle in mountain environments can be substantially altered by forest disturbance, leading to increased snow accumulation and snowmelt rates (Pomeroy and Gray, 1995; Boon, 2009; Burlles and Boon, 2011; Pomeroy et al., 2012; Ellis et al., 2013), enhanced surface runoff and peak flow (Whitaker et al., 2002; Pomeroy et al., 2012; Pomeroy et al., 2016a, b), and changing groundwater regimes (Rex and Dubé, 2006).

Needleleaf forest cover dominates many cold regions mountain basins, where snowmelt is the most important annual hydrological event (Gray and Male, 1981). Needleleaf forest foliage substantially reduces snow accumulation, with declines ranging from 30% to 50% compared to adjacent clearing sites (Pomeroy et al., 2002; Gelfan et al., 2004). The losses of snow accumulation in forests are attributed to the interception of snow by the evergreen needleleaf canopy (Lundberg and Halldin, 1994; Pomeroy and Gray, 1995; Hedstrom and Pomeroy, 1998; Gelfan et al., 2004). This intercepted snow is exposed to high rates of turbulent transfer and radiation input and sublimates rapidly (Pomeroy et al., 1998) resulting in greatly reduced snow accumulation on the ground at the time of snowmelt (Pomeroy and Gray, 1995). However, snow unloading response to energy inputs adds uncertainty about the partition of snowfall between interception and unloading by the forest canopies, and further development of these algorithms for mountain slopes and forests is needed (Rutter et al., 2009). Besides interception effects, needleleaf forest cover also affects energy exchanges to snow and therefore the timing and duration of snowmelt. The forest canopy dampens turbulent energy fluxes when compared with open snowfields (Harding and Pomeroy, 1996; Reba et al., 2011). As a result, energy to melt sub-canopy snow is dominated by radiation fluxes, which in turn are altered by extinction of shortwave transmission through the canopy and enhancement of longwave emission from canopies and trunks (Link et al., 2004; Sicart et al., 2004; Essery et al., 2008; Boon, 2009; Pomeroy et al., 2009; Ellis et al., 2012; Varhola et al., 2010).

Elevation exerts a strong influence on air temperature, precipitation depth and phase in mountain basins (Storr, 1967; Marks et al., 2012; Harder and Pomeroy, 2012), while slope and aspect are the additional factors controlling the patterns of snow accumulation and snowmelt in the mountain environments (Golding and Swanson, 1986; Pomeroy et al., 2003; DeBeer and Pomeroy, 2009; MacDonald et al., 2010; Ellis et al., 2011; Marsh et al., 2012). At high elevations above treeline, snow is redistributed by wind (Föhn and Meister, 1983; Doorschot et al., 2001; Bernhardt et al., 2009), of which some is lost via sublimation to the atmosphere (MacDonald et al., 2010; Musselman et al., 2015).

Temperate zone models have great difficulty in simulating the hydrological cycle of cold mountain regions (Swanson, 1998), and there remains a need for a model that is suitable for river basins originating in the Canadian Rockies. Cold regions hydrological processes have been represented in hydrological models such as ARHYTHM (Zhang et al., 2000), VIC (Bowling et al., 2004), and GENESYS (MacDonald et al., 2011). However, the Cold Regions Hydrological Modelling platform (CRHM) offers a more complete range of processes for the Canadian Rockies (i.e. blowing snow, interception and sublimation of snow, energy balance snowmelt, slope radiation, canopy influence on radiation, canopy gap effect on snow, infiltration to frozen soils) and the process algorithms have been extensively field tested in this environment. CRHM is a modular model assembling system that allows appropriate hydrological processes to be linked for simulating the hydrological cycle across a range of scales (Pomeroy et al., 2007). The underlying philosophy is to use CRHM to create a model of appropriate physical and spatial complexity for the level of understanding and information available for the basin being modelled. Insights from field investigations have largely guided CRHM's development, with the expectation that an improved understanding of the underlying hydrological processes will yield benefits in terms of prediction capability and so new algorithms from field studies are incrementally incorporated as modules in the platform. For example, new algorithms recently added to CRHM include those for estimating shortwave radiation through forest canopies on slopes (Ellis and Pomeroy, 2007), calculating enhanced longwave emissions from canopies (Pomeroy et al., 2009), estimating snow surface temperature (Ellis et al., 2010), calculating snowmelt energetics in forest gaps and clearings (Ellis et al., 2013); resistance-type evapotranspiration, hillslope hydrology and groundwater dynamics (Fang et al., 2013) and rain-on-snow processes and detention storage of overland flow in organic soil layers on hillslopes (Pomeroy et al., 2016; Fang and Pomeroy, 2016). CRHM also now accounts for canopy gap radiative transfer and unloading of intercepted snow in a mass and energy module for needleleaf forests (Ellis et al., 2010, 2013). Other recent additions are modules for simulating blowing snow and sublimation affected by local wind and topography in the alpine treeline environment (MacDonald et al., 2010), improved simulation for alpine snowmelt and snowmelt runoff (DeBeer and Pomeroy, 2010) and improved soil system representation for runoff generation (Dornes et al., 2008a; Fang et al., 2010; 2013).

A physically based hydrological model incorporating many of the new algorithms outlined above was assembled using CRHM to simulate forest snow hydrology in a headwater basin of Canadian Rockies, resulting in predictions for snow accumulation, melt, and snowmelt runoff (Pomeroy et al., 2012). Current model developments focus on incorporating a more physically realistic soil

and groundwater system in the model and simulating groundwater-surface water interactions on hillslopes to improve simulation of soil moisture, evapotranspiration, baseflow, and groundwater storage. A comprehensive model addressing all major processes in the basin hydrological cycle that can be parameterised based on field and remote sensing measurements is a powerful and robust tool for examining the impacts of land use and climate change on basin runoff response. Such a tool also provides a basis for identifying regionalized parameterizations for modelling similar, but ungauged, basins in the region or similar cold mountain environments (Dornes et al., 2008b) as well as helping identify those physical processes most critical in controlling the large-scale hydrology of the region (Pietroniro et al., 2007). Another advantage of CRHM is that it may be evaluated using multiple objectives to avoid equifinality problems (Bevan and Freer, 2001) by allowing a much more powerful evaluation of the model as a representation of many aspects of the hydrological cycle (Dornes et al., 2008b).

Results of Experiments

Task 1: Basin Process Studies and Data Collection

1.1 Canadian Rockies Hydrological Observatory

The Canadian Rockies Hydrological Observatory (CRHO) was used as the base of field and modelling studies for this project (Fig. 1). This comprises primarily the Bow and Elbow river basins (Fig. 1). The Canadian Rockies Hydrological Observatory obtains nested experimental study sites such as Marmot Creek Research Basin, Fortress Mountain Research Basin, and Peyto Glacier Research Basin. The research basins benefit from being nested within a relatively high density of federal and provincial meteorological, snow and hydrological monitoring stations as well as the 35 USask hydrometeorological stations, including some with sophisticated monitoring of radiation, turbulent transfer and snow properties that are located at the research basins. This CFI funded facility provides an unprecedented outdoor laboratory to make advances in the understanding and prediction of mountain hydrology.

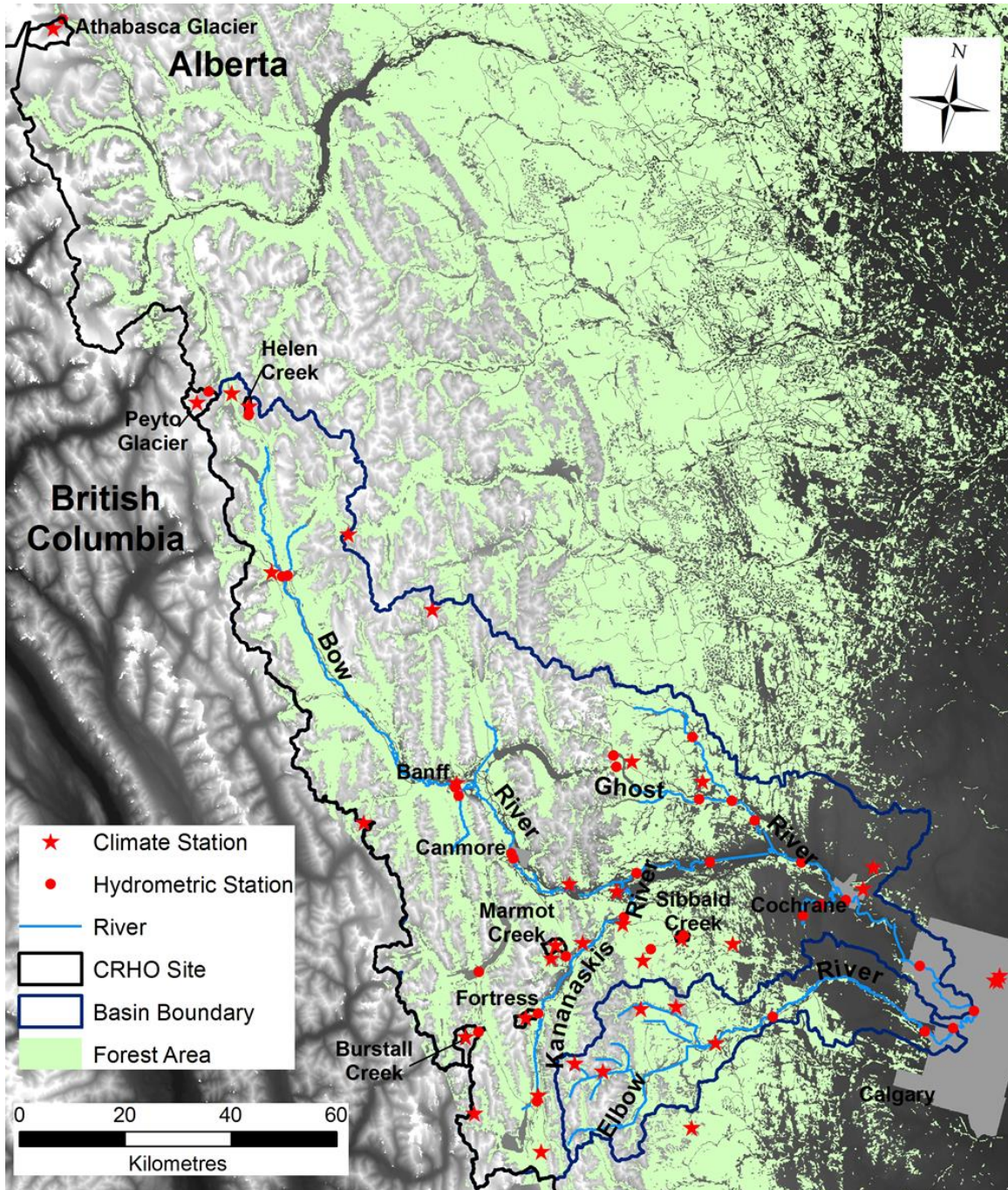


Figure 1. Map of the Canadian Rockies Hydrological Observatory climate and hydrometric station locations used within this study located in the Canadian Rocky Mountains, Alberta.

1.2 Mountain forest evapotranspiration

A key component to the understanding of mountain water resiliency is the understanding of subalpine vegetation and its role in the annual water budget. Presently, there is limited understanding of the quantity of water evaporated and transpired from these systems. Understanding the way water moves in mountain headwaters through forests and vegetation helps to gain an understanding of the overall vulnerability and resiliency of mountain headwaters. A series of studies were completed by graduate students under the supervision of Dr. Petrone to better understand this important component.

Subalpine forest evapotranspiration and water source investigation

Dr. Petrone's graduate student Lindsey Langs focussed on quantifying subalpine forest transpiration of two co-occurring tree species, subalpine fir and Engelmann spruce throughout the growing season of two hydrologically varying summers (2016 and 2017). The contrasts in years allowed for insight into fir and spruce water use behaviour, showing that trees transpired more throughout the drier summer (Fig. 2). Results indicated the sustained, large spring snowpack in 2017 helped encourage early growing season forest transpiration of a higher magnitude than 2016, the wet summer. This research also helped to quantify the relative proportion of forest transpiration to total evapotranspiration, helping to better understand the summer growing season water budget. In 2016, there was a positive gain of water to the system, replenishing groundwater and soil moisture stores (Fig. 3). In 2017, there was a net loss of water to the system, allowing no recharge during July and August (Fig. 4). If there are successive years of summer drought, younger trees may struggle to get enough water to sustain growth due to limited internal storage capacities and shallower rooting systems. This may alter the natural succession of forests in the Canadian Rockies, and could place further stress on these species in the event of a wildfire or biological pests.

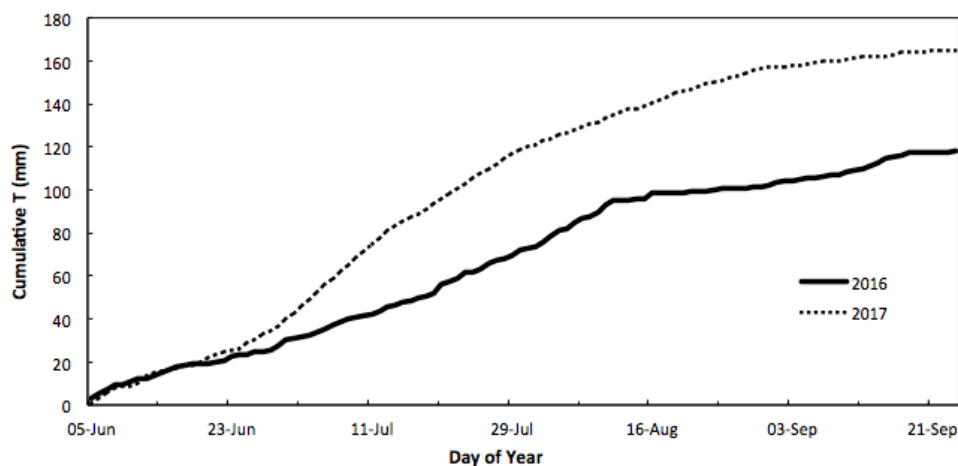


Figure 2. Cumulative transpiration (T) over the examined growing season, from June 5 – Sept 24 of both study years, 2016 and 2017. Of importance is the departure from similar early season totals on June 18, where T in 2017 surpasses that of 2016 due to a prolonged and more substantial winter snowpack.

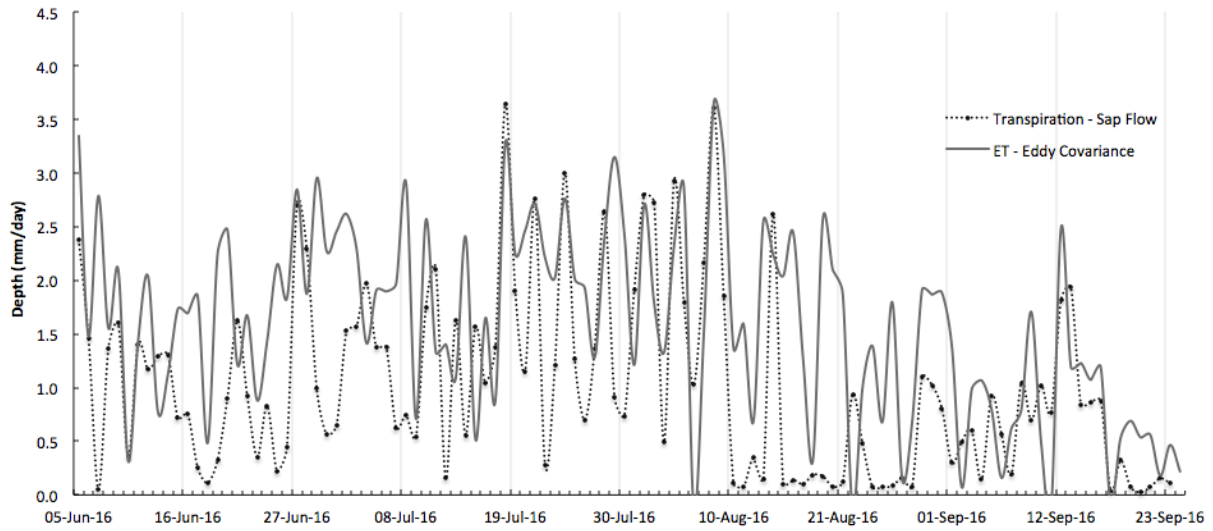


Figure 3. Forest transpiration plotted against entire forest-stand evapotranspiration for the 2016 wet growing season from June 5 – Sept 25 at Fortress Mountain, Kananaskis, AB.

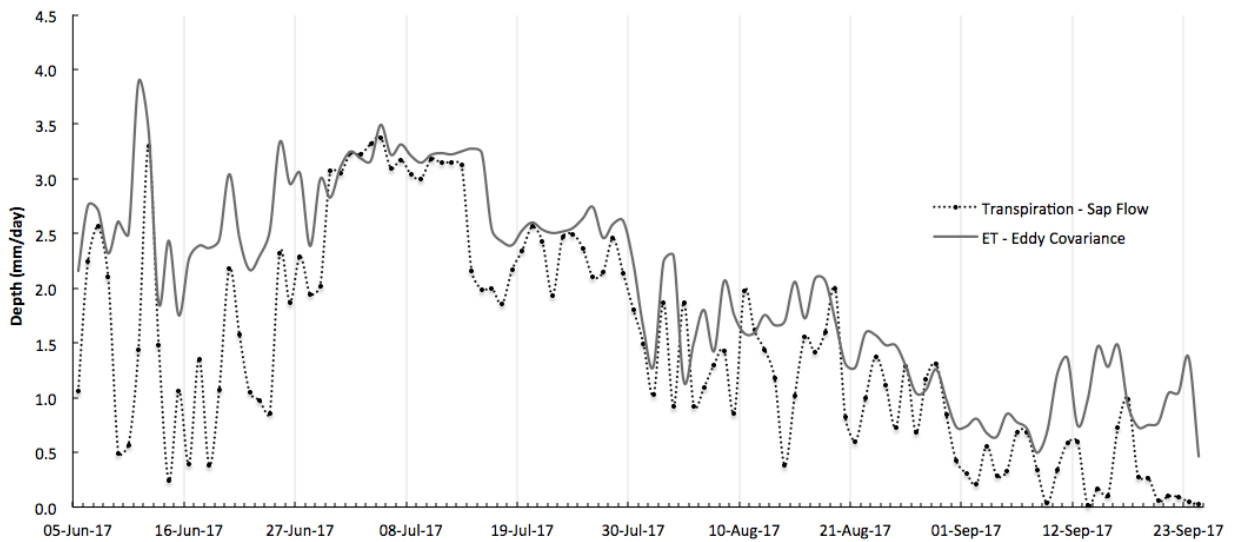


Figure 4. Forest transpiration plotted against entire forest-stand evapotranspiration for the 2017 dry growing season from June 5 – Sept 25 at Fortress Mountain, Kananaskis, AB

In conjunction with the hydrometeorological-based forest transpiration investigation, stable water isotopes were used to help tell the story of the sources for subalpine forest water use. By using isotopes $\delta^{18}\text{O}$ and $\delta^2\text{H}$, subalpine tree water sources were partitioned using a Bayesian mixing model, MixSIAR, for three points of the growing season. It was found that soil moisture was the most important water source for all trees, across both species and between two age classes (young, old), throughout the entire growing season (Fig. 5). Groundwater was the second most important source, being most valuable during spring snowmelt and at the beginning of the growing season as trees emerged from senescence. Like the hydrometeorological study, younger trees were found to rely on soil moisture more than older trees. There were minimal differences between species, although fir trees used more groundwater over the growing season, compared to spruce. This suggests that the rooting structure of fir may be better adapted to decreases in soil moisture during summer drought periods, allowing them to access deeper groundwater. Population abundance and succession may play a part in their successful adaption to access varied water sources, as fir were the most populous at the research location, comprising 70% of the local forest population.

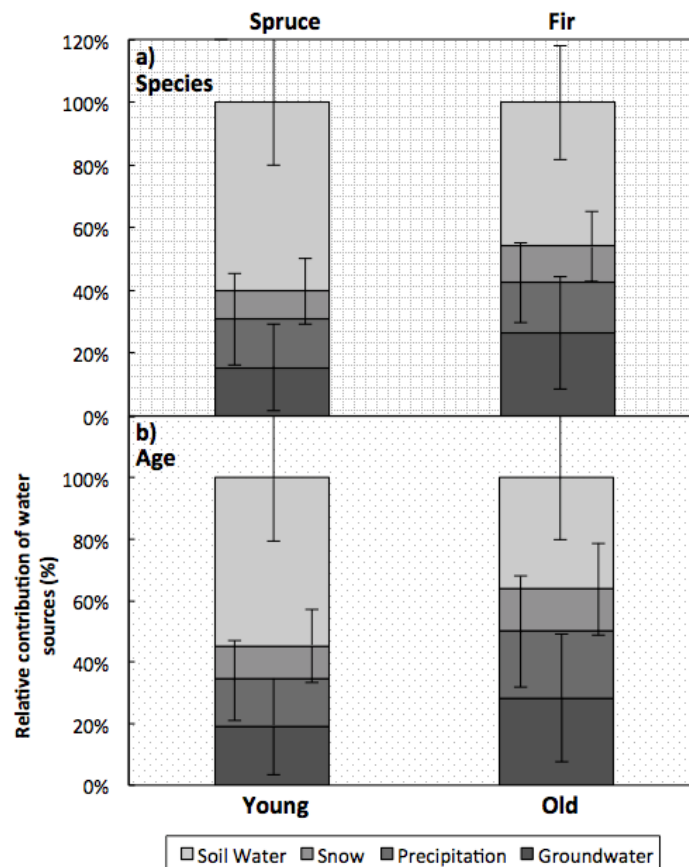


Figure 5. Relative source water contributions to xylem water for entire growing season (2017) length generated by MixSIAR BMM, partitioned by a) species (spruce, fir) and b) tree age (young, old). Standard deviations for each source depicted by error bars.

Treeline tree patch growth patterns and evapotranspiration

Dr. Petrone and Pomeroy's graduate student Jessica Williamson's research addressed the advancement of the treeline under climate change predictions, by focusing on how treeline expansion, in the form of tree islands and krummholz, interacts with alpine snowpacks and influences the evapotranspiration (ET) of a south-facing mountain ridge at Fortress Mountain in Kananaskis, Alberta. Open and closed canopy meteorological stations, atmometers and interception troughs were used to assess patterns in ET based on seasonal, vegetation and topographic changes. Additionally, snow surveys and a vegetation community analysis were performed to determine snow and growth patterns on a slope controlled by high wind speeds. Using atmometers, potential evapotranspiration (PET) was estimated within three closed-canopy tree islands and three surrounding open-canopy plots with scattered krummholz patches (Fig. 6). PET measurements were compared with dominant growth control factors, including temperature, wind speed, snowpack and microtopography. Positive feedbacks are anticipated between growth controls and the progression or stability of tree islands and krummholz.

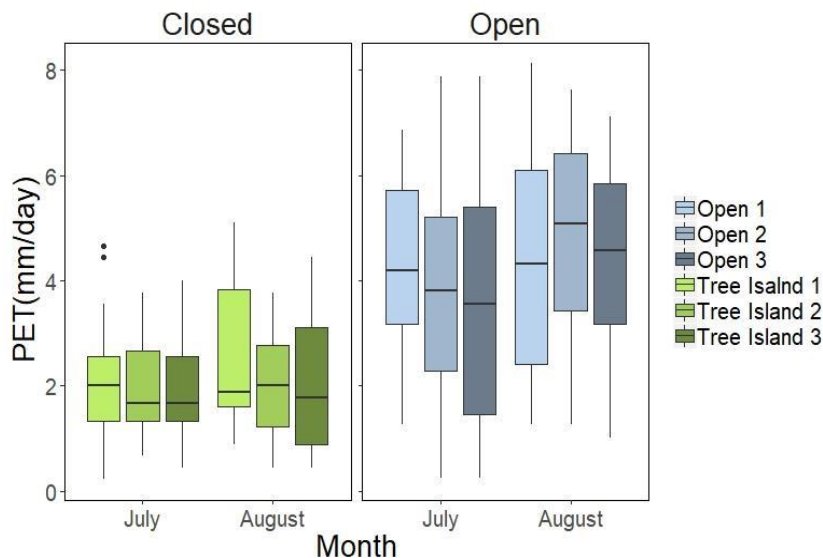


Figure 6. Potential evapotranspiration (PET) estimates for both closed and open study plots across the growing season. PET was higher in open areas, compared to within the tree islands.

Higher PET was measured in open-canopy plots, where exposure to wind and net radiation was increased and broad-leaved vegetation was present. PET rates in closed canopy tree islands were considerably lower, likely as a result of lower wind speeds and lower net radiation due to the presence of stunted subalpine firs and very little broad-leaved understory growth (Fig. 7). However, PET in closed canopy tree islands was shown to increase with stand density upslope. Krummholz and tree islands had a unique relationship with winter and spring snowpacks and snow coverage. By trapping windblown snow, shading snow from solar irradiance and reducing turbulent transfer, they sustained a snowpack that lasted later into the spring snowmelt period, resulting in increased moisture supply and continued growth. Canopy interception was greater within Tree Islands 1 and 2, further upslope, where patches had a dense understory of branch

offshoots that lay just over the ground and reduced throughfall. Higher interception rates within the denser tree islands could have caused higher rates of evaporation from the surface of the trees. These results suggest that the presence of trees above the existing treeline, with the potential for expansion under current and projected climate conditions, could result in more water being evaporated at higher elevations and potentially decreased downstream flows.

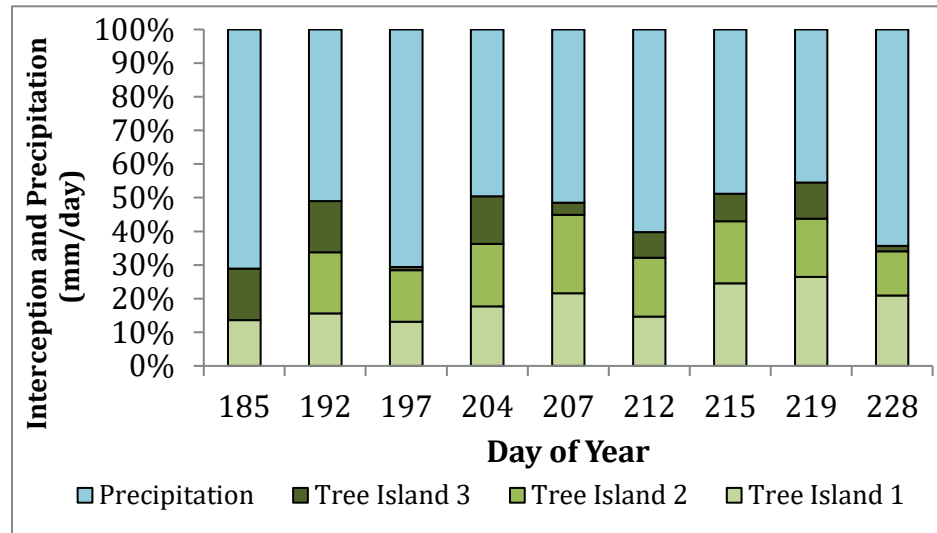


Figure 7. The relative proportions of interception and precipitation in the water budget, at different points of sampling throughout the summer growing season.

1.3 Storm runoff celerity as a function of soils and topography

Dr. Carey and a team of two graduate students focused on understanding storm runoff generation as a function of variable soils and topography. These studies combined simple models and analyses of climate data and in-field process based studies in order to understand these variables.

Infiltration into frozen soils and runoff generation in forested mountain catchments

Dr. Carey's graduate student Heather Bonn examined infiltration into frozen soils and their impact on runoff generation within forested mountain basins with both seasonal frozen soils and permafrost. The ground thermal and moisture regime along a topographic gradient was measured along with detailed surface observations and soil property information to set up and test a commercial finite element heat and mass transfer model GeoStudio. Once set up, the driving factors and influence of simple climate change scenarios on soil thermal and moisture regimes were assessed.

While some challenges exist, GeoStudio was able to simulate the patterns of ground temperature and moisture, although some parts of the water balance were poorly represented due to the simplicity of model formulation at the surface. Once the model was set up, simple delta change scenarios were evaluated by increasing and decreasing the temperature and precipitation. Fig. 8 shows how changes in temperature and the percentage of precipitation influence soil thermal

and moisture regimes. While increases in temperature and precipitation are relatively obvious (earlier melt, slightly warmer and wetter winter soils), a slightly cooler and drier scenario provides interesting results. Snowmelt completes earlier in a drier cooler scenario largely from a reduced snowpack, and soils achieve a much colder state, again more because of the decline in the snowpack than the decreased temperatures. This suggests that the greatest influence on winter thermal and moisture regimes is snow depth than air temperatures. This will strongly influence runoff generation processes in the spring.

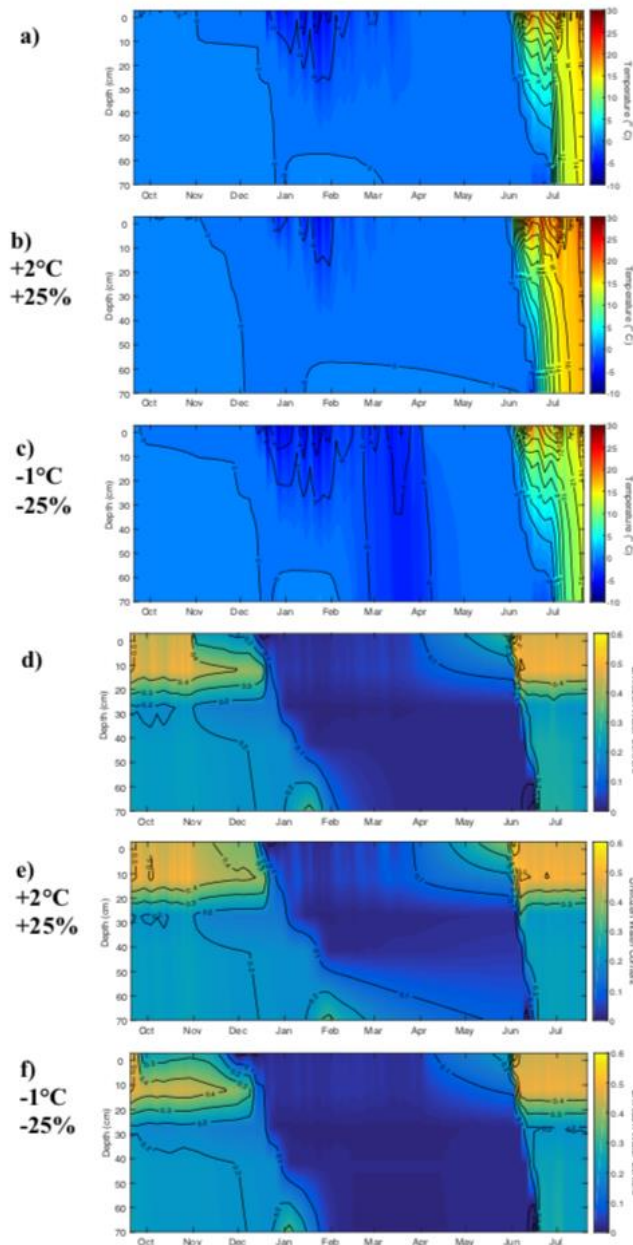


Figure 8. Soil temperature (a-c) and unfrozen water content (d-f) sensitivity from baseline model (a,d) to warmer and wetter (b,e) and cooler and drier (c,f) climate scenarios.

Hydrological change in runoff generation in the mountain West

Dr. Carey's PhD student Victor Tang examined hydrological change in the mountain west using multiple novel new techniques including deep learning (DL) algorithms combined with classical hydrometric analysis. In this work, Mr. Tang has worked with western North America's hydrometric data (Fig. 9) to use deep learning to assess shifts in hydrograph regimes using annual daily hydrographs. Deep learning algorithms are powerful new tools to detect hydrological change in mountain region, and can use various techniques to classify hydrometric regimes and then detect shifts associated with ecosystem change over time.

Results suggest that DL algorithms are effective at classifying hydrograph based on pattern recognition in their shapes. Once trained, these algorithms can be used to evaluate when changes occur in their general shape, and hence indicate when they flow regime is changing in a subtle manner. The power of DL is that they provide confidence scores in classification, so as hydrographs change with time, they can shift regimes (i.e. from a snowmelt towards rainfall driven regime) and the DL algorithm confidence scores will change to reflect this (Fig. 10). The impetus of this work is to develop new 'non-traditional' techniques to detect change and understand mountain hydrological processes, as we have relied overly on Mann-Kendall type analyses and other subjective metrics for some time.

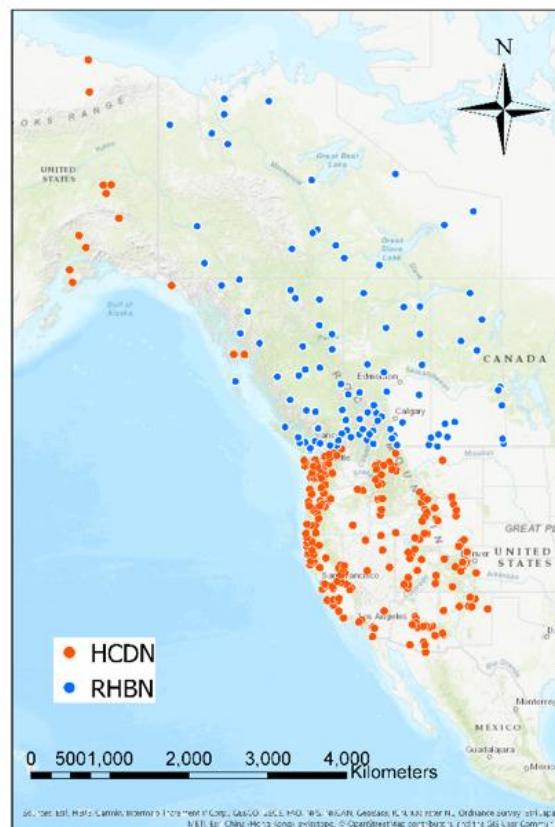


Figure 9. Hydrometric stations utilized for DL algorithms in western North America.

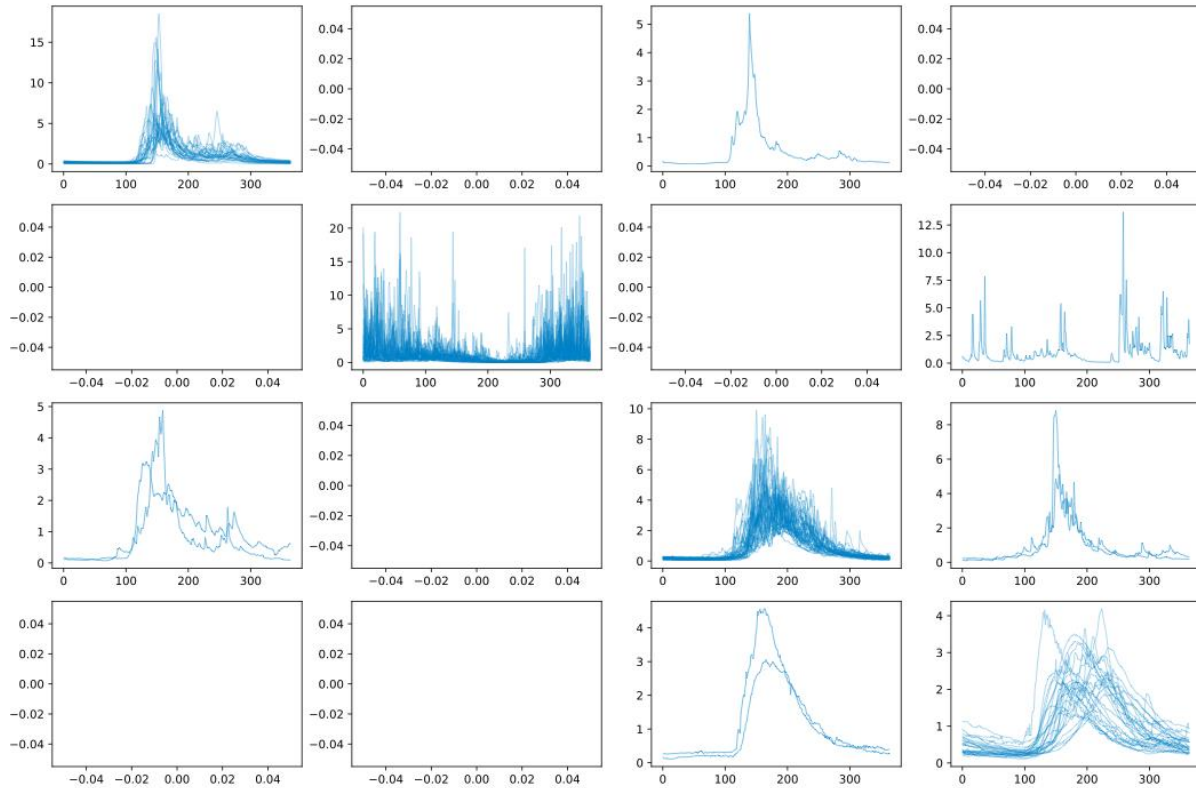


Figure 10. A confusion matrix from DL algorithm. Annual daily hydrographs along the diagonal are in a given class. Those outside the diagonal ‘confuse’ the algorithm’s classification. Confusion scores with time are used to assess change in flow regimes.

1.4 Snowmelt dynamics at forest edges

Dr. Pomeroy’s Post-Doctoral Fellows, Dr. Nicholas Wayand and Dr. Phillip Harder, and Research Scientist Dr. Joseph Shea focussed on measuring mountain snowpacks using remote sensing from Unmanned Aerial Vehicles (UAVs) and satellites. It is challenging to calculate mountain snowpacks in western Canada because of uncertain and sparse or non-existent precipitation measurements. Remotely sensed measurements of snow depth provide complementary approaches to the sparse network of ground observations and snow surveys. To meet the needs of catchment scale research, glacier mass balance, river basin scale data assimilation for streamflow predictions requires multiscale measurements with varying temporal return periods. No single platform available in the region can provide this. An integrated mountain snow measurement methodology has been devised that ranges from seasonal airborne laser altimetry measurements made over many hundreds of square km to more frequent surveys over small catchments using UAVs equipped with LiDAR and cameras permitting structure from motion estimation of the surface. Analysis of seasonal snow depth is also possible in sites of very high winter accumulation using high-resolution (< 1m) optical satellite imagery. A methodology was developed to collect these samples, results of initial measurements and a roadmap of how the air- and spaceborne snow observations will be integrated into research programmes, and snow

data assimilation schemes to support improved hydrological forecasting for Canada. An example of a UAV-LiDAR derived snow depth map for Fortress Ridge in Kananaskis is shown in Fig 11.

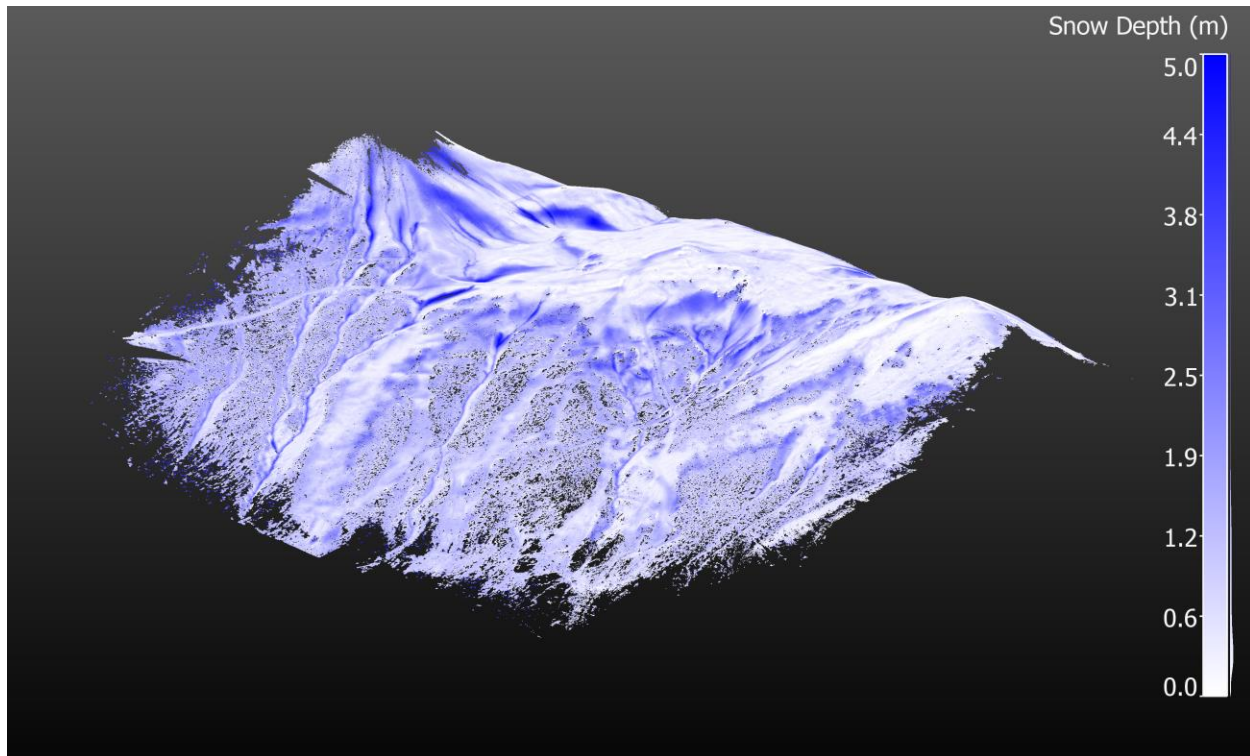


Figure 11. Snow depth map for 13 February 2019 derived from UAV-borne laser altimetry (LiDAR) over Fortress Ridge in the Fortress Research Basin, Kananaskis (Phillip Harder).

Dr. Pomeroy's graduate student and then Post-doctoral Fellow Dr. Nikolas Aksamit focused on studies of alpine blowing snow mechanics. Blowing snow in mountainous terrain is a complex nonlinear phenomenon driven by turbulent eddies with length scales ranging from millimetres to kilometres. Turbulent motions across a wide spectrum of sizes are superimposed on each other, interacting through a non-stationary energy and momentum cascade. In cold regions, snow redistribution by these turbulent motions impacts hydrology, glaciology, avalanche safety, and civil engineering. Blowing snow models typically rely on relating time-averaged turbulence statistics, which may oversimplify the complexity of the flow, especially in complex mountainous terrain, to steady-state snow transport. The present research sought to improve the understanding of the dominant structures in atmospheric surface layer turbulence relevant to snow transport, as well as characterize the short timescale response of blowing snow to specific eddy structures. A fundamental experiment was designed utilizing high-speed videography of laser illuminated near-surface blowing snow saltation coupled with adjacent 3D sonic anemometer wind measurements at two heights. The experiments were conducted at Fortress Mountain Snow Laboratory in the Canadian Rockies of Alberta during nighttime blowing snowstorms (Fig. 12). Novel applications of particle tracking velocimetry and binarization algorithms to blowing snow recordings allowed extraction of time resolved snow particle

velocities synchronized with instantaneous wind velocities, as well as time series of volumetric averages of blowing snow density in the first 30 mm above the surface. High-speed blowing snow video and measurements revealed the importance of the often-overlooked creep mode of transport to both transport initiation and flux. Blowing snow velocity and flux profiles were found to be temporally variable and dependent on instantaneous wind speed, with dominant modes of transport varying during turbulent gusts. Sweep and ejection wind events were coupled to blowing snow responses on sub-second timescales, with each quadrant event playing a unique role in transport initiation and sustaining snow fluxes. Finally, large low-frequency turbulent motions, hypothesized to follow a top-down characterization, were found to modulate the amplitude of near-surface turbulence, as well as directly contribute to blowing snow fluxes (Fig 13). The role of intermittent coherent turbulent structures challenges the ability of time-averaged turbulence statistics to represent the complexity of wind-snow coupling, especially in mountainous terrain. The strong relationship found between large-scale turbulence modulating eddies and near-surface turbulence, also challenges the efficacy of applying steady-state laboratory-derived flux relationships to model transport in the surface layer.

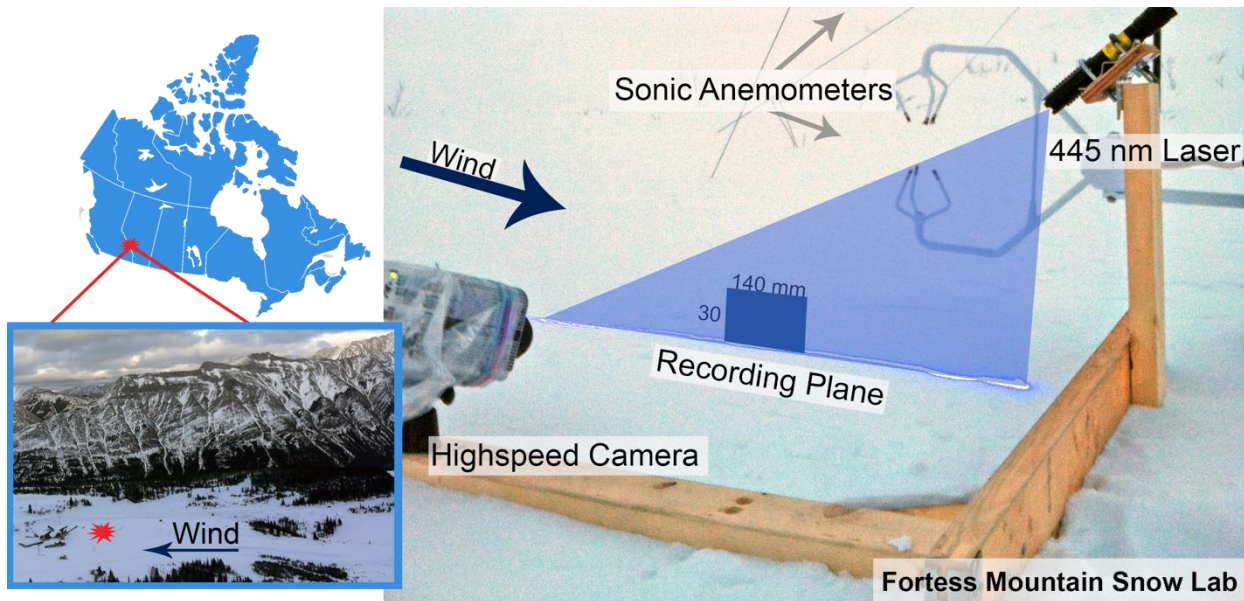


Figure 12. Field site location and recording apparatus setup with meteorological measurements, Fortress Mountain, Kananaskis, Alberta, Canada. The red mark indicates the location of the blowing snow measurement devices as viewed from the west with respect to the upwind fetch.

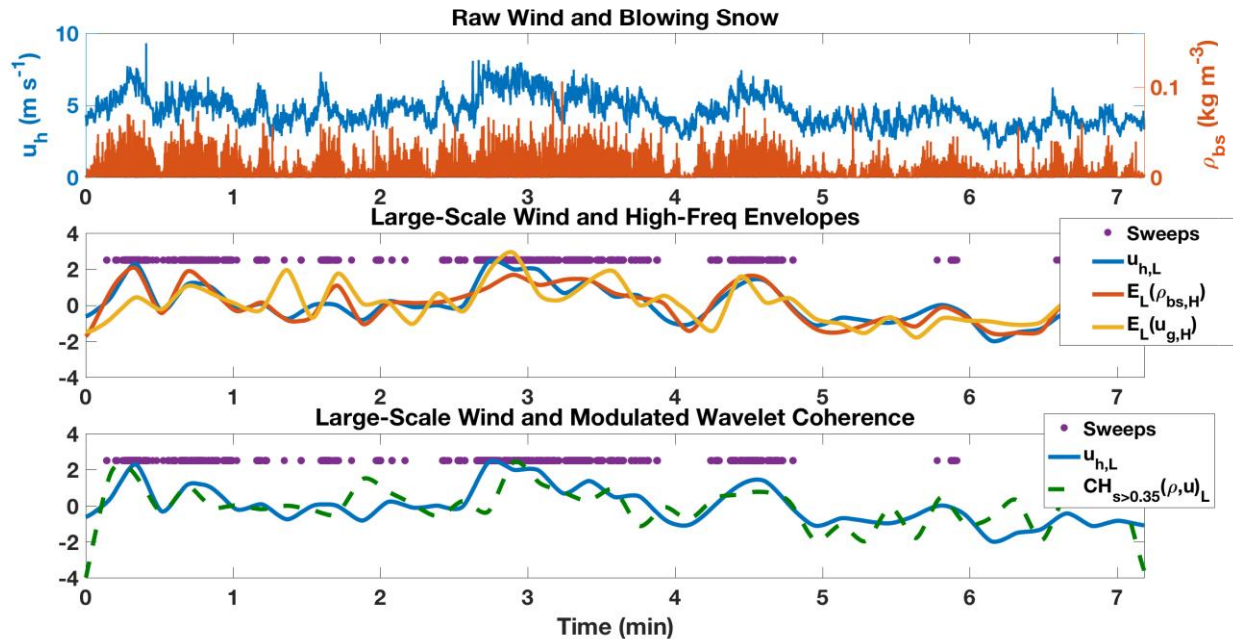


Figure 13. Figure showing modulation of wind-snow coupling measured with ultrasonic anemometry and PTV analysis of laser-illuminated alpine blowing snow particles. High frequency wavelet coherence between wind and snow is also modulated by large-scale turbulence events. Turbulent sweep motions are responsible for the strongest coupling, with decoupling occurring during their absence.

Dr. Pomeroy's graduate student and then Post-doctoral Fellow, Dr. Nicolas Leroux studied the flow of meltwater through snowpacks and the impact of snowpack heterogeneities on flow and energy dynamics. Accurate estimation of snowmelt runoff is of primary importance in streamflow prediction for water management and flood forecasting in cold regions. Lateral flow, preferential flow pathways, and distinctive wetting and drying water retention curves in porous media have proven critical to improving soil water flow models; the most sophisticated physically based snowmelt models only account for 1D matrix flow and employ a single drying water retention curve for both drying and wetting snowpacks. Thus, there is an immediate need to develop snowmelt models that represent lateral and preferential flows, as well as full capillary hysteresis to examine the potential to improve snowmelt hydrological modelling. In this research, the primary objective is to improve understanding and prediction of water flow through snow by investigating the formation of preferential flow paths and the coupling of heat and mass fluxes within snow. Of particular interest is the prediction of capillary pressure at macroscale, as it is of great importance for simulating preferential flow in porous media. A novel 2D numerical model is developed that enables an improved understanding of energy and water flows within deep heterogeneous snowpacks on flat and sloping terrains (Fig. 14). The numerical model simulates horizontal and lateral water flow through snow matrix and preferential flow paths and accounts for hysteresis in capillary pressure, internal energy fluxes, melt at the surface, and internal refreezing. Implementing a water entry pressure for initially dry snow was necessary for the formation of preferential flow paths. By coupling the simulation of preferential flow with heat transfer, ice layer formation was realistically simulated when water infiltrated an initially cold

snowpack. Heat convection was added to the model and coupled to the energy balance at the snow surface; the transfer of heat by topography-driven airflow affected the estimated snow surface temperature by transporting thermal energy from the warm snow-soil interface to the upper snowpack. Comparisons of the modelled meltwater flow predictions against snowmelt field data revealed limitations in the current theories of water flow through snow, such as the use of a single-valued capillary entry pressure that is limited to high-density snow. This suggested further concepts that would improve the representation of capillary pressure in snow models. This improved model, which considers a dynamic capillary pressure, gave better results than models based on previous theories when simulating capillary pressure overshoot. The research demonstrates how heterogeneous flow through snow can be modelled and how this research model furthers understanding of snowmelt flow processes and potential improvements in snowmelt-derived streamflow prediction.

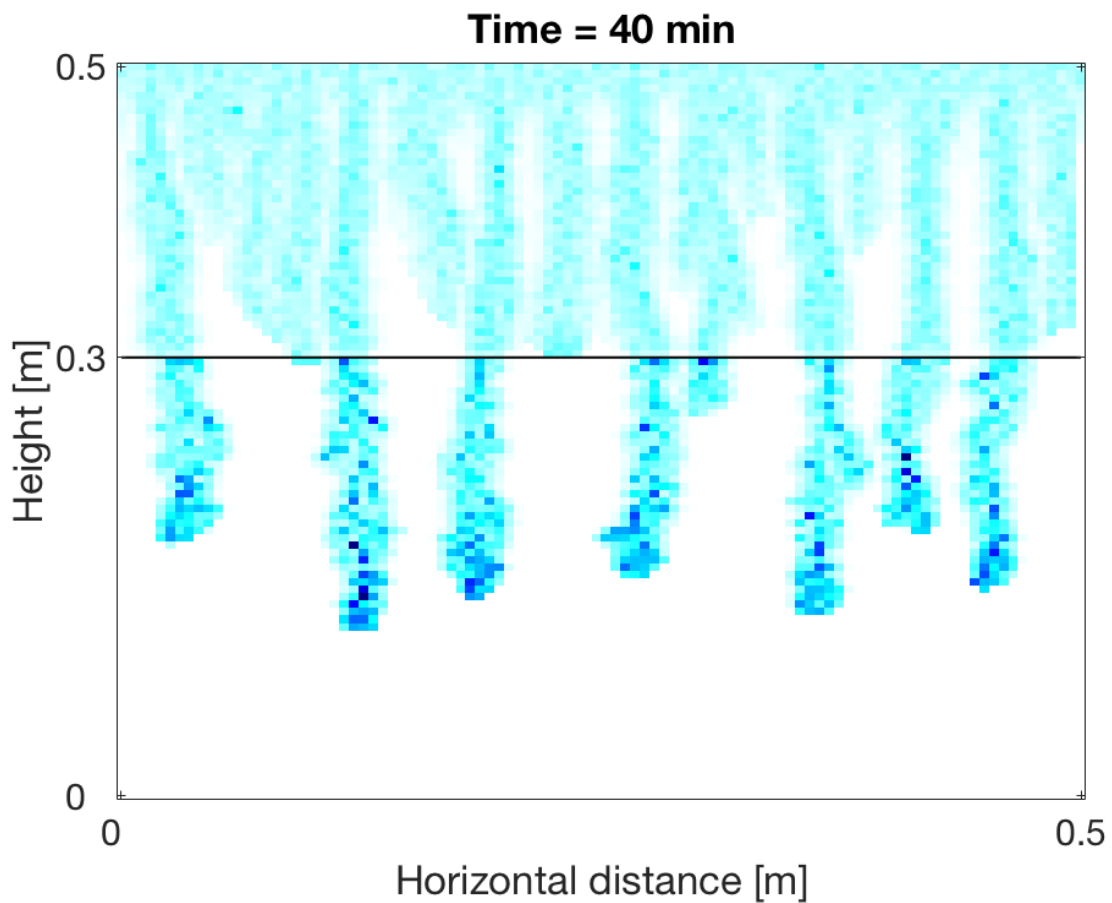


Figure 14. Rain-on-snow simulation of a coarse over a fine particle size snowpack from a 2D finite element snowmelt model.

1.5 Wetland storage and drainage

Wetlands perform important ecosystem services by regulating and storage large quantities of water, especially during and after large precipitation events. Understanding their hydrological function is important to the overall understanding of mountain headwater vulnerability by informing how these sensitive ecosystems contribute. Dr. Westbrook, Dr. Petrone and a various graduate students designed several research projects to address these questions.

Dr. Westbrook's wetland studies aimed to 1) characterize the dominant hydrological functions of a mountain valley bottom fen peatland during drought conditions; identify the primary controls over the fen's hydrological functions; 3) evaluate water storage retention capacity of beaver ponds during flood conditions; and 4) determine beaver dam persistence after the Alberta 2013 flood. The first two objectives were achieved through the work of graduate student, Stephanie Streich, who started the project in September 2016. The third objective was completed by undergraduate student, Amanda Ronnquist, who was recruited in June 2017. The following highlights the completed work of each objective. Dr. Petrone's master's student Dylan Hrach investigated a high subalpine wetland in comparison.

Hydrological Function of a Mountain Fen Peatland Under Dry Conditions

The study was conducted in a low elevation fen peatland unofficially called Sibbald fen. The fen is ~0.71 km² and situated in a valley-bottom position, typical of many peatlands throughout the Eastern Slopes (Morrison et al. 2015). The fen is surrounded by forested foothills reaching 1650 m, and the watershed area is 9.3 km². Peat is thinnest (<0.5 m) at the northern edge of the fen, and deepest (up to 6.5 m) towards its center. The upper 0.5 m of peat is mainly composed primarily of sedge (*Carex utriculata*), switching to peat composed mainly of *Sphagnum* spp. at 0.50-1.30 m below the peat surface (Wang et al. 2016). Underlying the peat is marine clay and alluvium. The fen is supplied by five streams several of which are ephemeral, and is drained by one perennial stream, Bateman Creek.

As Sibbald fen has been an active research site since 2006 (Westbrook and Bedard-Haughn 2016), several long-term installations have been put in place in it to gather hydrometric data (Fig. 15). These were used to detail the water balance for the fen during the very dry summer of 2017. Spence's (2007) hydrological function model was applied, with modification, at a daily time step using the water balance values. As well, ground frost was monitored every 1-2 weeks during the 2017 field season until the ground fully thawed to evaluate its regulatory effect on fen hydrological function.

The observations reveal that Sibbald fen regulated runoff in four different ways during the study: it transmitted, contributed, stored and evapotranspired water (Fig. 16). Shifts in hydrological function were driven primarily by the presence/absence of seasonal ground frost and timing of rainfall events. In the spring and early summer, the dominant hydrological function of the peatland was transmission. When frozen, the fen released very little water from its internal stores. Rainstorms during this time led to a temporary switch in hydrological function to contribution. The evapotranspiration function was dominant only for a brief period in late June and early July when rainfall was low and the ground was still partially frozen, even though

evapotranspiration accounted for the largest loss of storage from the system. Once the ground thawed, the fen's dominant hydrological function became contribution. With very little precipitation and consistent rates of evapotranspiration each day, the fen water table dropped nearly 1 m by the end of the growing season. The release of the fen's internally stored water maintained baseflow in Bateman Creek, whereas some of the inflowing streams to the fen ran dry (Fig. 17). The larger rainstorm that occurred when the ground was thawed transiently switched hydrological function to recharge, but did not cause the fen to generate runoff.

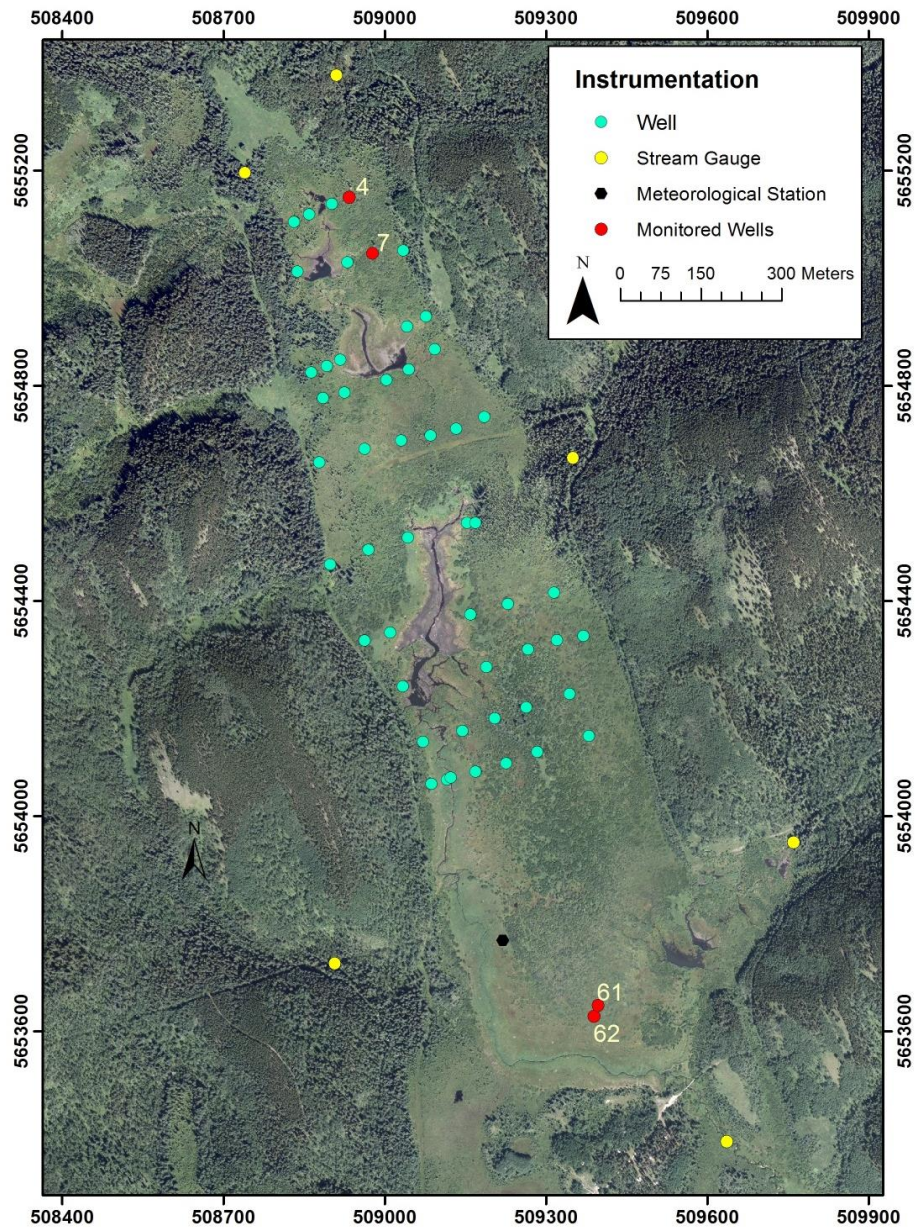


Figure 15. Map of Sibbald fen near Sibbald Flats showing hydrometric instrumentation. The wells shown are the approximate locations of frost measurements taken on each survey day.

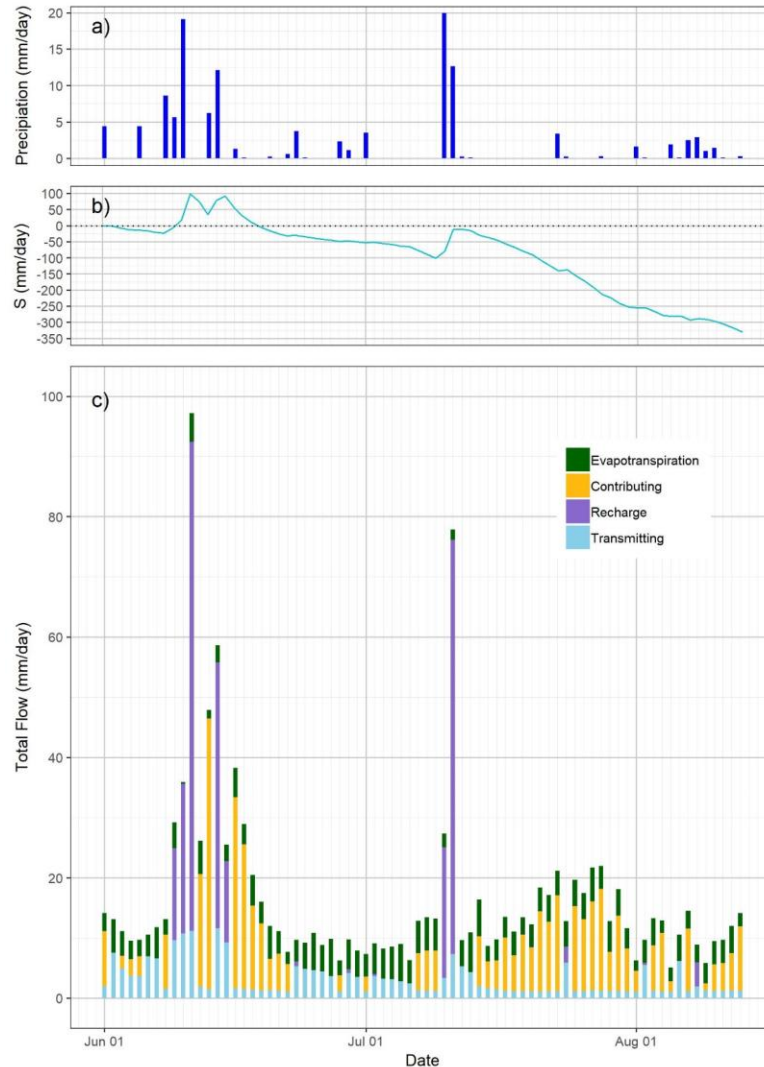


Figure 16. Daily distribution of wetland hydrological function at Sibbald fen (c). Changes in dominant function occur in response to rainfall events (a) and changes in ground thaw (not shown) and water storage (b). Ground frost was present in the fen until the first week of July. Afterward, the fen was frost-free.

This research highlights the mechanisms by which mountain peatlands supply baseflow during drought conditions, which will prove useful to modelling regional baseflow. Also better understood is the importance of frozen ground and rainfall in regulating fen hydrological function. A follow-up study of ground frost presence in Rocky Mountain fens at different elevations, and how frozen ground influences fen peat (carbon) accumulation is underway (PhD student María Elisa Sanchez Garces). Results should provide new understanding of the sustainability of fens at high and low elevation, and determine which are expected to be most jeopardized by climate change.

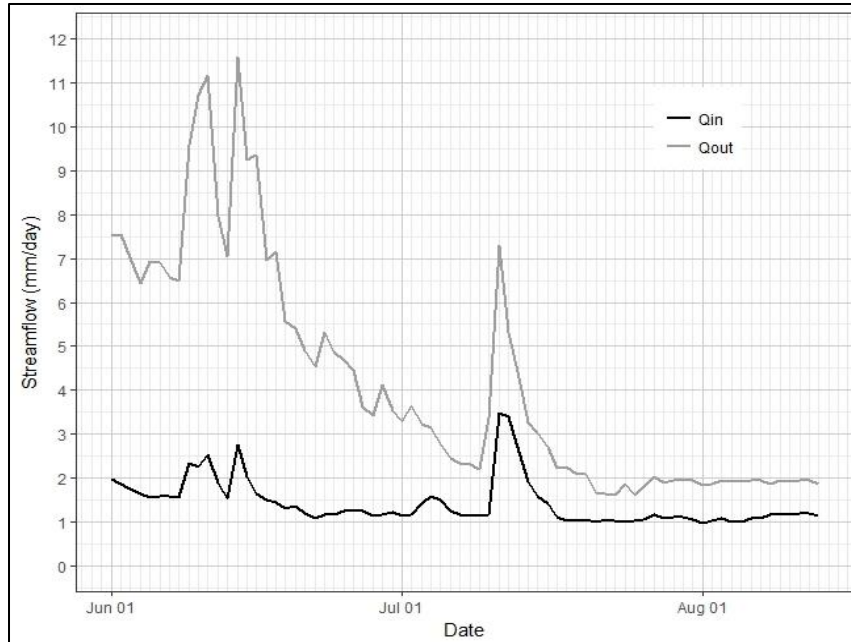


Figure 17. Total inflow (Q_{in}) from all inlet streams and outflow (Q_{out}) in Bateman Creek for Sibbald fen, 1 June-13 August 2017. Streamflow was scaled to the area of the peatland (0.71 km^2).

Flood Attenuation Offered by Beaver Ponds

There is growing interest in using beaver to help restore ecosystem resilience to floods and droughts, especially in western North America. The problem with the concept of relying on beaver ponds to attenuate floods is that they, when full, should offer little storage of floodwaters. Beaver commonly live in wetlands situated in valley-bottom positions throughout the Eastern Slopes (Morrison et al, 2015) where water drained from the alpine zone funnels through before reaching the populated lowlands. The Alberta 2013 flood triggered the largest recorded flood in the Rockies west of Calgary, Alberta. It provides a natural experiment from which one can learn more about the ways in which green infrastructure, using the example of beaver dams, function in mountain environments during floods. The opportunity was used to test two long-standing hypotheses: one, that beaver ponds have limited flood attenuation capacity; and two, that beaver dams commonly breach during large flood events.

The study was carried out at two spatial scales. At the local scale, the valley-bottom wetland that has been studied for a decade (Sibbald fen, described above) was instrumented with a meteorological station, stream gauge, groundwater well, and three beaver pond level recorders at the time of the flood (Fig. 18). All instrumentation survived the flood. Regionally, we had fortuitously inventoried wetlands and beaver ponds in 2012 (i.e. pre-flood) via image analysis and field verification (Morison et al, 2015). Determined herein was post-flood beaver dam conditions across 74% of Morrison et al.'s 7912 km^2 study area, as that was the extent of the post-flood (July 2013) ortho photographs (0.30 m resolution) provided by Alberta Environment and Parks. The area assessed included 74 sites with beaver dam sequences known to be intact in

the Morrison et al. study. The sites with sequences of beaver dams were categorized as 'breached', 'persisted', or 'persisted but affected'. Categories were based on the collective status of all the dams within a site.

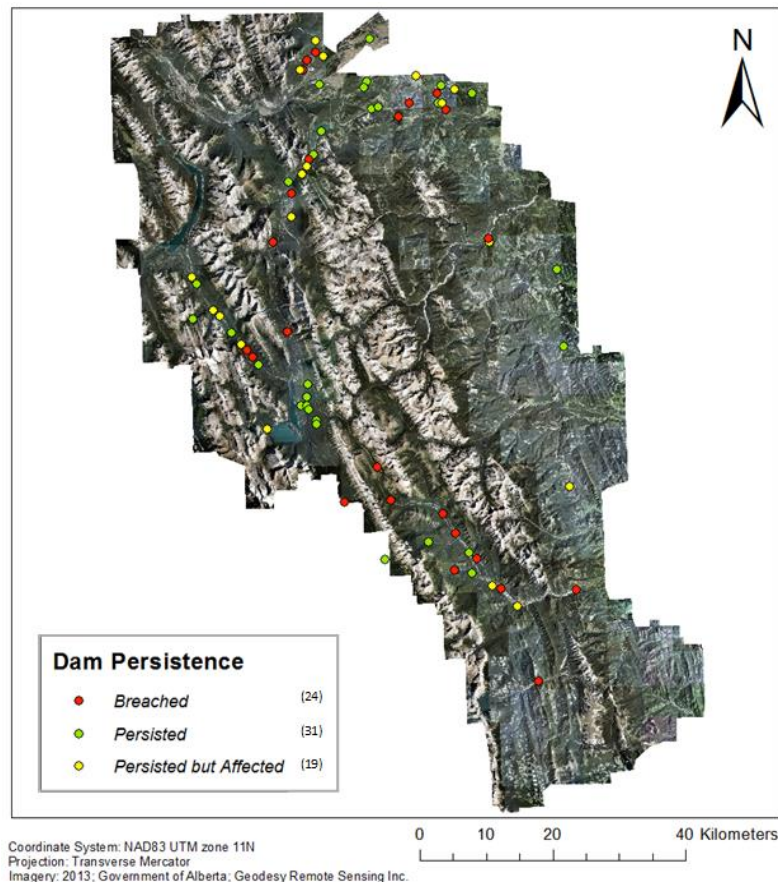


Figure 18. Persistence of beaver dam cascade systems throughout Kananaskis Country as inventoried following the Alberta 2013 flood.

The analyses indicate that the majority of beaver dams across Kananaskis Country, including at Sibbald fen, survived the flood (Fig. 18; 42% of the beaver dam cascade systems studied persisted, 32% were breached, and 26% persisted but were affected). This was surprising given that beaver dam failures are common during high intensity rainstorms when landscapes have limited water infiltration capacity (Butler and Malanson, 2005), such as was the case in the study area at the time of the flood (Pomeroy et al. 2016). Regionally, there was spatial clustering of sites where beaver dam sequences persisted or failed during the flood event that was unrelated to pond water retention capacity or the amount of rainfall received. Beaver dams survived the flood mostly intact in valleys that were broad and flat, or where beaver dammed groundwater seepage. Higher than average dam failure rates were observed for beaver dam complexes situated in steep, narrow valleys. The failure of one beaver dam in a cascade system, particularly if it has a high dammed water volume (Gurnell, 1998), can create a water or water-sediment

surge great enough to have a domino effect wherein downstream beaver dams also fail (Marston, 1994; Butler and Malanson, 2005). Thus, we were surprised by the failure of often only the upstream dam in a cascade sequence for sites in the persisted but affected category (26% of all sites). The detailed study at Sibbald revealed that pond fullness, in addition to the magnitude of the water-sediment surge, appears to be important in determining the fate of dams in a cascade sequence when an upstream beaver dam fails.

Sibbald fen received 194.6 mm of rain during the 19-22 June 2013 event. The four largest beaver ponds in the peatland collectively stored $1.9 \times 10^4 \text{ m}^3$ of water when filled to their dam crests. Water level loggers from the three instrumented beaver ponds (W52, W53 and W54) indicate pond levels were dynamic (Fig. 19). Early in the storm event, all three beaver ponds quickly over-filled. Only one of the three monitored beaver dams – pond 53 – failed during the rain event. The other two dams developed some holes, but did not rupture. A 10-m long section of the dam at pond 53 failed on 20 June between 11:15 and 11:30 am after five hours of heavy rain (44 mm, intensities of 7.5 – 10.0 mm/hr). The pond lost 7474 m^3 of water over 5.0 hrs. The outburst flood mobilized the two beaver lodges in the pond, all the dam’s woody material along the 10-m breach, and blocks of peat from a depth previously dated as ~4100 years before present (Janzen and Westbrook, 2011). Floodwaters rushed over top of the downstream dam without rupturing it. Despite sustaining a considerable breach, pond 53 did not fully drain. The pond continued to retain water after the breach, and had a secondary peak in level following the 6-hr lull in the rain event, transiently storing 18% of its capacity.

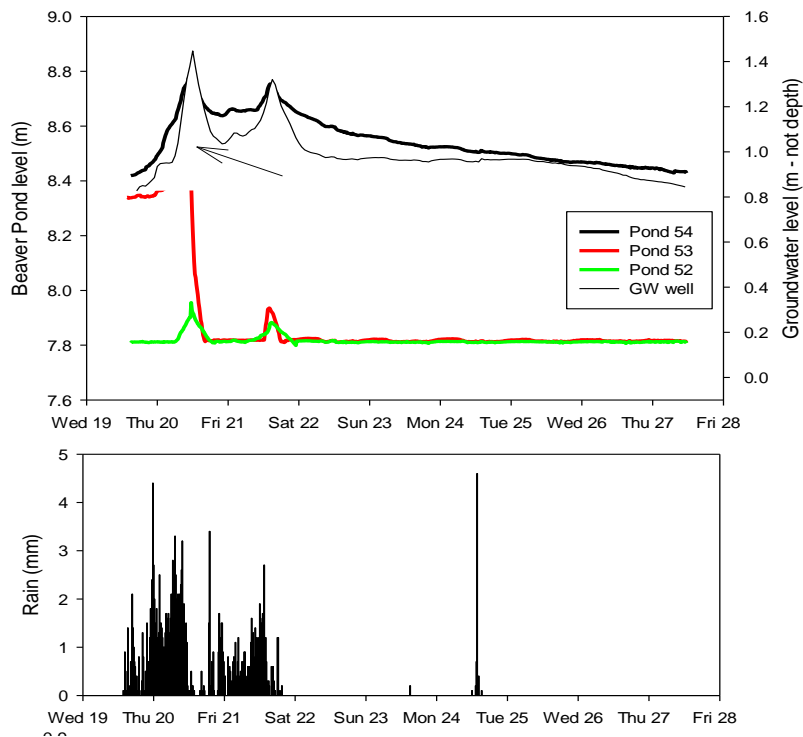


Figure 19. Hydrographs (top) of the three instrumented beaver ponds at Sibbald fen (Ponds 52-54) and the groundwater well (GW well) located near the meteorological station during the Alberta 2013 flood event. The hyetograph (bottom) shows hourly rain received

Stormflow volume at Sibbald was estimated as $1.69 \times 10^5 \text{ m}^3$ between 19 June at 1:00 pm and 22 June at 4:00 pm. Since beaver ponds in Sibbald store an average of 4750 m^3 , 35 ponds would be needed to provide 100% flood reduction (i.e. to hold all of the stormflow from the 2013 event). For 50% flood reduction, 18 beaver ponds would be needed, and for 10% flood reduction, 4 beaver ponds would be needed.

Overall, these findings suggest that beaver ponds could prove useful in flood reduction, even for large floods such as happened in Alberta in 2013. The journal manuscript is currently being finalized and will be submitted in July 2019. Follow-up research on the conditions under which beaver ponds can offer enhanced hydrological resilience to floods is being carried out as part of a new Alberta Innovates funded MSc project (Amanda Ronnquist).

Dr. Westbrook has initiated follow-up research goals that started late 2018 to determine whether the groundwater source of subalpine wetlands is local (recently recharged snowmelt water) or regional. Results hope to provide a new understanding of the sustainability of fen wetlands at higher and low elevations and which could be most jeopardized by climate change. This continued work will be tackled by new PhD student Maria Elisa Sanchez and MSc student Selena Schut.

Seasonal evapotranspiration and shading dynamics of a subalpine wetland

Dr. Petrone’s graduate student Dylan Hrach focussed on understanding the influencing of shading and complex topography on the classification, climate and energy balance of a subalpine wetland. This is being accomplished by characterizing the soil, vegetation and microclimate of

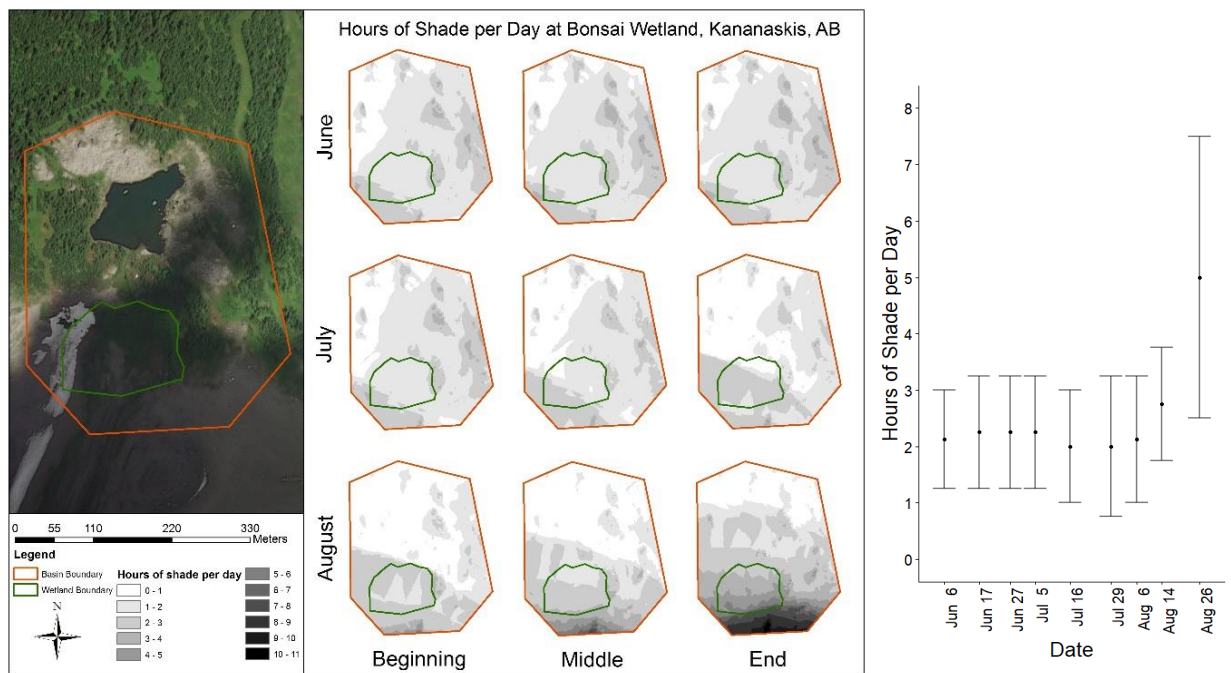


Figure 20. Shading from a 400m tall headwall on a 2100 masl subalpine wetland over the summer growing season. Hours of available sunlight, and photosynthetic driving radiation, to the wetland at varying points of the growing season.

the wetland in question, in addition to determining how the complex topography of a mountain headwall influences shading and the surface energy balance (Fig. 20). In addition, the turbulent fluxes of CO₂ and H₂O are being used to generate an understanding of water use efficiency of vegetation within the wetland. Of particular importance is considering how shading creates a microclimate that influences the turbulent fluxes throughout the growing season.

Shading of the wetland changes significantly over the growing season from June – August. In June, there is 1-4 hours of shade per day within the wetland boundary (green, in Fig. 21). Shade increases from SW to NE. In July, there is 1-4 of shade per day in the wetland boundary, shade also increases from SW to NE. Following the summer solstice, there is a rapid increase of shading hours. In August, there is 3-8 hours of shade within the wetland boundary. Shade increases from N to S. Maximum daily ET occurred on July 17th, with 3.9 mm. The highest period of ET occurred following the end of snowmelt, and was from July 5th to the 20th, with a total of 44.3 mm during this period. This was 28% of the cumulative growing season ET that occurred in a two week period.

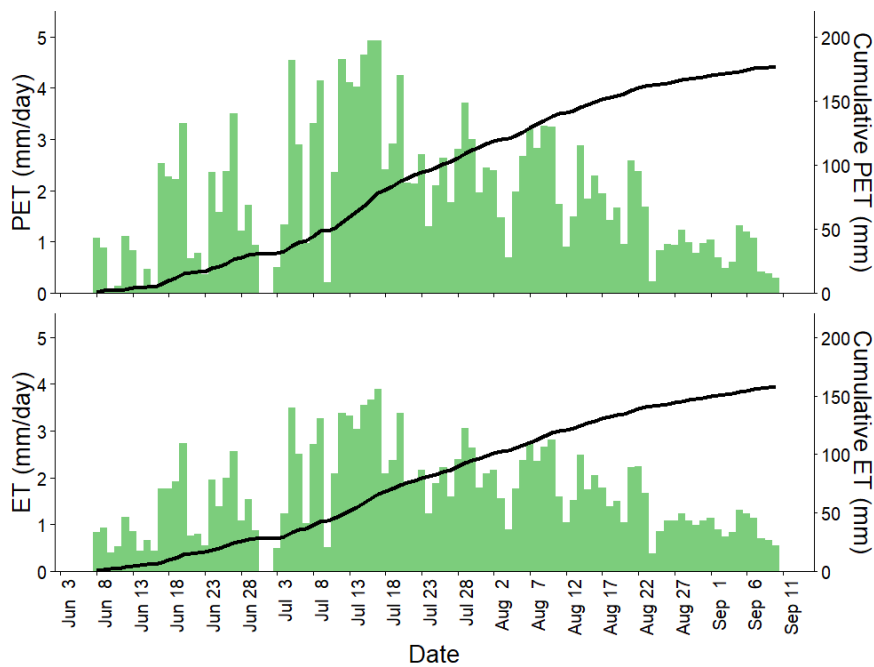


Figure 21. Graph showing ET and Potential ET seasonal progression for the subalpine wetland over the growing season.

Dr. Petrone recruited three new students in early 2019 to continue work developed from both Dr. Westbrook and Petrone’s recent findings on mountain catchment wetlands. PhD student Abby Wang will study three subalpine wetlands over an altitudinal gradient within the Kananaskis region, while MSc candidates Sheryl Chau and Julia Hathaway will focus on smaller scale wetlands process, with the goal of scaling up the processes they see to larger areas, helping to model wetland processes in mountain headwater regions.

1.5 Groundwater storage, flow paths and hydraulic response time

Dr. Masaki and his students lead the groundwater contribution task. The objectives of the groundwater component of this study are to 1) identify unique headwater aquifer systems that represent common conditions of the Eastern Slopes; 2) quantify the hydrogeological response of these systems to water inputs by glacier melt, snowmelt, and rainfall; 3) characterize the effects of stream-groundwater exchange processes on distribution and extent of thermal refugia, and 4) develop practical tools to estimate groundwater contribution, which are applicable to many headwater streams in the Eastern Slopes. The first two objectives were achieved through the work of graduate student, Craig Christiansen. Two other graduate students were recruited to work on the last two objectives, and their work is still in progress. This report will highlight the completed work by Christiansen.

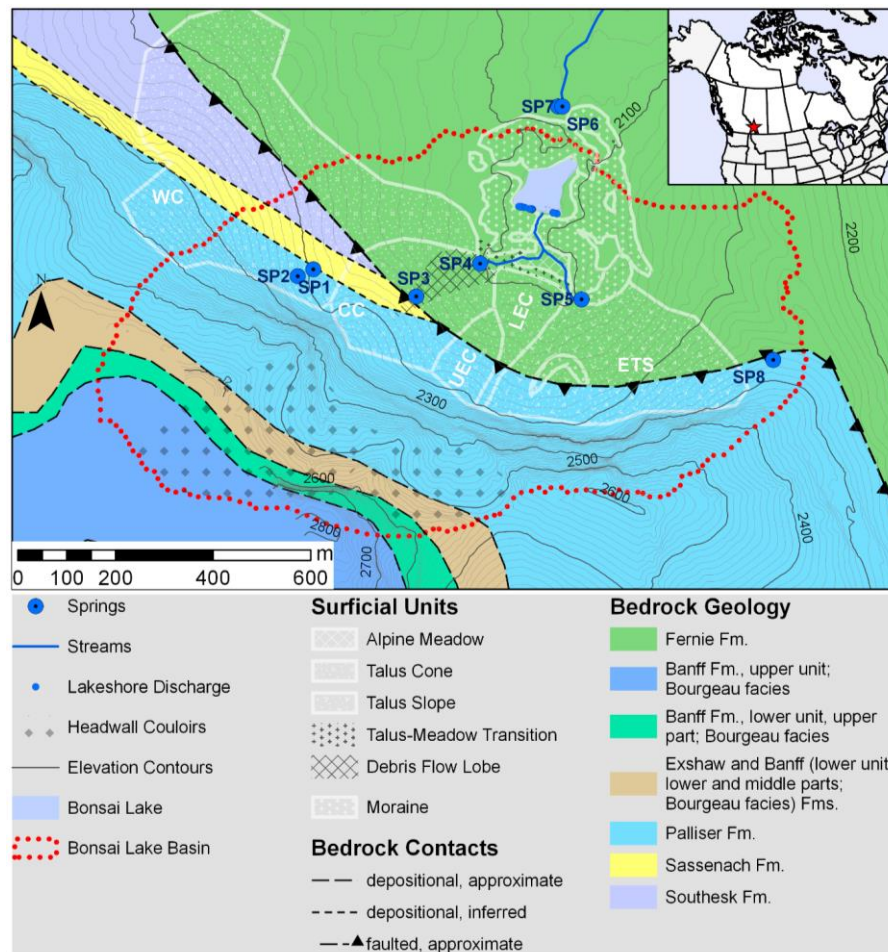


Figure 22. Map of Bonsai Lake Basin near Fortress Mountain showing bedrock lithology, surficial geology, and hydrology. White lettering notes the abbreviated names of the West Cone (WC), Central Cone (CC), Upper East Cone (UEC), Lower East Cone (LEC), and Eastern Talus Slope (ETS), and the red arrows denote the drainage direction within the headwall couloirs. Red star in the inset map shows the location of the site within Canada. Bedrock spatial data from McMechan (2012).

The study was conducted in a headwater catchment unofficially called the Bonsai Lake watershed, partially coinciding with the evapotranspiration study area within the project. The watershed consists of typical alpine landforms of exposed bedrock, talus slope and cone, moraine (Fig. 1, Fig. 2). Bedrock geology is mainly characterized by older and harder Devonian limestone in the southern part, and younger and softer Jurassic shale (Fig. 1). Several springs (marked SP in Fig. 3) occur on talus slopes, and the groundwater discharging from these springs provides baseflow to a stream flowing through an alpine meadow (Fig. 1), where evapotranspiration study was conducted.

Hydrogeological and geophysical investigations showed that the streams flowing through the meadow were “losing streams”. Therefore, springs discharging at the bottom of talus slopes are recharging the groundwater under the meadow and sustaining evapotranspiration by meadow vegetation. Detailed geophysical imaging was conducted on talus, meadow, and moraine (see Fig. 3 for location of survey lines) using electrical resistivity tomography (ERT), seismic refraction tomography (SRT), and ground-penetrating radar (GPR) (Christensen 2017). Geophysical data revealed that the talus deposits are up to 60 m thick and include internal layers of fine sediments embedded in coarse gravels and boulders. This is in contrast to previous hydrogeological studies conducted in the Main Range of the Canadian Rockies characterized by hard quartzite bedrock, where talus slopes have relatively simple internal structure (e.g., Muir et al. 2011; Harrington et al. 2018). The findings of the present study indicate the important effects of underlying bedrock geology on hydrogeological characteristics of alpine landforms such as talus.

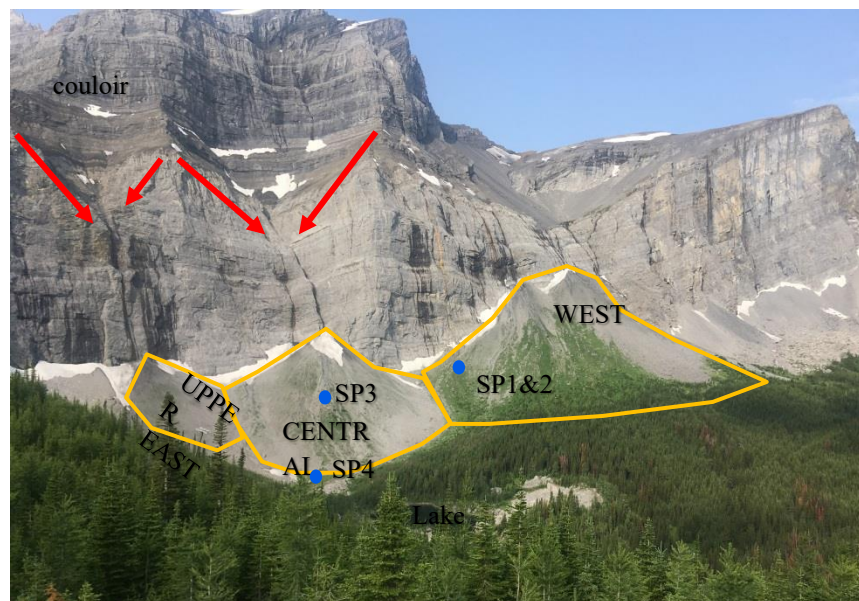


Figure 24. An oblique photo (facing southwest) of the talus deposits in the study area taken on July 26, 2018. Orange lines outline the three of the four talus cones. (The Lower East cone is obscured by trees). Also noted are important springs (blue circles), waterfalls (blue dashed lines), and couloirs above the Upper East and Central Cones (red arrows).

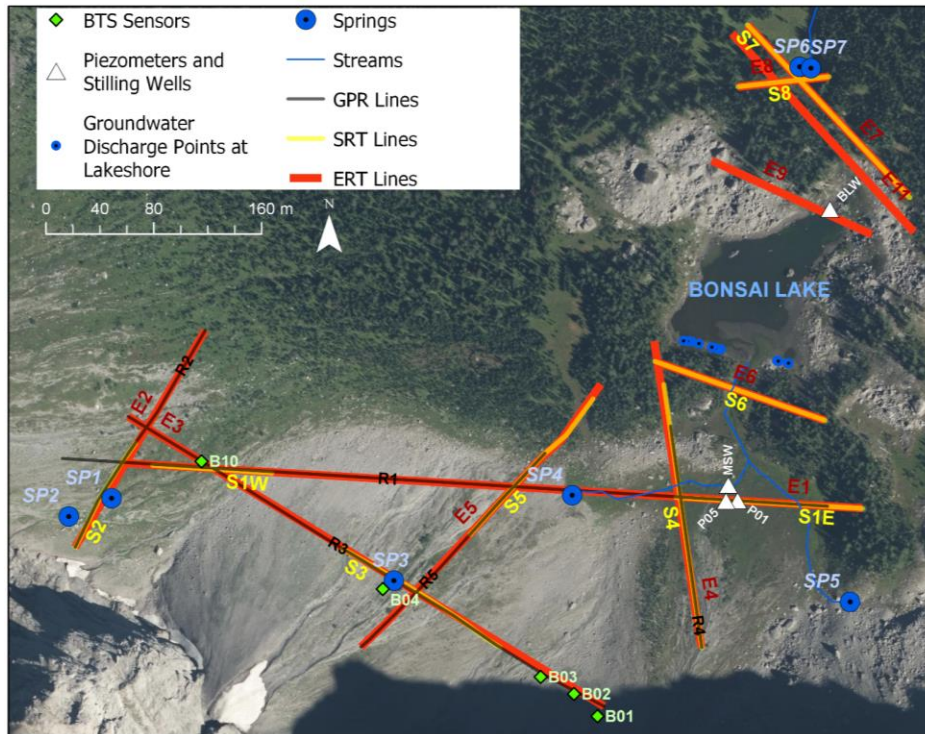


Figure 25. Map showing the locations of geophysical lines and other sensors. Note that ERT lines are labeled “EX”, SRT lines labeled “SX”, and GPR lines labeled “RX”, with “X” being the line number. Line S1 has two segments: S1W at the west and S1E to the east. Air photos from Alberta Environment and Parks (2013).

Hydrological and geophysical data showed that Bonsai Lake (Fig. 22) is a seasonal water body, or a surface expression of the water table within the moraine aquifer. A large spring complex on the north side of the lake (SP6 and SP7 in Fig. 25) is the headwater of the stream draining the watershed. This stream is a tributary of Galatea Creek, which in turn is a tributary of Kananaskis River. Winter baseflow of streams in the Canadian Rockies is almost entirely provided by groundwater discharge and hence, is a good indicator of groundwater retention capacity of watersheds (Paznekas and Hayashi, 2016). Winter baseflow expressed as the basin-average runoff in the rivers originating in the Rockies ranges from 0.1 to 0.4 mm/d (Paznekas and Hayashi, 2016). Winter baseflow of the stream draining the Bonsai Lake watershed during 2016-2017 was 0.7-1 mm/d, much higher than the common range in the Rockies, indicating a uniquely high capacity of the watershed to store groundwater and release it slowly during the fall and winter months.

Synthesizing all geophysical, geological, and hydrological data, Fig. 26 shows the conceptual model of the aquifer system in the watershed. Talus slopes receive rainfall and snowmelt water from the bedrock cliffs above, much of which is funneled through couloirs (Fig. 24), which provides the first step of groundwater retention. Groundwater from the talus slopes is transferred to the meadow, and to the moraine complex, within which Bonsai Lake is located. The moraine provides the second step of groundwater retention, before it is release to the

stream. Therefore, the alpine landform complex in the watershed serves a “gate keeper” function of water during dry and cold periods, and sustains baseflow in the headwater stream. This is a common setting in many other mountain ranges in Canada and elsewhere, and alpine landforms consisting of coarse sediments (talus, moraine, rock glacier) are expected to play an important role in temporary storage of glacier melt, snowmelt, and rain.

Building on the conceptual model (Fig. 26) is the development of a numerical groundwater model of the basin by graduate student Jesse He, and a detailed study of the interaction between groundwater and the stream originating from the Bonsai Lake basin by graduate student Benjamin Roeksy. These studies will be completed when the students defend their theses in December 2019.

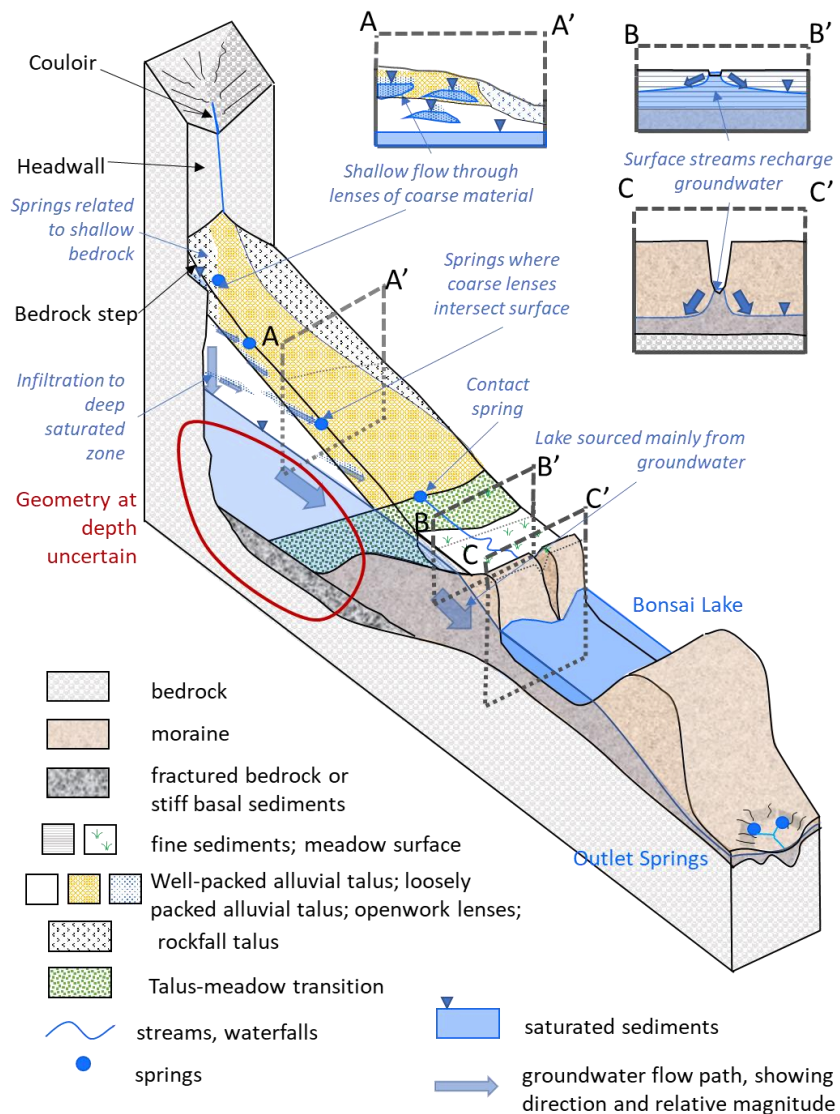


Figure 26. Conceptual model developed by Craig Christiansen of hydrogeological processes in alpine headwater basins.

Task 2: Develop and Improve a Hydrological Model Based on Process Studies

2.1 Cold Regions Hydrological Model (CRHM) setup on Upper Bow River Basin and testing at Fortress Mountain Basin and Marmot Creek

Dr. Pomeroy's research with research officer Xing Fang explored use of a physically based hydrological model for Marmot Creek Research Basin (MCRB) using the Cold Regions Hydrological Modelling platform (CRHM) for climate change research. The model was originally developed several years ago (Pomeroy et al., 2012; Fang et al., 2013) and recently improved to accommodate rain-on-snow flow through snowpacks, subsurface storage and evapotranspiration parameterisations based on research in this project (Pomeroy et al., 2016; Fang and Pomeroy, 2016; Fang et al., 2019). Marmot Creek Research Basin (~9.4 km²) is located in the Front Ranges of the Canadian Rockies (Fig. 27). It is composed of ecozones ranging from montane forests to tundra to alpine exposed rock and includes both large and small clearcuts. The CRHM model includes blowing and intercepted snow redistribution, sublimation, energy-balance snowmelt, slope and canopy effects on melt, Penman-Monteith evapotranspiration, infiltration to frozen and unfrozen soils, hillslope hydrology, streamflow routing and groundwater

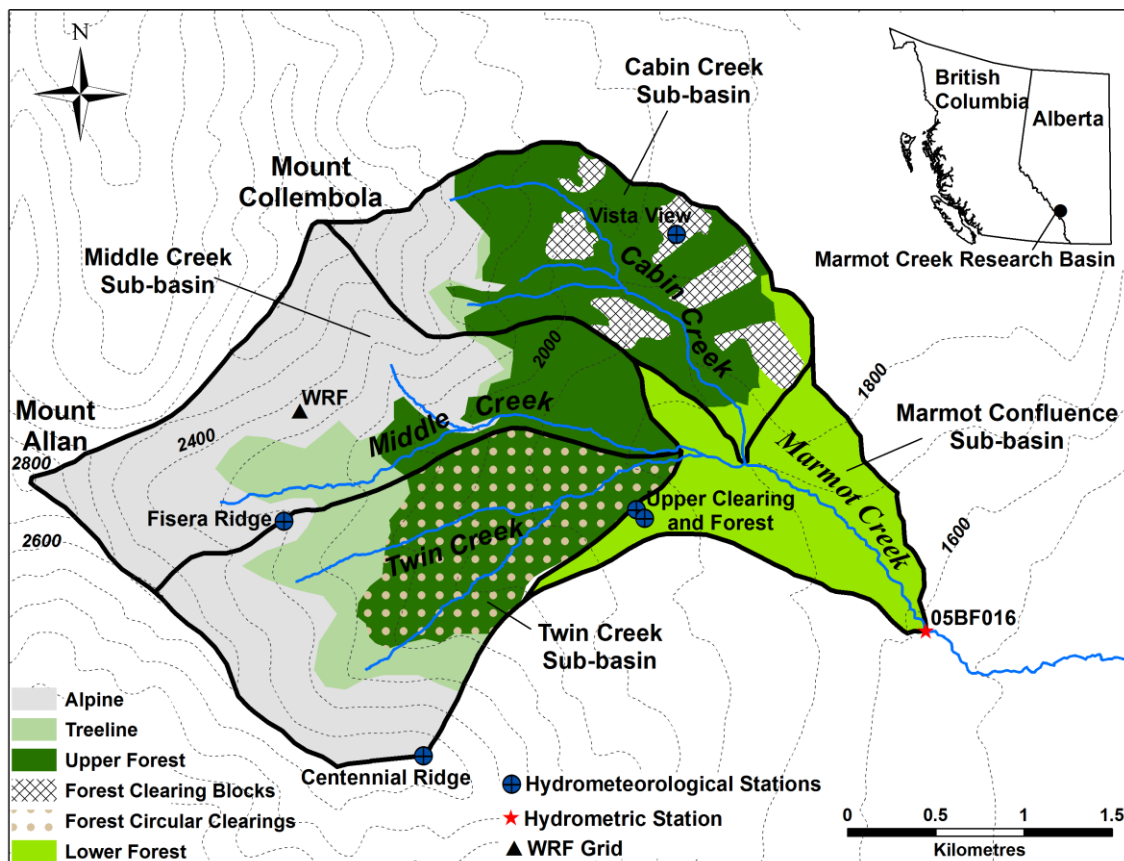


Figure 27. Location and contour map of the Marmot Creek Research Basin (MCRB), showing hydrometeorological stations, hydrometric station, and WRF grid centroid, and ecozones of the MCRB: alpine, treeline, upper forest, forest clearing blocks, forest circular clearings, and lower forest. Note that the size and areas of circular clearings in Twin Creek are not to scale.

components and was parameterised without calibration from streamflow. Near-surface outputs from the 4-km resolution Weather Research and Forecasting (WRF) model, run and bounded by ERA-Interim reanalysis data, were bias corrected using the quantile delta mapping method with respect to meteorological data from meteorological stations located from valley bottom to mountaintop in MCRB during October 2005–September 2013. The bias corrected WRF outputs during the current period (CTRL, 1 October 2005 to 30 September 2013) and future period (PGW, 1 October 2091 to 30 September 2099) were used to drive CRHM model simulations to assess changes in Marmot Creek’s hydrology. Model tests against basin observations showed good representation of both the snowpack regime at several elevations and landcovers (Fig. 28) and good representation of the basin streamflow regime (Fig. 29).

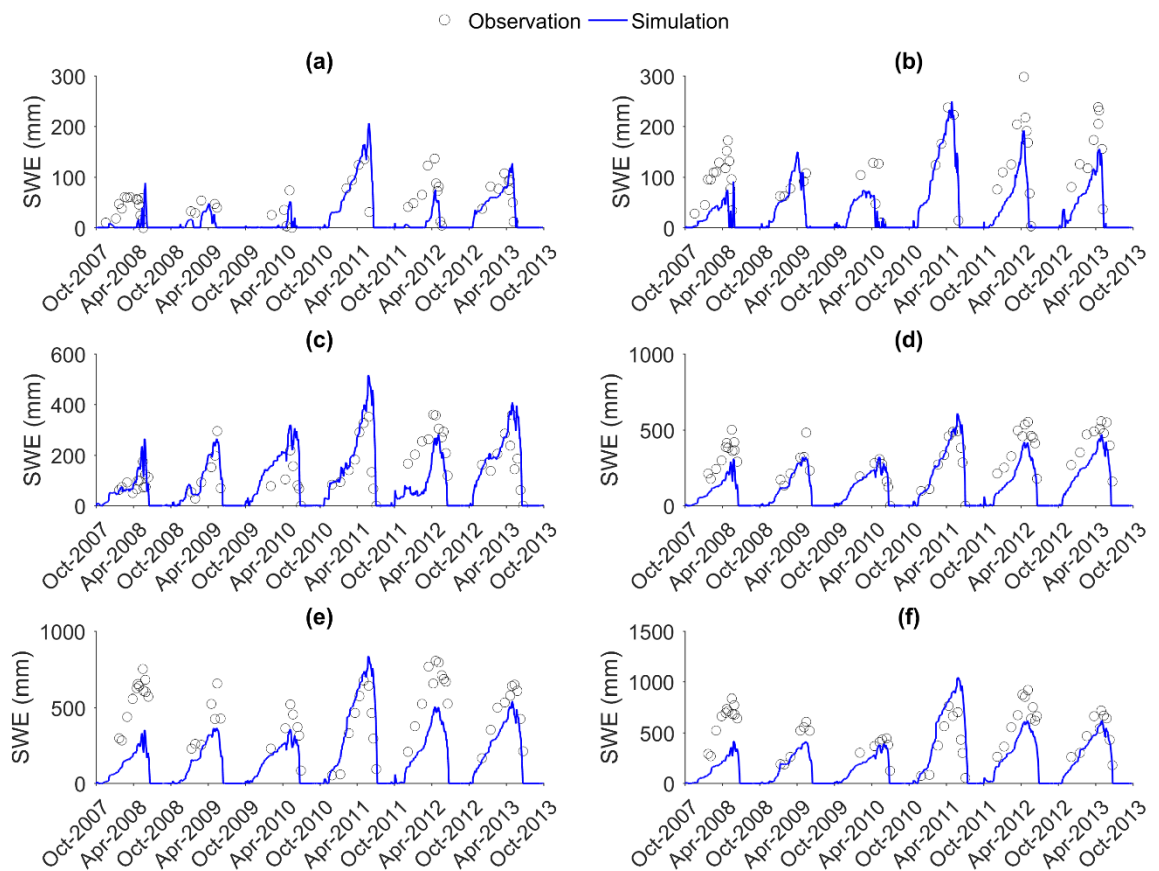


Figure 28. Comparisons of the observed and WRF-CRHM simulated snow accumulation (SWE) for 2007-2013 at the sheltered, mid-elevation Upper Forest/Clearing and the wind-blown, high-elevation Fisera Ridge sites in MCRB. (a) Mature spruce forest, (b) forest clearing, (c) ridge top, (d) upper alpine south-facing slope, (e) lower upper alpine south-facing slope, and (f) larch forest treeline.

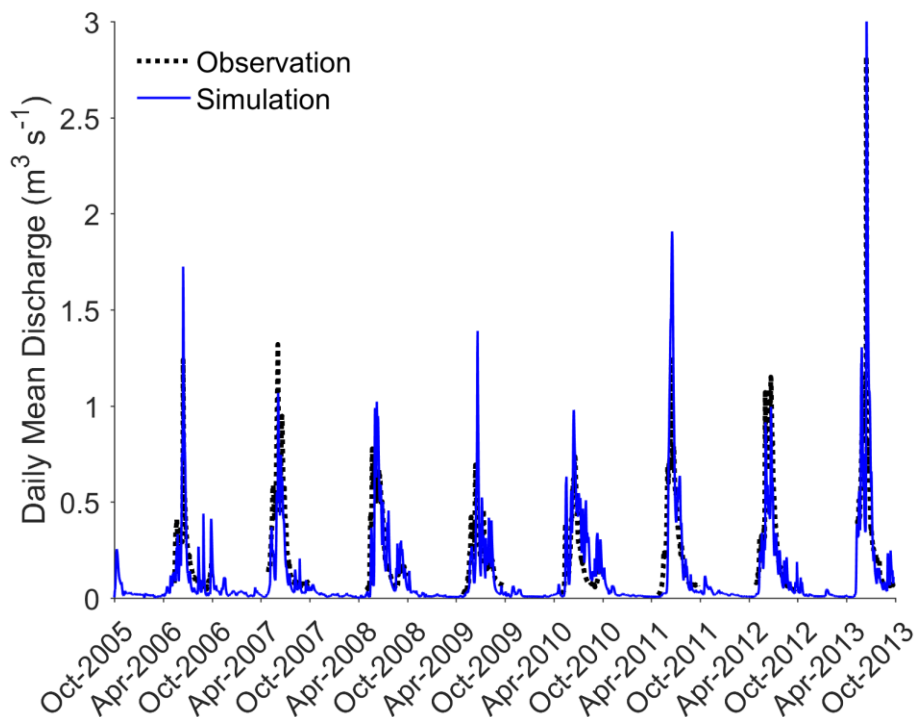


Figure 29. Comparisons of the observed and WRF-CRHM simulated daily streamflow for 2005-2013 for Marmot Creek.

Under a “business as usual” forcing scenario : representative concentration pathway 8.5 (RCP8.5) in PGW, the MCRB warms up on average by 4.7 °C and receives 16% more precipitation over the 21st C, which leads to a 40 mm decline in seasonal peak snowpack, 84 mm decrease in snowmelt volume, and 49 days shorter snowcover duration (Fig. 30). The alpine snow season will be shortened by almost one month, but at lower elevations, there are large decreases in peak snowpack (~50%) as well as a shorter snow season. Losses of peak snowpack will be much greater in clearcuts than under forest canopies. In alpine and treeline ecozones blowing snow transport and sublimation will be suppressed by higher threshold wind speeds for transport, in forest canopies sublimation losses from intercepted snow will decrease due to faster unloaded and drip, and for all ecozones evapotranspiration will increase due to longer snow-free seasons and more rainfall. Runoff will begin earlier in all ecozones, but as result of variability in surface and subsurface hydrology, forested and alpine ecozones generate larger runoff volumes, ranging from 12% to 27%, whereas the treeline ecozone has a small (3%) decrease in runoff volume due to decreased melt volumes from smaller snowdrifts (Fig. 31). The shift in timing in streamflow is notable, with higher flows in spring months and lower flows in late summer and higher flows in fall (Fig. 32). Overall, Marmot Creek basin annual streamflow discharge will increase by 18% with PGW, but its streamflow generation efficiency will not change despite the basin shifting towards a rainfall-dominated runoff generation.

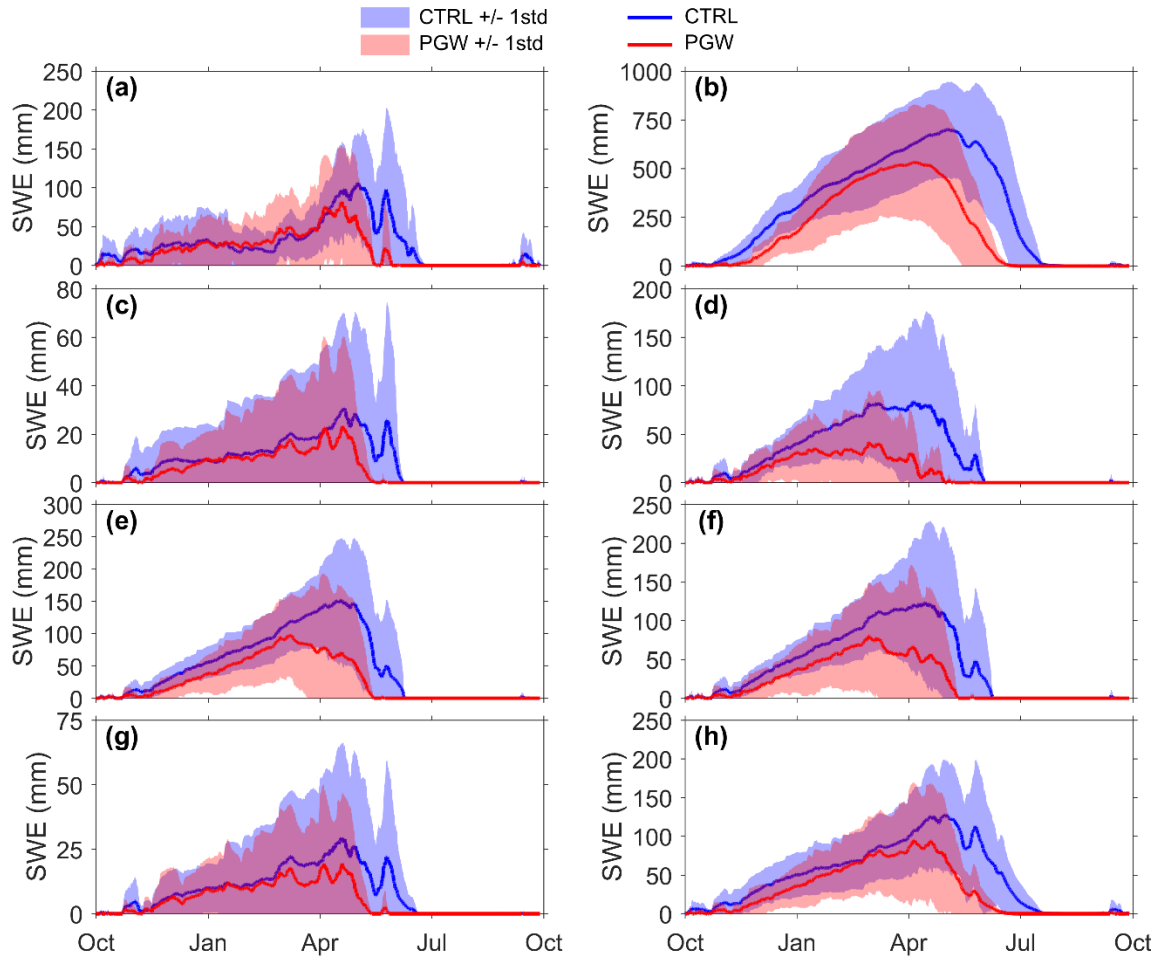


Figure 30. Simulated annual mean snow accumulation (SWE) for WRF CTRL and PGW. (a) Alpine, (b) treeline, (c) upper forest, (d) forest clearing blocks, (e) forest circular clearing north-facing, (f) forest circular clearing south-facing, (g) lower forest ecozones, and (h) Marmot Creek basin. Line represents the annual mean and the shadow represents the standard deviation of the eight-water year SWE.

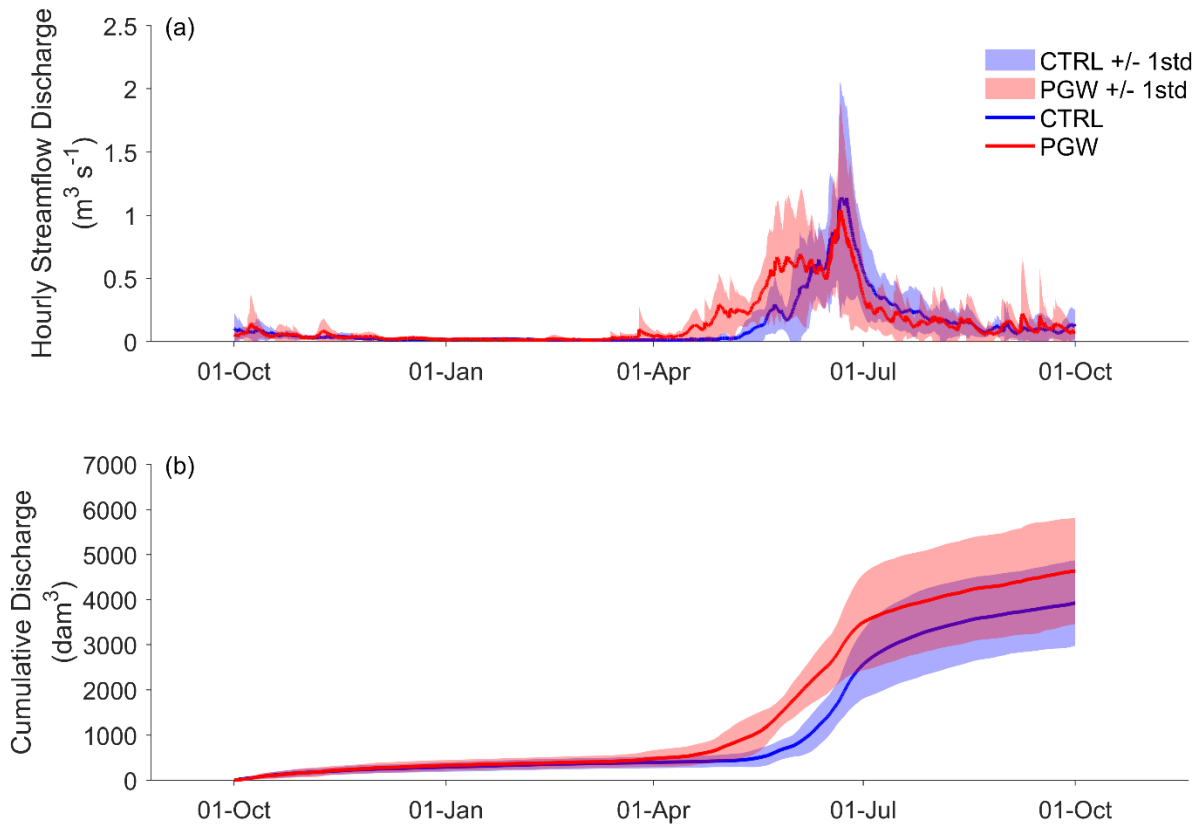


Figure 31. Simulated annual mean (a) Marmot Creek hourly streamflow discharge and (b) cumulative discharge for WRF CTRL and PGW. Line represents the annual mean and the shadow represents the standard deviation of the eight-water year streamflow discharge.

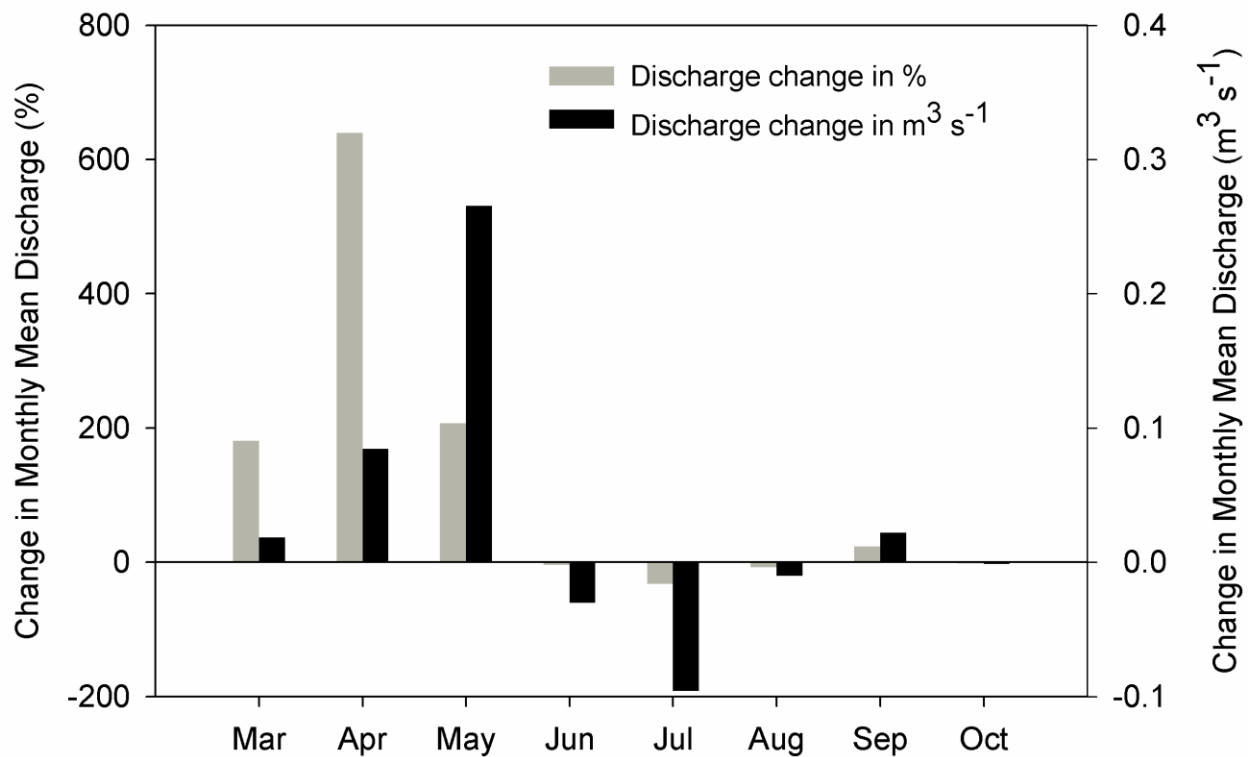


Figure 32. Change in monthly mean discharge due to pseudo global warming simulation of RCP8.5 for Marmot Creek Research Basin.

2.2 Hydrological model of Fortress Mountain Basin

Dr. Pomeroy's investigation supported by research associate Xing Fang was to evaluate two sources of meteorological forcing for simulating snowpack and streamflow in the headwater basins of Canadian Rocky Mountains: intensively observed station data, and the 2.5-km Global Environmental Multiscale (GEM) output available as a forecast product from Environment and Climate Change Canada. The purpose was to answer the question: can numerical weather prediction model outputs be a viable alternative for forcing hydrological process models in mountain basins? Snowpack simulations using GEM 2.5km output had some success for evergreen forests, but were poor for alpine ridges, likely due to GEM misrepresentation of local winds and seasonal precipitation. Streamflow was better simulated using station data than with GEM output, which missed the timing and magnitude of seasonal flow (Fig. 33). The poor streamflow simulation using GEM output is attributed to underestimation of late-lying snowpacks in the alpine drift area due to an inability to simulate snow transport. 2015 was an exceptional drought year and so may not be representative of a longer period, but it is clear that GEM 2.5 km data requires bias correcting before it can be used to drive hydrological models in the region.

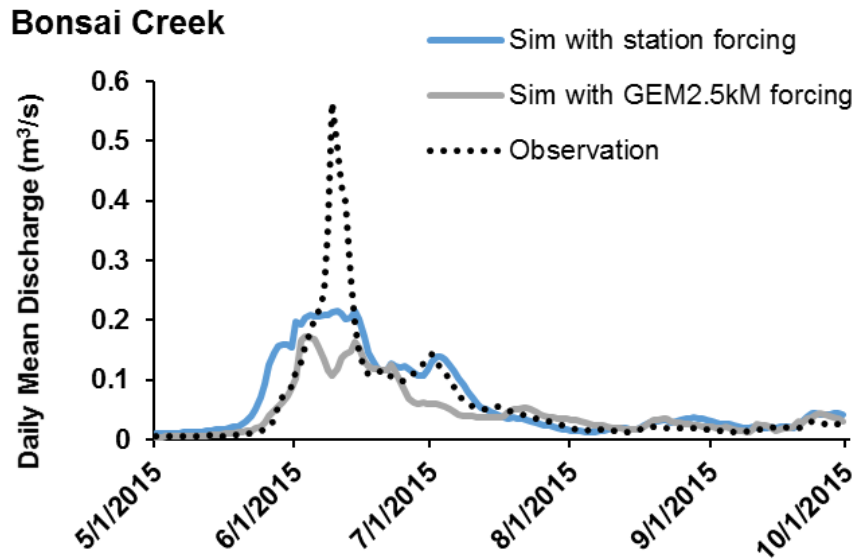


Figure 33. Simulations of Bonsai Creek in Fortress Mountain area, with a CRHM model driven by station data and driven by GEM atmospheric model data.

Dr. Helgason and Pomeroy's graduate student Hailey Robichaud found that snowpacks in the Canadian Rockies provide large amounts of freshwater for downstream environmental and socio-economic demands. Modifications to the snowpack storage can have severe implications for these uses. Mountain streamflow and snow accumulation and ablation have been studied in Europe and in the Canadian Rockies; however there is a lack of understanding of how hydrological processes in the complex terrain of high alpine catchments in the Canadian Rockies will respond to climatic changes. Helen Creek Research Basin is a small, high elevation alpine basin (~2.5 km², 2600 m mean elevation) in the Canadian Rockies with complex terrain, a relict rock glacier and an alpine lake. The Cold Regions Hydrological Modelling platform was used to create an alpine hydrological model to simulate the dominant hydrological processes of this basin, in order to understand the recent hydrological regime. The model was constructed and parameterized based on the current understanding of alpine hydrology, field research in the basin, and studies in the surrounding regions. Observations taken during a 2-year control period were used to evaluate model predictions of snow accumulation, ablation and streamflow. The model adequately simulated snowpacks and streamflow, and provided a diagnosis of the processes controlling these regimes. The results help to understand the hydrology of alpine basins in the Canadian Rockies.

2.3 Evapotranspiration modelling in mountain terrain

Large-scale wind fluxes influencing evapotranspiration in complex mountainous terrain

Dr. Pomeroy and Dr. Petrone's PhD student Mina Rohanzadegan focused on modeling using primary using the WRF model. Simulations were performed using WRF (Weather Research and Forecasting) model at high resolution (90 m horizontal, and 20 m vertical) and were evaluated against data collected at various locations in Kananaskis valley located in Rocky mountains of

Canada. The measurements were made using atmospheric sounding by Kite-sonde, SODAR, and several automatic micrometeorological stations located in both high altitude ridge tops and valley bottoms, providing regular measurements of the main atmospheric variables, such as air temperature, humidity, atmospheric pressure, solar irradiance, wind speed and direction.

The simulations were first generated for a lower resolution setting at 180 m with a PBL scheme (YSU) to provide comparisons with higher resolution LES for July 19, 2016. The LES simulations were then performed at two different sets; one with general smoothing and the other with the use of a local filtering technique (selective smoothing of terrain at angles only above 45 degree) to alleviate the problems (model instability/contamination by unrealistic flow) arising from steep terrain in terrain following coordinate of WRF (Fig. 34).

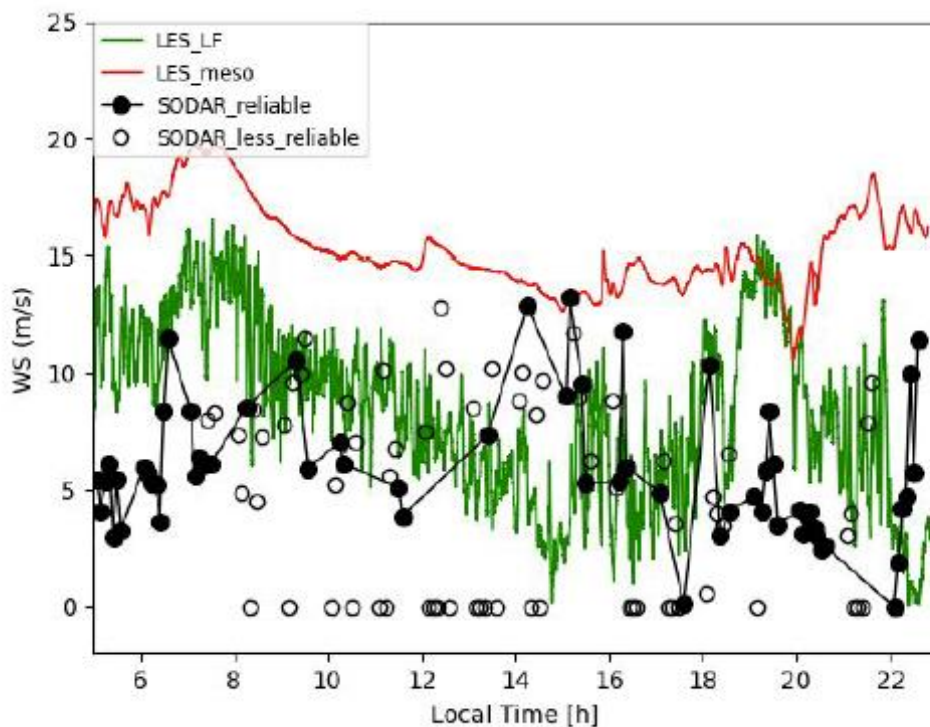


Figure 34. Figure showing wind speed for LES_LF at 90 m resolution and LES_meso at 900 m resolution versus SODAR reliable data profiles reached 300 m AGL versus SODAR less reliable (data profiles reached less than 300 m AGL).

2.4 CRHM Glacier development and testing

Dr. Pomeroy's graduate students Caroline Aubry-Wake and Dhiraj Pradhananga found that in glacierized alpine catchments, glaciers are typically conceptualized as acting to buffer inter-annual hydrological variability by accumulating snow during wet/cool years, and releasing more meltwater in dry/warm years. This glacier compensation effect is considered particularly important in late summer, when other sources of runoff are low. However, glacier meltwater does not always augment streamflow during low flow years. It can also accentuate high flow

years, with no clear relationship with either increased winter accumulation or warmer summer temperatures. This is coincident with recent research showing that during cold years, glacier meltwater can be significantly reduced and cause “glacier melt drought”. Both these results hints at the complex interactions between winter snow accumulation, seasonal meteorology and glacier melt to generate streamflow, and ultimately, provide a hydrological buffering effect in years with extreme conditions. To understand how glacier hydrology might change in future climates and glacial configurations, it is important to understand the drivers of glacier meltwater generation, and the processes governing this “glacier buffering” effect. Here, the influence of snow accumulation and seasonal weather on glacier mass balance and streamflow generation were examined through a combination of distributed, physically based glacier hydrology modelling and intensive field observations. The examination focusses on recent hydrological extremes of flood and drought experienced in the Canadian Rockies over 2013-2017. During this period, strong positive and negative anomalies in snowpack accumulation, and summer precipitation and air temperature occurred resulting in record peak streamflow and record negative glacier mass balances. The research site is the glacierized catchment of Peyto Glacier Research Basin. Peyto Glacier, an outlet glacier of the Wapta Icefield in Banff National Park, Alberta, Canada ranges between 2100-3190 m a.s.l. and has an area of 5.3 km². The distributed, physically based Cold Region Hydrological Modelling Platform, including a newly developed glacier-hydrology module, was used to simulate snow accumulation and redistribution processes, glacier melt and mass balance and streamflow generation. CRHM includes an energy balance representation of glacier and snowmelt, snow redistribution by blowing snow and avalanching. It also includes glacier mass balance and dynamics and surface cover change to include the expansion of a pro-glacial lake and debris-covered area. Preliminary model results indicate an increase in runoff between historical values and recent years at the PGRB. This increasing trend suggest the glacier is still able to provide a significant contribution to streamflow and buffer low water years. However, the melt patterns are changing; snowmelt peak is now a month earlier than historical values and glacier melt extends further into the fall. For the 2013-2017 period,

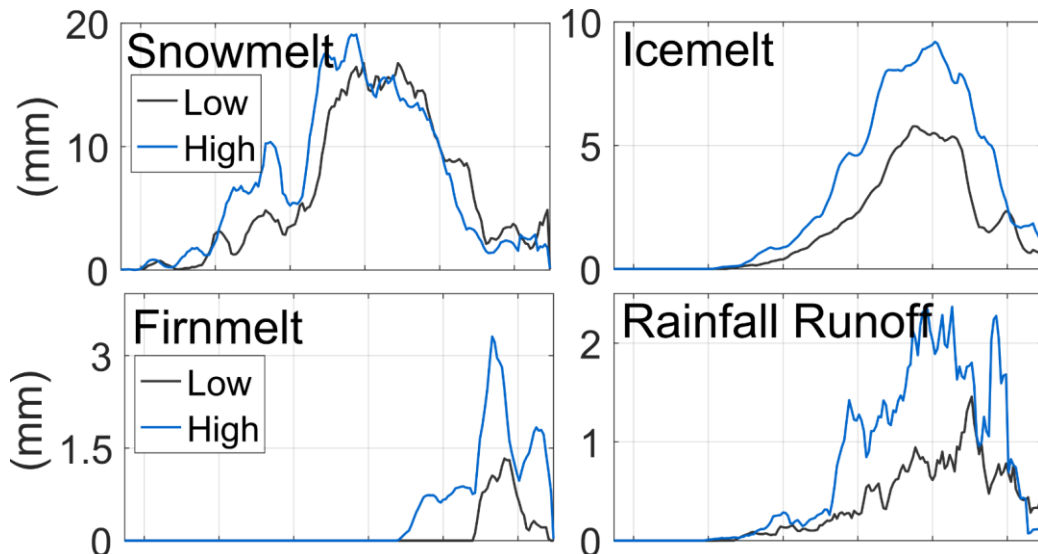


Figure 35. Contributions of runoff from snowmelt, icemelt, firnmelt and rainfall-runoff for high and low streamflow years in Peyto Glacier Research Basin.

there is a strong variation in the timing of the beginning and end of melt, as well as the in transition from snow to ice dominated streamflow. These changes are linked to increase in temperatures, with summer temperature and fall consistently up to 4 °C warmer than historical values. However, this increased fall melt is somewhat balance with colder spring temperatures, which results in spring precipitation to accumulate as snow on the glacier. Simulations are showing that high flow years have 34% more annual streamflow than low flow years, the source of extra streamflow in high flow years is from: + 13% snowmelt, + 80% icemelt, + 280% firn melt, + 106% rainfall runoff and visible changes in transition season, with earlier spring melt and increased fall rainfall-runoff (Fig. 35)

2.5 Canadian Hydrological Model (CHM) development

Dr. Pomeroy's graduate student Chris Marsh found that despite debate in the rainfall-runoff hydrology literature about the merits of physics-based and spatially distributed models, substantial work in cold regions hydrology has shown improved predictive capacity by including physics-based process representations, relatively high-resolution semi- and fully-distributed discretizations, and use of physically identifiable parameters with limited calibration (Fig. 36). While there is increasing motivation for modelling at hyper-resolution (< 1 km) and snow-drift resolving scales (~1 m to 100 m), the capabilities of existing cold-region hydrological models are computationally limited at these scales. The Canadian Hydrological Model (CHM) was designed to be applied generally, but it has a focus for application where cold-region processes play a role

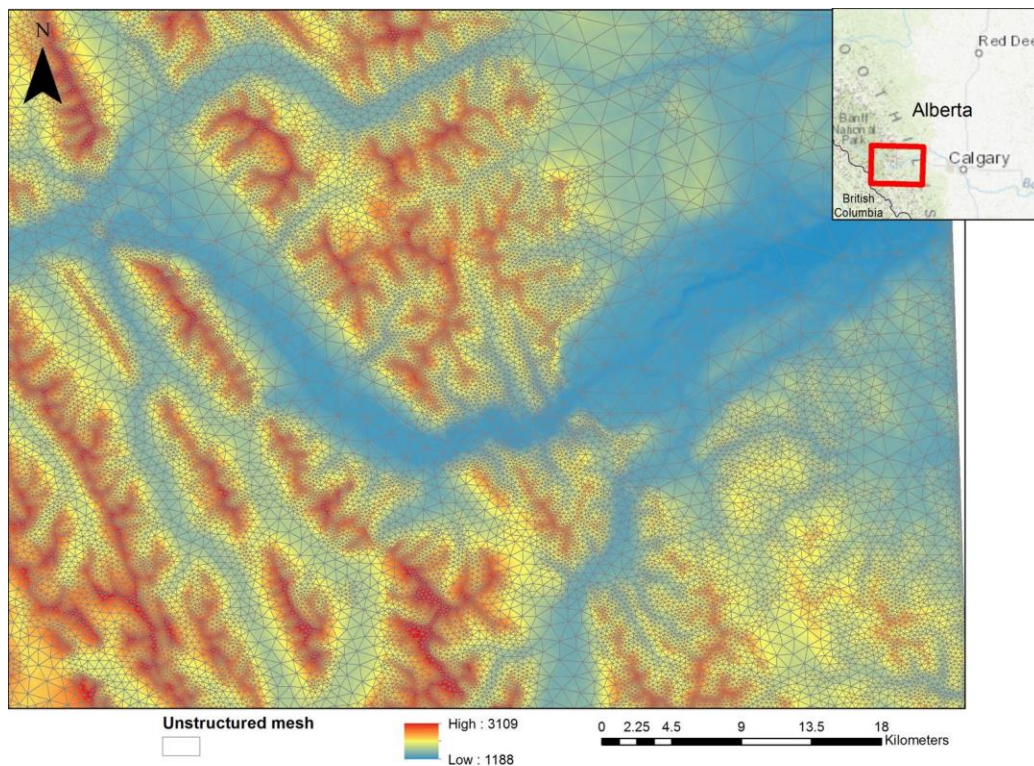


Figure 36: Example of variable resolution triangulation mesh as produced by Mesher for a region west of Calgary in the Canadian Rocky Mountains. The triangular edges are shown as grey lines overlain on the original DEM.

in hydrology. Key features include the ability to capture spatial heterogeneity in the surface discretization in an efficient manner; to include multiple process representations; to be able to change, remove, and decouple hydrological process algorithms; to work both at a point and spatially distributed; the ability to scale to multiple spatial extents and scale; and to utilize a variety of forcing fields (boundary and initial conditions). CHM has been deployed with a full snow model including avalanching to provide spatially detailed snowpack forecasts for the Canadian Rockies west of Calgary. It is driven by the GEM atmospheric model to provide 2 day and 6 day forecasts which can be publically accessed here www.snowcast.ca . Future modelling in the region will focus on deploying CHM.

Task 3: Assemble Basin and Past/Future Climate Information for Modelling

Modelling Approach and Results

3.1 Modelling Objectives

The objective of the modelling components of this study are to determine how forest cover controls streamflow generation in the Bow River and Elbow River basins. It assesses whether forest management, including soil compaction control, can be used as tool to promote water resource enhancement and evaluates impact on floods. More specifically, the objectives are to:

- 1) Evaluate the impacts of forest harvesting and other forest disturbances on drainage basin hydrology in Bow River and Elbow River basins above Calgary.
- 2) Examine the potential hydrological impact of current forest and soil disturbances on hydrology including floods and droughts for Bow River and Elbow River basins above Calgary.
- 3) Set up hydrological model for Bow River and Elbow River basins above Calgary using Cold Regions Hydrological Modelling platform (CRHM) to predict basin streamflow. The hydrological model will have forest disturbance scenarios applied to it to assess impacts of these scenarios on basin streamflow.

CRHM background

The Cold Regions Hydrological Modelling platform (CRHM) was used to set up a hydrological model for Bow River and Elbow River basins above Calgary. CRHM is an object-oriented, modular and flexible platform for assembling physically based hydrological models. With CRHM, the user constructs a purpose-built model from a selection of possible basin spatial configurations, spatial resolutions and physical process modules of varying degrees of physical complexity. Basin discretization is performed via dynamic networks of hydrological response units (HRUs) whose number and nature are selected based on the variability of basin attributes and the level of physical complexity chosen for the model. The user in light of hydrological understanding, parameter availability, basin complexity, meteorological data availability and the objective flux or state for prediction selects physical complexity. Pomeroy et al. (2007) provide a full description of CRHM.

CRHM offers a full suite of streamflow generation processes for Canadian Rockies and foothills (i.e. wind redistribution of alpine snow, snow avalanching on steep alpine slopes, snow interception, sublimation, drip and unloading from forest canopies, infiltration to frozen and unfrozen soils, overland and detention flow, hillslope sub-surface water redistribution, and evapotranspiration from forests, clearings and alpine tundra). Physically based algorithms in CRHM have been developed from field studies in the boreal forest and Canadian Rockies (Pomeroy et al., 2009; Ellis et al., 2010; MacDonald et al., 2010; Harder and Pomeroy, 2013; DeBeer and Pomeroy, 2017) and have been extensively evaluated in mountain headwater basins (Fang et al., 2013; Pomeroy et al., 2013; Pomeroy et al., 2016; Rasouli et al., 2019). CRHM was evaluated in the recent Earth System Models Snow Model Intercomparison Project (ESM-SnowMIP) and performed relatively well in modelling snowmelt at forest and alpine sites in Canada, France, USA, Japan, Finland and Switzerland (Krinner et al., 2018). In addition, CRHM was used in snow accumulation, snowmelt, and streamflow prediction and climate change impact studies in the mountains of Spain (López-Moreno et al., 2013), western China (Zhou et al., 2014), Germany (Weber et al., 2016), USA (Rasouli et al., 2019) and Chile (Krogh et al., 2015).

3.2 CRHM setup and parameterization

Model domain delineation

GIS terrain preprocessing analysis was conducted to delineate model basins for the Bow and Elbow river drainage basins above Calgary using a resampled 20 m Canadian digital elevation model (cdem). Three model domains were generated for simulating basin streamflow for Bow River and Elbow River basins above Calgary. For the Bow River above Calgary, the total basin area delineated for modelling is approximately 7,823.6 km² at the Environment and Climate Change Canada's (ECCC) Water Survey of Canada streamflow gauge (05BH004), and two model domains: Upper Bow River at Banff and Upper Bow River between Banff and Calgary were created (Fig. 37). Upper Bow River at Banff model domain has approximate 2,192.2 km² for total basin area at the ECCC Water Survey of Canada streamflow gauge (05BB001), while the Upper Bow River between Banff and Calgary domain has about 5,631.4 km² total basin area. For the Elbow River at Calgary model domain, the total area is about 1,191.9 km² at the ECCC Water Survey of Canada streamflow gauge (05BJ010). In addition, sub-basins were delineated and aggregated corresponding to their stream segments during the stream segmentation process in GIS terrain preprocessing analysis. There are 50, 92, and 25 sub-basins for Upper Bow River at Banff, Upper Bow River between Banff and Calgary, and Elbow River at Calgary model domains, respectively. A sub-basin map for Bow River and Elbow River basins above Calgary is shown in Appendix 1.

HRU determination

Elevation, aspect, slope, and land cover GIS layers were used and intersected in ArcGIS to determine hydrological response units or HRU. Elevation, aspect, and slope were extracted from the 20 m cdem and are shown in Figures 38 to 39. Land cover was obtained from open access Alberta Biodiversity Monitoring Institute (ABMI) land cover polygon circa 2000, and available pine forest coverage from Alberta forest species (AVIE) inventory for the Upper Bow River between Banff and Calgary and the Elbow River at Calgary model domains was used to separate pine and spruce forest for these domains (Fig. 40). In addition, the water course in Alberta drainage

network inventory was used to determine river channel valley HRU. Flowcharts of HRU determination are shown in Appendix 2.

As there are higher glacier and alpine rock coverages in the Upper Bow River at Banff domain, more details were considered for HRU determination (Figure A2). For glacier HRU, seven elevation bands, aspects of north-facing, south-facing, and east-facing, and slope gradients of gentle slope, medium slope, and steep slope were taken into consideration. For rock HRU, upper and lower elevation, aspects of north-facing, south-facing, and east-facing, and slope gradients of gentle slope, medium slope, and steep slope were taken into consideration. For alpine tundra, alpine sparse forest, and valley shrubland HRUs, slope/aspects of north-facing, south-facing, and east-facing were considered. For all forests, open water, river valley, developed and exposed HRUs, elevation, aspect, and slope were not used in determining these HRUs. While for the Upper Bow River between Banff and Calgary and Elbow River at Calgary model domains, fewer criteria were considered for HRU determination. For glacier, rock, and alpine tundra HRUs, slope/aspects of north-facing, south-facing, and east-facing were taken into consideration. For the rest of HRUs, elevation, aspect, and slope were not considered. In total, there are 1,512, 1,068, and 257 HRUs for Upper Bow River at Banff, Upper Bow River between Banff and Calgary, and Elbow River at Calgary model domains, respectively.

There are four types of sub-basins: glacier mountain basin, non-glacier mountain basin, foothill plain basin, and agriculture basin. A glacier mountain basin is a sub-basin with at least glacier and rock HRUs in addition to other HRUs; a non-glacier mountain basin is a sub-basin with rock HRU but without glacier HRU in addition to other HRUs. A foothill plain basin is a sub-basin that has forest HRUs but does not have glacier, rock and cropland HRUs. An agriculture basin is a sub-basin that has cropland HRUs but without glacier and rock HRUs. These diverse sub-basin types are similar to those sub-basins based on “ecoregion types” in the previous CRHM modelling for Smoky River Basin (52,000 km²) (Pomeroy et al., 2013). The sub-basin name, sub-basin type, sub-basin HRU numbers, and sub-basin area for Bow River and Elbow River basins above Calgary are provided in Appendix 3.

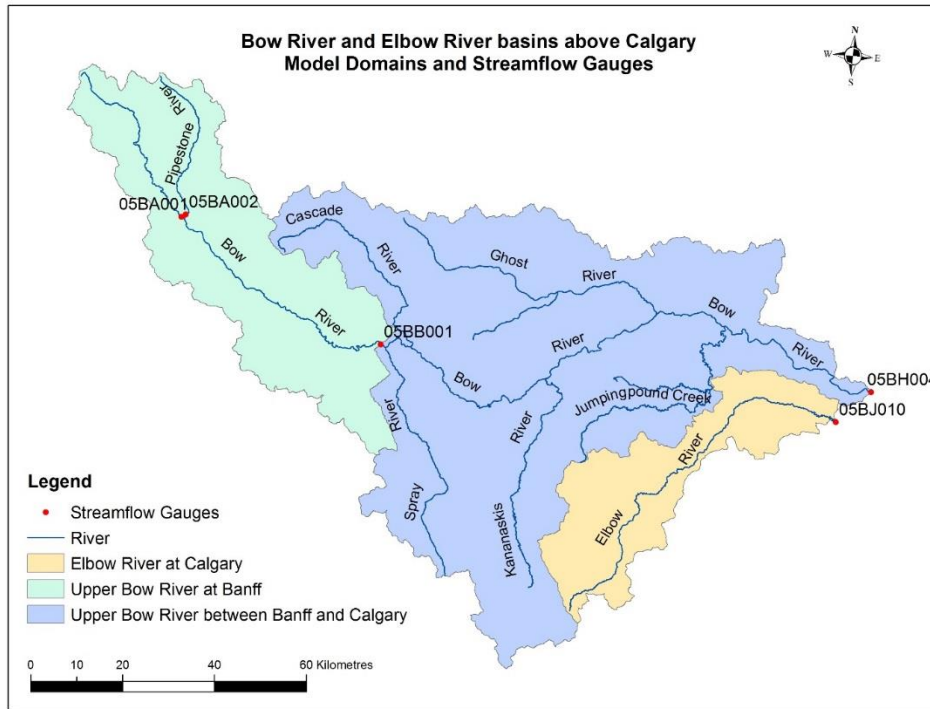


Figure 37. Bow River and Elbow River basins above Calgary model domains and streamflow gauges.

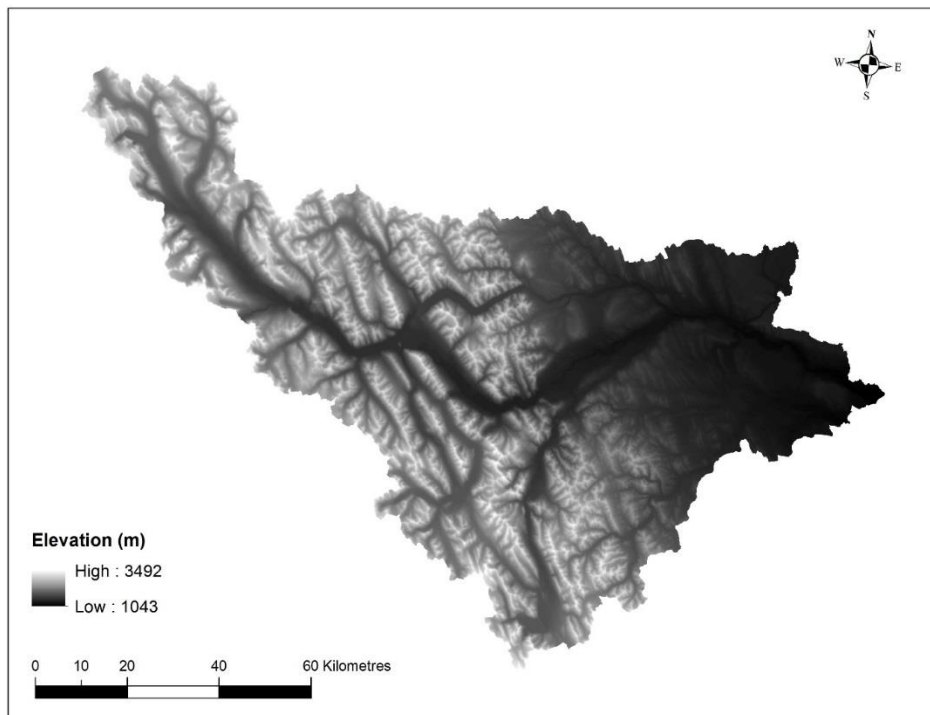


Figure 38. Resampled 20 m Canadian digital elevation model (cdem) for Bow River and Elbow River basins above Calgary.

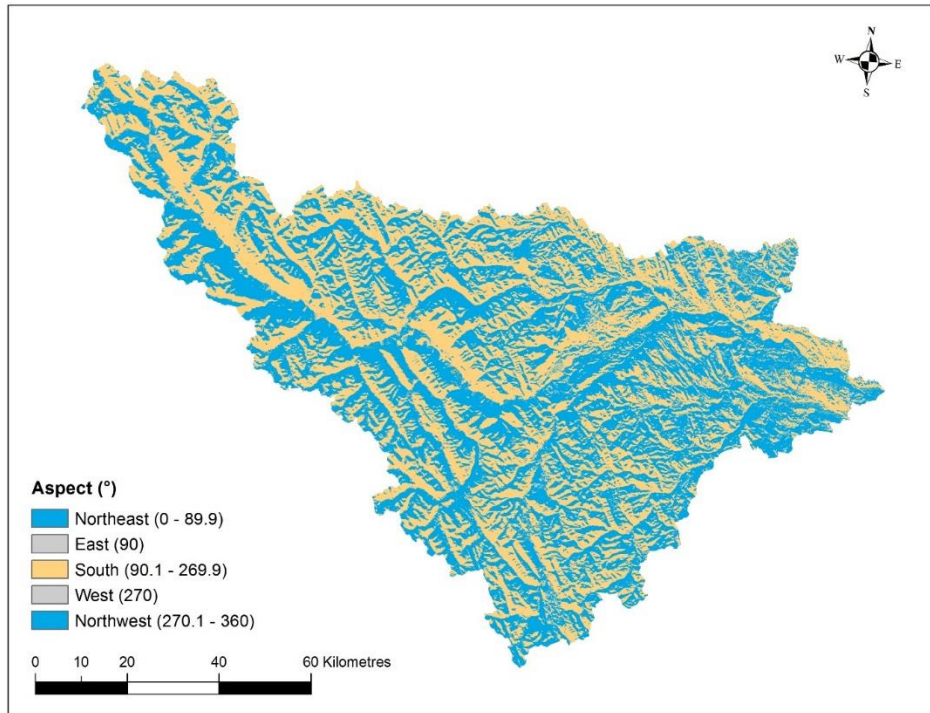


Figure 39. Aspect of slopes for Bow River and Elbow River basins above Calgary, derived from the 20 m cdem.

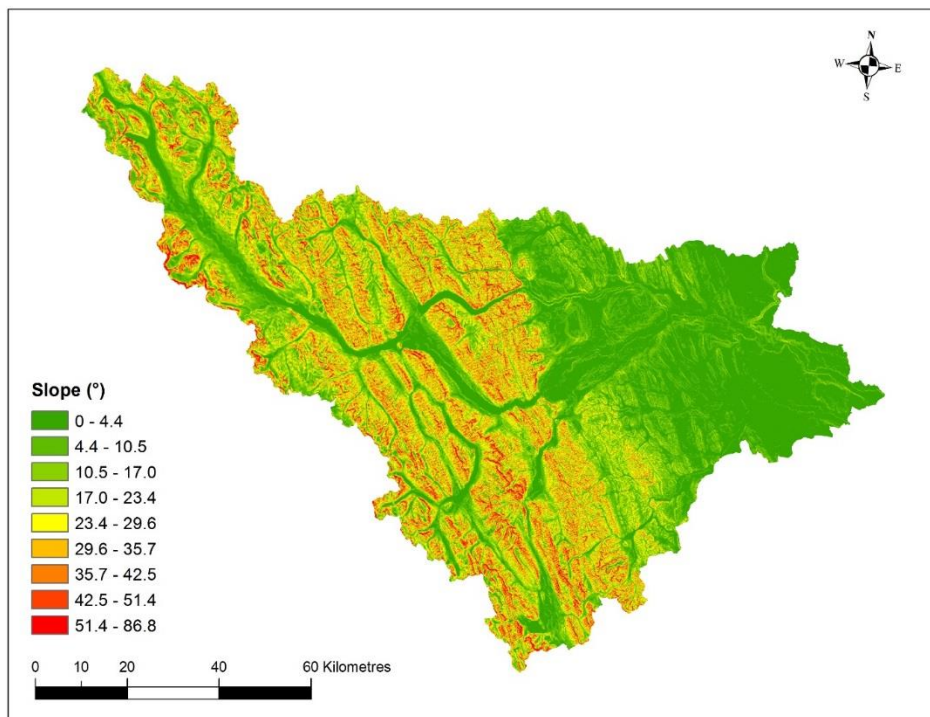


Figure 40. Slope angle for Bow River and Elbow River basins above Calgary, derived from the 20 m cdem.

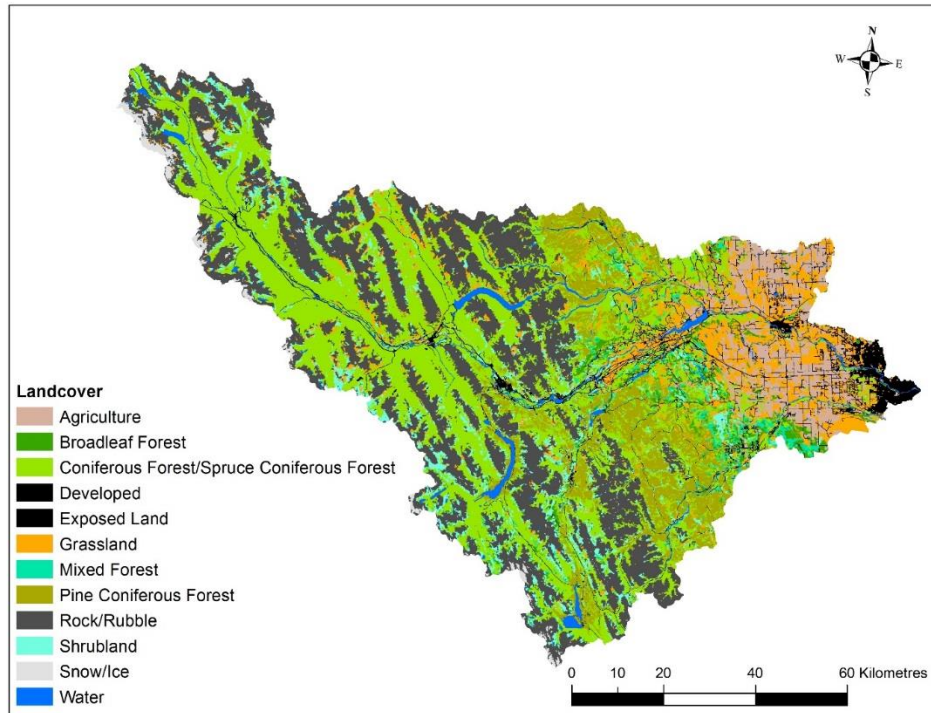


Figure 41. Land cover for Bow River and Elbow River basins above Calgary, derived from the ABMI land cover polygon with update for pine forest from AVIE inventory.

Module structure

A set of physically based modules was constructed in a sequential manner to simulate the dominant hydrological processes for Bow River and Elbow River basins above Calgary. Figure 6 shows the schematic setup of these modules, which include:

- 1). Observation module: reads the meteorological data (temperature, wind speed, relative humidity, vapour pressure, precipitation, and radiation), adjusting temperature with environmental lapse rate and precipitation with elevation and wind-induced undercatch, and providing these inputs to other modules.
- 2). Solar radiation module (Garnier and Ohmura, 1970): calculates the theoretical global radiation, direct and diffuse solar radiation, as well as maximum sunshine hours based on latitude, elevation, ground slope, and azimuth, providing radiation inputs to the sunshine hour module, the energy-balance snowmelt module, and the summer net radiation module.
- 3). Sunshine hour module: estimates sunshine hours from shortwave irradiance to a level surface and maximum sunshine hours, generating inputs to the energy-balance snowmelt module and the summer net radiation module.
- 4). Slope radiation module: estimates shortwave irradiance to a slope using measurement of shortwave irradiance on a level surface. The measured shortwave irradiance from the observation module and the calculated direct and diffuse shortwave irradiance from the radiation module are used to calculate the ratio for adjusting the shortwave irradiance on the slope.

- 5). Longwave radiation module (Sicart et al., 2006): estimates longwave irradiance using measured or estimated shortwave irradiance. This is input to the energy-balance snowmelt module.
- 6). Albedo module (Verseghy, 1991): estimates snow albedo throughout the winter and into the melt period and also indicates the beginning of melt for the energy-balance snowmelt module.
- 7). Canopy module (Ellis et al., 2010): estimates the snowfall and rainfall intercepted by the forest canopy and updates the sub-canopy snowfall and rainfall and calculates shortwave and longwave sub-canopy irradiance. This module has options for open environment (no canopy adjustment of snow mass and energy), small forest clearing environment (adjustment of snow mass and energy based on diameter of clearing and surrounding forest height), and forest environment (adjustment of snow mass and energy from forest canopy).
- 8). Blowing snow module (Pomeroy and Li, 2000): simulates the inter-HRU wind redistribution of snow transport and blowing snow sublimation losses throughout the winter period.
- 9). Energy-balance snowmelt module (Marks et al., 1998): this is a version of the SNOBAL model developed to simulate the mass and energy balance of deep mountain snowpacks. This module estimates snowmelt and flow through snow by calculating the energy balance of radiation, sensible heat, latent heat, ground heat, advection from rainfall, and the change in internal energy for snowpack layers consisting of a top active layer and layer underneath it.
- 10). Gravitational snow transport module (Bernhardt and Schulz, 2010): simulates the inter-HRU snow transport by gravity along steep slope, and this is topographic driven distribution of snow.
- 11). Glacier module: estimates icemelt from glacier ice, firmelt from firn layers and snowmelt from snowpack above glacier or firn layers based on energy-balance model, then movement of icemelt, firmelt and snowmelt through glacier ice, firn and snowpack are handled by a simple lag and route method.
- 12). Summer net radiation module (Granger and Gray, 1990): calculates the net all-wave radiation from short-wave radiation for input to the evaporation module for snow-free conditions.
- 13). Infiltration module: Gray's parametric snowmelt infiltration algorithm (Zhao and Gray, 1999) estimates snowmelt infiltration into frozen soils; Ayers' infiltration (Ayers, 1959) estimates rainfall infiltration into unfrozen soils based on soil texture and ground cover. Both infiltration algorithms link moisture content to the soil column in the hillslope module. Surface runoff forms when snowmelt or rainfall exceeds the infiltration rate.
- 14). Fall soil moisture module: this is a module to set the fall soil moisture status for running the multiple-year simulation. The amount of soil moisture and the maximum soil moisture storage in the soil column are used to estimate the fall soil moisture status, which provides the initial fall soil saturation for the infiltration module.
- 15). Evaporation module: Penman-Monteith (P-M) evapotranspiration algorithm (Monteith, 1965) with a Jarvis-style resistance formulation (Verseghy, 1991) estimates actual evapotranspiration from unsaturated surfaces. The P-M method includes stomatal and aerodynamic resistances which control water vapour transfer to the atmosphere, representing the diffusion path lengths through vegetation and the boundary layer, respectively. Stomatal resistance varies with the biophysical properties of vegetation (i.e. leaf area index, plant height, rooting zone) and is affected by four environmental stress factors: light limitation, vapour pressure deficit, soil moisture tension or air entry pressure, and air temperature. Priestley and

Taylor evaporation expression (Priestley and Taylor, 1972) estimates evaporation from saturated surfaces such as wetland, open water, and river channel valley. Both evaporation algorithms modify moisture content in the interception store, ponded surface water store and soil column and are restricted by water availability to ensure continuity of mass, and the Priestley and Taylor evaporation also updates moisture content in the wetland, open water, and river channel.

16). Hillslope soil module: this recently developed module is for calculating sub-surface flow and simulating groundwater-surface water interactions using physically-based parameters and principles on hillslopes. This module was revised from an original soil moisture balance routine developed by Leavesley et al. (1983) and modified by Dornes et al. (2008) and Fang et al. (2010) and now calculates the soil moisture balance, groundwater storage, subsurface and groundwater discharge, depressional storage, and runoff for control volumes of two soil layers, a groundwater layer and surface depressions as well as a near-surface detention layer. The detention layer is a new interface between the soil and atmospheric processes and allows the surface runoff to flow through a porous medium as a transient flow pathway (Pomeroy et al., 2016). It was incorporated to address temporary snow damming (Fang et al., 2013) and water storage in loose organic material in the alpine tundra (Beke, 1969) and forest floor (Keith et al., 2010). In addition, thawing and freezing fronts are allowed in two soils layers, in which moisture movement is restricted where portion of soil has freezing front presented and is free where portion of soil has thawing front presented. A conceptual representation of this module is shown in Figure 42.

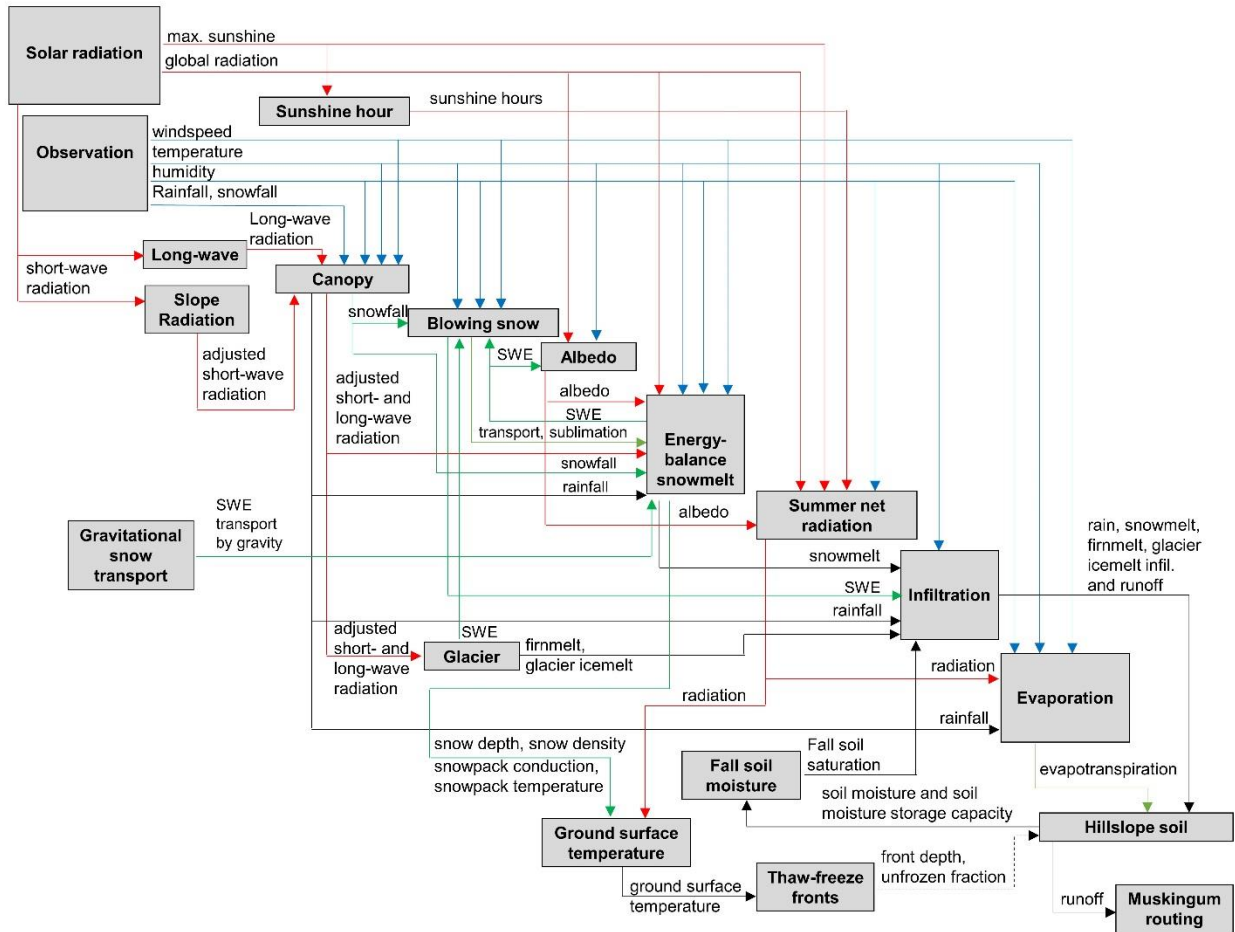


Figure 42. Module structure of physically based hydrological model for Bow River and Elbow River basins above Calgary showing process and data modules and flow of variables dealing with radiation (red line), meteorology (blue line), evaporation, sublimation and snow (green line) and soil moisture content, ground surface temperature and water (black line).

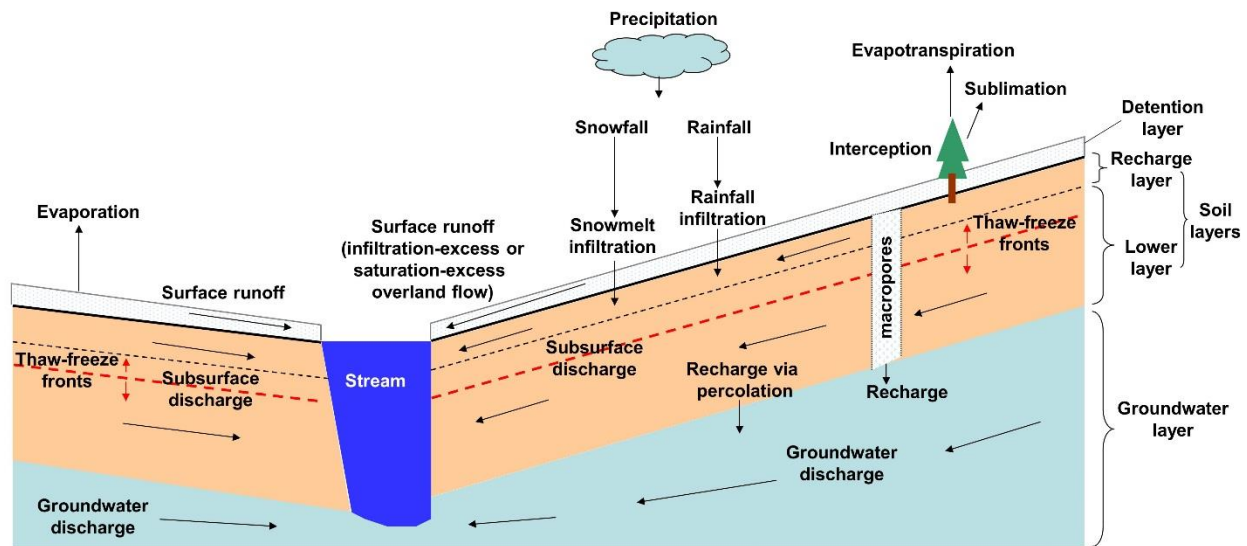


Figure 43. Conceptual representation of hillslope soil module with control volumes for detention layer, two soil layers, a groundwater layer and surface depressions or macropores, with thaw-freeze fronts enabled in soil layers. Note that saturated porous media flow always occurs in the groundwater layer and can episodically occur in the detention and soil layers.

17). Thaw-freeze fronts module (Xie and Gough, 2013): simulates the freezing and thawing fronts in seasonal frost or permafrost soil based on a modified Stefan's heat flow equation for user specified number of soil layers (Krogh et al., 2018) This provides status of thawing and freezing fronts for hillslope soil module.

18). Ground surface temperature module: calculates the ground surface temperature using air temperature and thermal conductivity and energy of snowpack during snowcover period based on conduction approach (Luce and Tarboton, 2010) and using air temperature and net radiation for snow-free period based on radiative-conductive-convective approach (Williams et al., 2015). This provides ground surface temperature input for thaw-freeze fronts module.

19). Muskingum routing module: the Muskingum method is based on a variable discharge-storage relationship (Chow, 1964) and is used to route runoff between HRUs in the sub-basins. The routing storage constant is estimated from the average distance from the HRU to the main channel and average flow velocity; the average flow velocity is calculated by Manning's equation (Chow, 1959) based on the average HRU distance to the main channel, average change in HRU elevation, overland flow depth and HRU roughness. For subsurface and groundwater flows, Clark's lag and route algorithm (Clark, 1945) is used.

Sub-basin group structure

For modelling large basins such as Bow River and Elbow River, the CRHM model structure "representative basin" (RB) group was used, in which a set of physically based modules are assembled with a number of HRUs to represent a sub-basin. The RB can be repeated as necessary in a basin, with each sub-basin having the same modules but differing parameter sets as needed. Streamflow output from a number of RBs is then routed along the main river channel using a

modelling structure comprising of Muskingum routing. Figure 8 shows the sub-basin group structure for Upper Bow River at Banff, Upper Bow River between Banff and Calgary, and Elbow River at Calgary model domains.

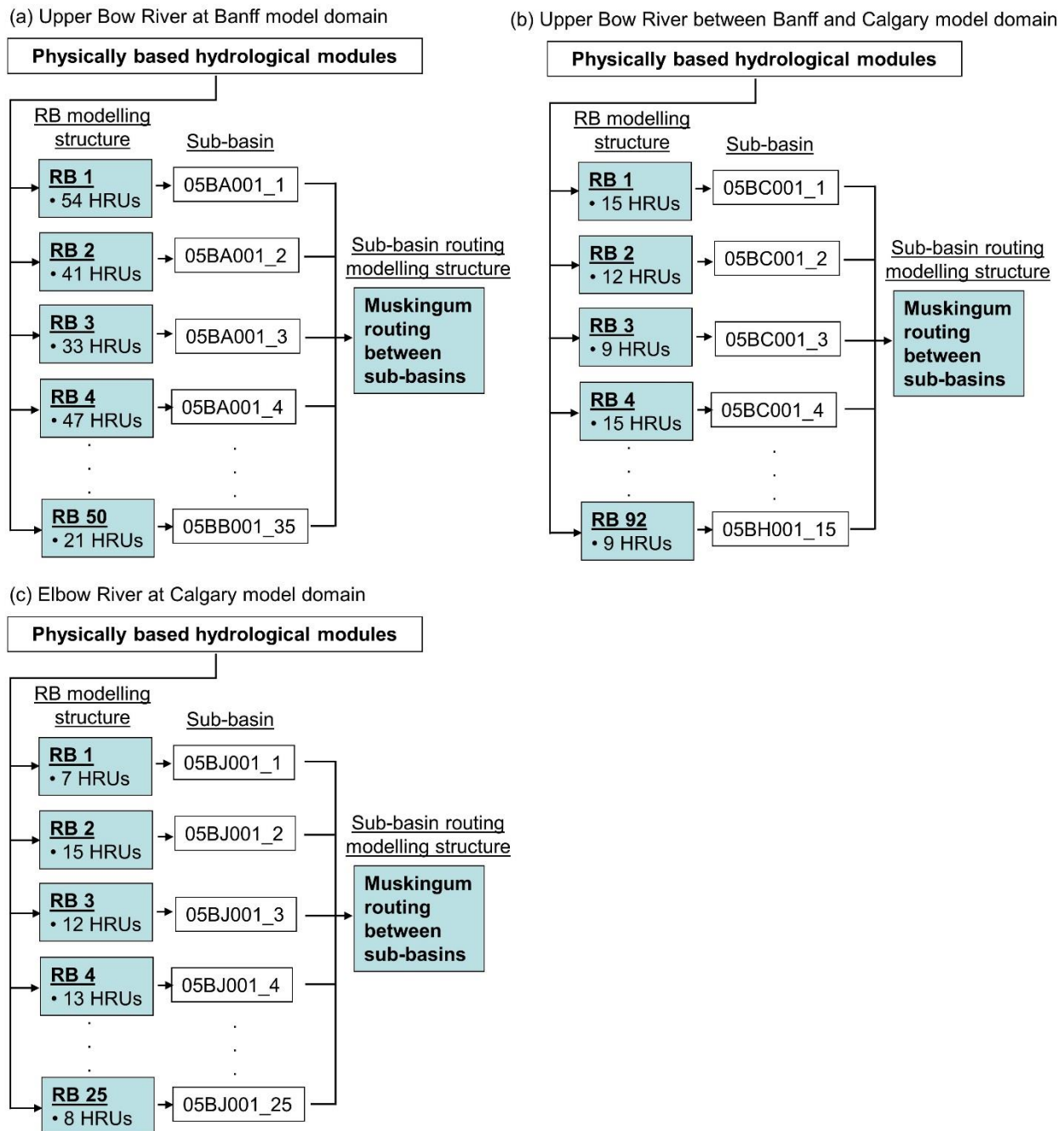


Figure 44. Sub-basin group structure for Upper Bow River at Banff, Upper Bow River between Banff and Calgary, and Elbow River at Calgary model domains. Sub-basins are simulated by modelling structure “representative basin” (RB) group. Modelling structure of Muskingum

routing connects all RBs. Note not all sub-basins in three model domains are shown due to number of them, and information for all sub-basins is summarized in Appendix 3.

Model parameterization

CRHM parameters values were determined based on field studies conducted in Canadian Rocky Mountains and Canadian Prairies, through either understanding of processes or direct field measurements. In addition, GIS analysis of basin characteristics: aspect, slope, elevation, terrain view, and river channel length was used to set up basin physiographic, terrain visibility, and routing parameters. The following lists some of parameters values for key hydrological processes.

Blowing snow parameters

Table 1 shows the values of blowing snow module parameters for HRUs. Blowing snow fetch distance is the upwind distance without disruption to the flow of blowing snow. Fetch distances were set to 1000 m for 'Cropland' and 'Grassland' HRUs. A 300 m fetch length was assigned for other HRUs such as 'developed and exposed land', 'rock', 'alpine tundra', 'forest', 'wetland', 'open water' and 'river channel valley'. These values are comparable to the estimated values for the prairie fields by Fang et al. (2010) using the computer program "FetchR" (Lapen and Martz, 1993) and for alpine zones set by MacDonald et al. (2010) in the Canadian Rockies. Values of vegetation height, stalk density and stalk diameter were set for these HRUs to represent them in the prairie and mountain forest environments during fall and winter; these parameters values are comparable to those reported for the prairie by Fang et al. (2010) and for the alpine region in the Canadian Rockies (MacDonald et al., 2010; Fang et al., 2013).

Table 1. Blowing snow module parameters.

HRU Name	Fetch Distance (m)	Vegetation Height (m)	Stalk Diameter (m)	Stalk Density (#/m ²)
Glacier	300	0.001	0	1
Rock	300	0.001	0.003	1
Alpine tundra	300	0.25	0.01	100
Alpine sparse forest	300	5	0.6	1
Valley shrubland	300	0.5	0.003	100
Coniferous forest edge	300	15	0.6	1
Coniferous forest	300	15	0.6	1
Spruce coniferous forest	300	15	0.6	1
Pine coniferous forest	300	15	0.5	1
Deciduous forest	300	10	0.4	1
Mixed forest	300	15	0.6	1
Regenerated forest clear-cut	300	1.5	0.6	1
Wetland	300	2	0.05	100
Grassland	1000	0.7	0.003	200
Cropland	1000	0.15	0.003	250
Developed and exposed land	300	0.001	0.003	1
Open water	300	0.001	0.003	1
River channel valley	300	2	0.003	1

Albedo and canopy parameters

Table 2 presents the values of albedo and canopy parameters for HRUs. For the albedo of bare ground, measured values in the prairie by Armstrong (2011) were used to set values for ‘tundra’, ‘grassland’, ‘cropland’ and ‘wetland’ HRUs, whilst measured values in the boreal forest environment by Granger and Pomeroy (1997) were used for the forest HRUs. The albedo of fresh snow was set to 0.85 based on recommended values by Male and Gray (1981) and measurements in the Canadian Rockies and northern prairies. For the leaf area index (LAI), a value of 0.5 was assigned for the deciduous forest HRU and this is similar to the value used for aspen forest in the prairie during winter (Pomeroy et al. 1999). Measured values in the boreal forests (Hedstrom and Pomeroy, 1998; Pomeroy et al., 2002) were used for coniferous, mixed and regenerated forest HRUs, which is comparable to the values for northern Canadian Rockies and forests (Pomeroy et al., 2013). The canopy snow interception capacity values were set for coniferous, mixed, and regenerated forest HRUs based on similar forest types in the Western Cordillera and boreal forest (Schmidt and Gluns, 1991; Pomeroy et al., 2002). Small values were set for the deciduous forest HRU as it does not have high capacity to intercept and hold snow (Pomeroy and Gray, 1995).

Table 2. Albedo and canopy parameters. Note LAI is leaf area index, S_{min} is the minimum snowfall needed to refresh snow albedo, and (-) means parameter is dimensionless.

HRU Name	Albedo Parameter			Canopy Parameter	
	Albedo_bar e ground (-)	Albedo_sno w (-)	S_{min} (mm)	LAI (-)	Canopy Snow Interception Capacity (kg/m ²)
Glacier	0.17	0.85	1	0	0
Rock	0.152	0.85	1	0	0
Alpine tundra	0.17	0.85	1	0	0
Alpine sparse forest	0.091	0.85	5	0.8	6.6
Valley shrubland	0.17	0.85	1	0	0
Coniferous forest edge	0.091	0.85	5	2.8	8.8
Coniferous forest	0.091	0.85	5	2.8	8.8
Spruce coniferous forest	0.091	0.85	5	2.8	8.8
Pine coniferous forest	0.091	0.85	5	1.5	6.6
Deciduous forest	0.145	0.85	1	0.5	0.1
Mixed forest	0.145	0.85	5	4	2.1
Regenerated forest clearcut	0.129	0.85	1	0.3	0
Wetland	0.11	0.85	1	0	0
Grassland	0.17	0.85	1	0	0
Cropland	0.18	0.85	1	0	0
Developed and exposed land	0.152	0.85	1	0	0
Open water	0	0.85	1	0	0
River channel valley	0.17	0.85	1	0	0

Hillslope soil parameters

Table 3 lists the values of hillslope soil parameters for HRUs. Both saturated hydraulic conductivity and pore size distribution parameters are used in the Brooks and Corey (1964) relationship to calculate the drainage factors for lateral flow in detention layer, soil layers and the groundwater layer as well as the vertical flow of excess soil water to groundwater. Saturated hydraulic conductivities and pore size distributions for various layers were determined based on well-established experimental relationships to soil texture (Brooks and Corey, 1964; Zhang et al., 2010).

The water storage capacities of recharge and soil layers were determined by multiplying soil layer depth by soil porosity. For the soil depth and porosity, averaged values for 'cropland', 'grassland' HRUs were estimated from information of predominant soil texture in the region (Soil Landscapes of Canada Working Group, 2011). For the 'rock', 'alpine tundra' and 'forest' HRUs, the water storage capacity in the recharge and soil layers were set based on the values reported for Marmot Creek Research Basin (Beke, 1969; Fang et al. 2013). For the 'glacier' HRU, the water storage capacity in the recharge and soil layers were set based on modelling values used for Peyto Glacier

in Icefields Parkway. For the water storage capacities of detention layer, values were set from studies conducted in Marmot Creek Research Basin (Beke, 1969; Keith et al., 2010; Pomeroy et al., 2016). For groundwater storage capacity that is relatively unknown, values of 200 mm and 500 mm were set for 'glacier' and 'rock' HRUs; a value of 750 mm was set for rest of HRUs. For surface depressional storage capacities, values of 300 mm and 500 mm were set for 'wetland' and 'open water' HRUs, which is similar to values found in other prairie environment (Fang et al., 2010). Small value of 10 mm was set for 'glacier', 'grassland' and 'cropland' to represent the temporal depressional storage for these HRUs.

Routing parameters

Figures 45 and 46 show the routing sequence between HRUs within the sub-basin and routing sequence between sub-basins, respectively. The routing sequence within the sub-basin is modelled using routing distribution parameter (Fang et al., 2010; 2013) to represent typical sequence of flow relationship among HRUs for of glacier mountain, non-glacier mountain, foothill plain, and agriculture sub-basin types. The routing sequence between sub-basins follows the channel flow order from the upstream part to the downstream part of the basin. The Muskingum routing method was used and flow travel times were estimated from the routing length and average flow velocity. For routing between HRUs within sub-basins, the routing lengths for the non-river channel valley HRUs were calculated based on the Hack's law length-area relationship (Hack, 1957). Routing lengths for the 'river channel valley' HRU within sub-basins and routings lengths between the sub-basins were calculated from the channel length in water course in Alberta drainage network GIS inventory. Manning's equation (Chow, 1959) was used to calculate the average streamflow velocity based on longitudinal channel slope, Manning's roughness coefficient, and hydraulic radius as parameters. The longitudinal channel slope of a HRU or a sub-basin was estimated from the average slope of the HRU or sub-basin. Manning's roughness coefficient was approximated based on surface cover and channel condition using a Manning's roughness lookup table (Mays, 2001). The hydraulic radius was determined from the lookup table using channel shape and channel depth as criteria.

Table 3. Hillslope soil parameters. K_{s_gw} , K_{s_upper} , K_{s_lower} and $K_{s_organic}$ are the saturated hydraulic conductivity in the groundwater, upper and lower of soil layers, and organic detention layer, respectively. λ is the pore size distribution index. $soil_{rechr_max}$, $soil_{moist_max}$ and gw_{max} are the available water storage capacity for the recharge, soil of both recharge and lower, and groundwater layers, respectively. sd_{max} is the depressional storage capacity. $Dts_{organic_max}$ and Dts_{snow_max} are the water storage of organic detention layer and snowcover detention layer, respectively. Note (-) means parameter is dimensionless.

HRU Name	K_{s_gw} (m/s)	K_{s_upper} (m/s)	K_{s_lower} (m/s)	$K_{s_organic}$ (m/s)	λ (-)	$soil_{rechr_max}$ (mm)	$soil_{moist_max}$ (mm)	gw_{max} (mm)	sd_{max} (mm)	$Dts_{organic_max}$ (mm)	Dts_{snow_max} (mm)
Glacier	6.9×10^{-7}	2.3×10^{-3}	1.7×10^{-5}	3.3×10^{-3}	0.252	50	100	200	10	0	50
Rock	6.9×10^{-7}	2.3×10^{-4}	1.7×10^{-5}	3.3×10^{-3}	0.252	100	250	500	0	50	100
Alpine tundra	6.9×10^{-7}	6.9×10^{-5}	1.7×10^{-5}	3.3×10^{-3}	0.252	200	750	750	0	100	100
Alpine sparse forest	6.9×10^{-7}	6.9×10^{-5}	1.7×10^{-5}	3.3×10^{-3}	0.252	200	750	750	0	100	100
Valley shrubland	6.9×10^{-7}	6.9×10^{-5}	1.7×10^{-5}	3.3×10^{-3}	0.252	200	750	750	0	100	100
Coniferous forest edge	6.9×10^{-7}	6.9×10^{-5}	1.7×10^{-5}	3.3×10^{-3}	0.252	200	750	750	0	100	100
Coniferous forest	6.9×10^{-7}	6.9×10^{-5}	1.7×10^{-5}	3.3×10^{-3}	0.252	200	750	750	0	100	100
Spruce coniferous forest	6.9×10^{-7}	6.9×10^{-5}	1.7×10^{-5}	3.3×10^{-3}	0.252	200	750	750	0	100	100
Pine coniferous forest	6.9×10^{-7}	6.9×10^{-5}	1.7×10^{-5}	3.3×10^{-3}	0.252	200	750	750	0	100	100
Deciduous forest	6.9×10^{-7}	6.9×10^{-5}	1.7×10^{-5}	3.3×10^{-3}	0.252	200	750	750	0	100	100
Mixed forest	6.9×10^{-7}	6.9×10^{-5}	1.7×10^{-5}	3.3×10^{-3}	0.252	200	750	750	0	100	100
Regenerated forest clearcut	6.9×10^{-7}	6.9×10^{-5}	1.7×10^{-5}	3.3×10^{-3}	0.252	200	750	750	0	100	100
Wetland	6.9×10^{-7}	6.9×10^{-5}	1.7×10^{-5}	3.3×10^{-3}	0.252	200	750	750	300	100	100

Grassland	6.9×10^{-7}	6.9×10^{-5}	1.7×10^{-5}	3.3×10^{-3}	0.252	200	750	750	10	50	100
Cropland	6.9×10^{-7}	6.9×10^{-5}	1.7×10^{-5}	3.3×10^{-3}	0.252	200	750	750	10	50	100
Developed and exposed land	6.9×10^{-7}	6.9×10^{-5}	1.7×10^{-5}	3.3×10^{-3}	0.252	200	750	750	0	0	100
Open water	6.9×10^{-7}	6.9×10^{-5}	1.7×10^{-5}	3.3×10^{-3}	0.252	200	500	750	500	100	100
River channel valley	6.9×10^{-7}	6.9×10^{-5}	1.7×10^{-5}	3.3×10^{-3}	0.252	200	1000	750	0	100	100

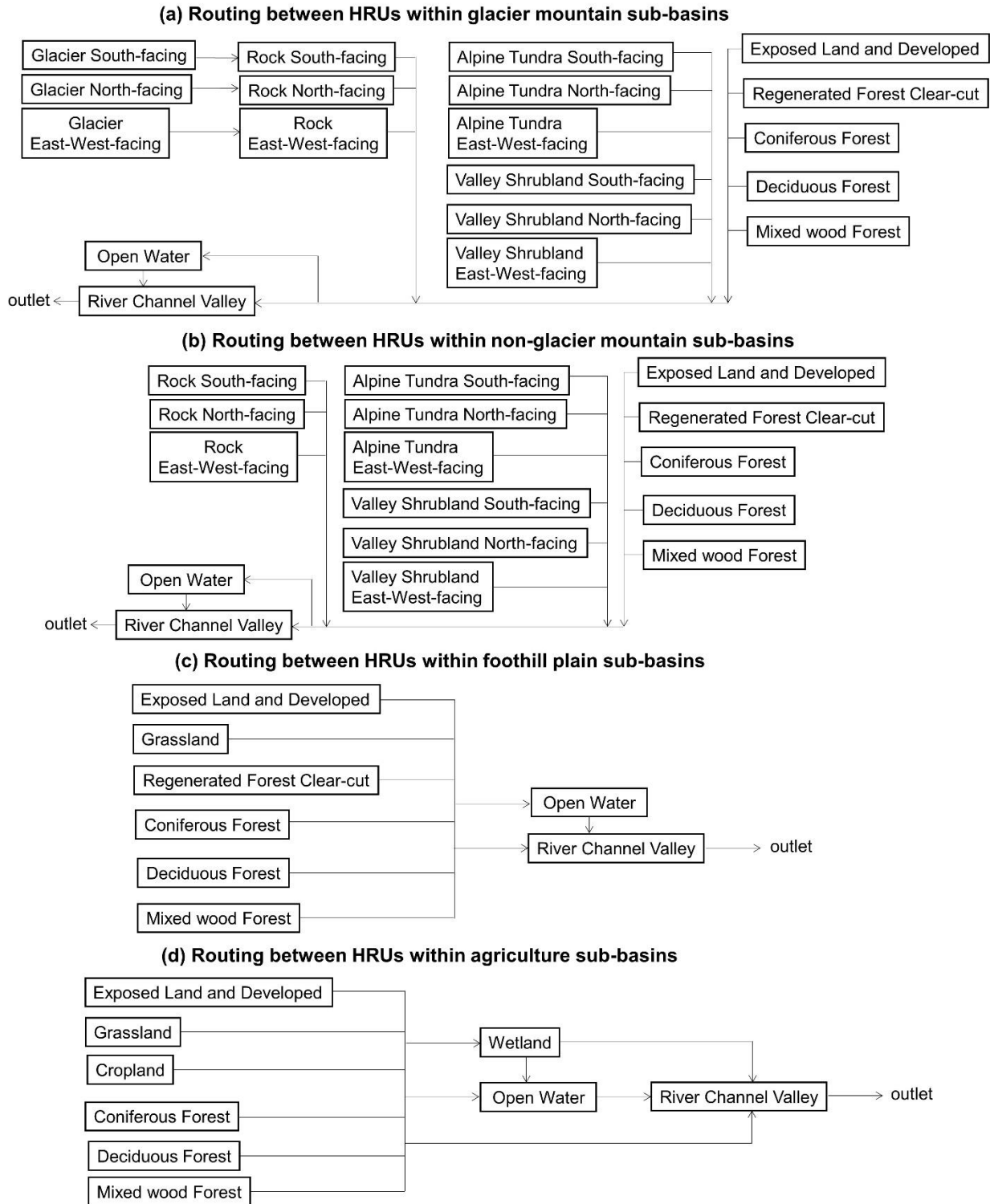
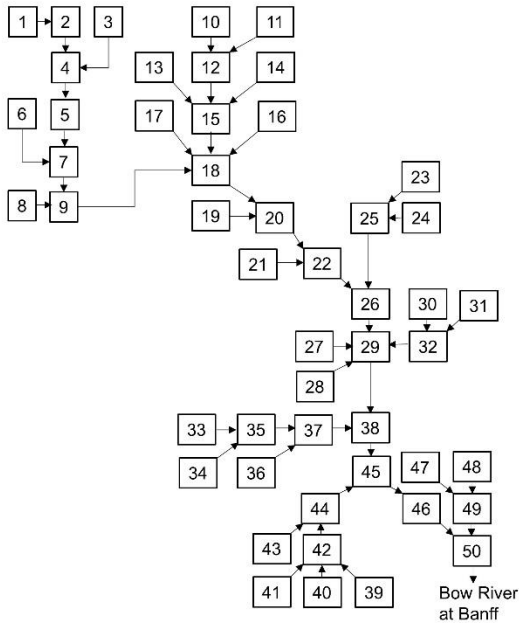
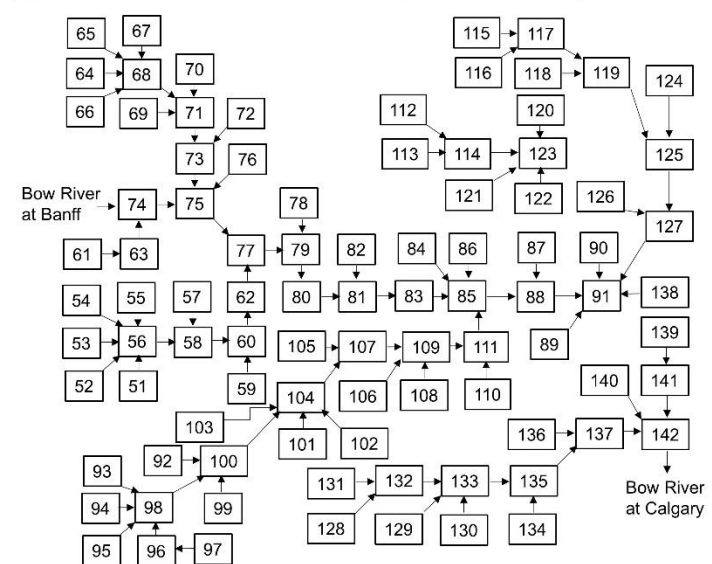


Figure 45. Routing sequence between HRUs within the modelled sub-basins in Upper Bow River at Banff, Upper Bow River between Banff and Calgary, and Elbow River at Calgary model domains.

Upper Bow River at Banff model domain:



Upper Bow River between Banff and Calgary model domain:



Elbow River at Calgary model domain:

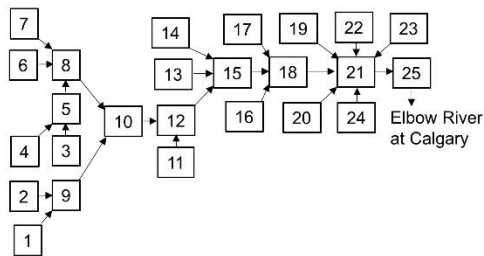


Figure 46. Routing sequence between the modelled sub-basins in Upper Bow River at Banff, Upper Bow River between Banff and Calgary, and Elbow River at Calgary model domains. Note that the sub-basin number is shown in the routing sequence, and sub-basin name and other information for these sub-basins are summarized in Appendix 3.

Model forcing

The CRHM hydrological models were driven by the model outputs from the CCRN runs (Dr. Yanping Li, GIWS, Univ. Saskatchewan) of the Weather Research and Forecasting (WRF) model, available from 1 October 2000 to 25 September 2015, include air temperature, vapour pressure, wind speed, shortwave irradiance, and precipitation. These variables from a 4-km WRF model version 3.6.1 were bias-corrected using the same outputs from 10-km Global Environmental Multiscale and Canadian Precipitation Analysis (GEM-CaPA) based on multi-variate bias correction method (Cannon et al., 2018), resulting in 10-km bias corrected WRF model outputs. In total, there are 17, 50, and 12 grids of these 10-km WRF model outputs used to forcing the hydrological models for Upper Bow River at Banff, Upper Bow River between Banff and Calgary, and Elbow River at Calgary model domains, respectively. Information for these WRF grids is provided in Appendix 4.

Forest disturbance scenarios

Three types of forest disturbance scenarios: fire, harvesting, and pine beetle were created. More details are provided as follows.

Fire scenarios

In the fire scenarios, all types of forest are burned with three different severities:

- Low severity: 20% reduction in values of LAI and canopy snow interception capacity parameters,
- Moderate severity: 50% reduction in values of LAI and canopy snow interception capacity parameters, with 67% reduction in rainfall infiltrability for soil defined by ground cover and texture parameters,
- High severity: 80% reduction in values of LAI and canopy snow interception capacity parameters, with about 99% reduction in rainfall infiltrability for soil defined by ground cover and texture parameters, and high fall soil saturation for snowmelt infiltration.

Table 4 lists the values of canopy and soil infiltration parameters for fire scenarios. For maximum LAI (i.e. LAI_{max}) and minimum LAI (i.e. LAI_{min}) parameters, values were adjusted accordingly to the changes in LAI parameter. Both LAI_{max} and LAI_{min} parameters affect the seasonal stomatal resistance in evaporation from forests such as alpine sparse forest (e.g. larch), deciduous forest (e.g. aspen), and mixed forest HRUs. In addition, for both low and moderate fire severity scenarios, the fall soil saturation parameter was set 0, same as for the healthy forest condition, which allows unlimited snowmelt infiltration into seasonal frozen soil due to coarse soil texture on the forest floor with high organic content on the top. For the moderate fire severity scenario, the rainfall infiltrability was reduced to 25.4 mm/hour, a 67% reduction; this represents a reduced infiltration ability of soil for the summer intense rainfall. For the high fire severity scenario, the fall soil saturation parameter was set to a high value of 0.6 based on field measurement for the disturbed forest in Barrier Lake forest clear-cut site, Kananaskis Country, and this represents limited condition for snowmelt infiltration into seasonal frozen soil. Rainfall infiltrability was set to minimum value of 0.5 mm/hour to represent a very limited rainfall infiltration capacity for soil after high fire severity.

Harvesting scenarios

In the harvesting scenarios, only the pine coniferous forest is harvested with two levels of harvesting area:

- Harvest half maximum: harvesting 25% of pine coniferous forest area,
- Harvest maximum: harvesting 50% of pine coniferous forest area.

In CRHM, the harvested pine forest area was converted to a new HRU called 'disturbance' with the following parameter values, also listed in Table 5:

- set both vegetation height (i.e. Ht) and maximum vegetation height (Ht_{max}) to 0.5 m;
- set LAI and LAI_{min} to 0.5 and LAI_{max} to 1;
- set available water storage capacity for the recharge layer (i.e. $soil_{rechr_max}$) to 167 mm and entire soil column (i.e. $soil_{moist_max}$) to 625 mm, both are 17% reduction compared to the

healthy pine forest; this reduction was used to represent soil compaction during harvesting and was set based on field measurements of soil moisture for intact forest and forest clear-cut in Barrier Lake forest clear-cut site, Kananaskis Country;

- set to minimum value of 0.5 mm/hour for rainfall infiltrability to represent a very limited rainfall infiltration capacity for the compacted soil;
- set soil withdrawal function for evaporation to loam, this reduces amount of evaporation flux withdrawn from soil storage, compared to the organic soil withdrawal function for healthy pine forest.

Pine beetle scenarios

In the pine beetle scenarios, infested pine coniferous forest represents the final stage of pine beetle infestation, affected area is 100% of pine forest with two cases:

- Pine beetle with salvage: salvage logging the 100% of infested pine forest,
- Pine beetle without salvage: retaining the 100% of infested pine forest.

In CRHM, the infested pine forest area was converted to a new HRU called 'disturbance' with the following parameter values, also listed in Table 5:

- for pine beetle with salvage scenario, parameter changes are the same as those in harvesting scenarios;
- for pine beetle without salvage scenario:
 - set LAI, LAI_{min}, and LAI_{max} to 1;
 - set Ht and Ht_{max} to 15 m, same as healthy pine forest;
 - restore soil_{rechr_max}, soil_{moist_max}, soil withdrawal function for evaporation, and rainfall infiltrability parameters to same values as healthy pine forest, as there is no soil compaction in this scenario.
 -

In total, three simulations of fire scenarios were conducted for each of three model domains. Two simulations of harvesting scenarios and two simulations of pine beetle scenarios were conducted for only Upper Bow River between Banff and Calgary and Elbow River at Calgary model domains, as there is no pine forest coverage from Alberta forest species (AVIE) inventory for Upper Bow River at Banff model domain.

Table 4. Canopy and soil infiltration parameters for health forest and forest in fire scenarios. LAI_{max} and LAI_{min} are maximum and minimum of leaf area index (LAI). Note (-) means parameter is dimensionless.

Scenario	Healthy Forest	Low Severity	Moderate Severity	High Severity	Healthy Forest	Low Severity	Moderate Severity	High Severity
HRU Name	LAI (-)				Canopy Snow Interception Capacity (kg/m ²)			
Alpine sparse forest	0.8	0.64	0.4	0.16	6.6	5.28	3.3	1.32
Coniferous forest	2.8	2.24	1.4	0.56	8.8	7.04	4.4	1.76
Coniferous forest edge	2.8	2.24	1.4	0.56	8.8	7.04	4.4	1.76
Spruce coniferous forest	2.8	2.24	1.4	0.56	8.8	7.04	4.4	1.76
Pine coniferous forest	1.5	1.2	0.75	0.3	6.6	5.28	3.3	1.32
Deciduous forest	0.5	0.4	0.25	0.1	0.1	0.08	0.05	0.02
Mixed forest	0.54	0.432	0.27	0.108	2.1	1.68	1.05	0.42
HRU Name	LAI _{max} (-)				LAI _{min} (-)			
Alpine sparse forest	1.5	1.2	0.75	0.3	0.8	0.64	0.4	0.16
Coniferous forest	2.8	2.24	1.4	0.56	2.8	2.24	1.4	0.56
Coniferous forest edge	2.8	2.24	1.4	0.56	2.8	2.24	1.4	0.56
Spruce coniferous forest	2.8	2.24	1.4	0.56	2.8	2.24	1.4	0.56
Pine coniferous forest	1.5	1.2	0.75	0.3	1.5	1.2	0.75	0.3
Deciduous forest	1.4	1.12	0.7	0.28	0.5	0.4	0.25	0.1
Mixed forest	1.4	1.12	0.7	0.28	0.54	0.432	0.27	0.108
HRU Name	Rainfall infiltrability (mm/hour)				Fall soil saturation (-)			
Alpine sparse forest	76.2	76.2	25.4	0.5	0	0	0	0.6
Coniferous forest	76.2	76.2	25.4	0.5	0	0	0	0.6
Coniferous forest edge	76.2	76.2	25.4	0.5	0	0	0	0.6
Spruce coniferous forest	76.2	76.2	25.4	0.5	0	0	0	0.6
Pine coniferous forest	76.2	76.2	25.4	0.5	0	0	0	0.6
Deciduous forest	76.2	76.2	25.4	0.5	0	0	0	0.6
Mixed forest	76.2	76.2	25.4	0.5	0	0	0	0.6

Table 5. Canopy, soil infiltration and soil withdrawal function parameters for ‘disturbance’ HRU in harvesting and pine beetle scenarios. Note that Ht and Ht_{max} are the vegetation height and maximum vegetation height; LAI_{max} and LAI_{min} are maximum and minimum of leaf area index (LAI). soil_{rechr_max} and soil_{moist_max} are the available water storage capacity for the recharge layer and entire soil column. (-) means parameter is dimensionless.

Scenario		Ht (m)	Ht _{max} (m)	LA I (-)	LAI _{min} in (-)	LAI _{max} ax (-)	soil _{rechr_max} (mm)	soil _{moist_max} (mm)	Rainfall infiltrability (mm/hour)	Soil withdrawal function (-)
Harvest half maximum	0.5	0.5	0.5	0.5	1	167	625	0.5	loam	
Harvest maximum	0.5	0.5	0.5	0.5	1	167	625	0.5	loam	
Pine beetle with salvage	0.5	0.5	0.5	0.5	1	167	625	0.5	loam	
Pine beetle without salvage	15	15	1	1	1	200	750	76.2	organic	

3.2 Results of simulations

Streamflow test using the WRF forcing

Model simulations of streamflow using the 10-km bias corrected WRF forcing were conducted for about 15 water years (from 1 October 2000 to 25 September 2015) and were compared to the observed discharge from four ECCC Water Survey of Canada natural flow streamflow gauges: 05BA001, 05BA002, 05BB001, and 05BJ010 (Figs. 47 to 50). Statistical indexes: Nash-Sutcliffe efficiency (NSE) (Nash and Sutcliffe, 1970) and model bias (MB) (Fang et al., 2013) were used to assess model performance. Results show that the 15-water year NSE values ranged from -0.12 for Bow River at Lake Louise to 0.61 for Pipestone River near Lake Louise, with 15-water year MB values ranging from -0.21 for Pipestone River near Lake Louise to -0.4 for both Bow River at Lake Louise and Elbow River at Calgary. This suggests that model did not capture the time evolution of streamflow for Bow River at Lake Louise, which had a negative NSE value. Although the model had some predictability for the time evolution of streamflow for other three gauges, with positive NSE values, especially the moderate value of 0.61 for Pipestone River near Lake Louise, it failed to estimate the total flow volume well for all four gauges. That is, model consistently underestimated total flow volume for these gauges, ranging from 21% to 40% underestimation.

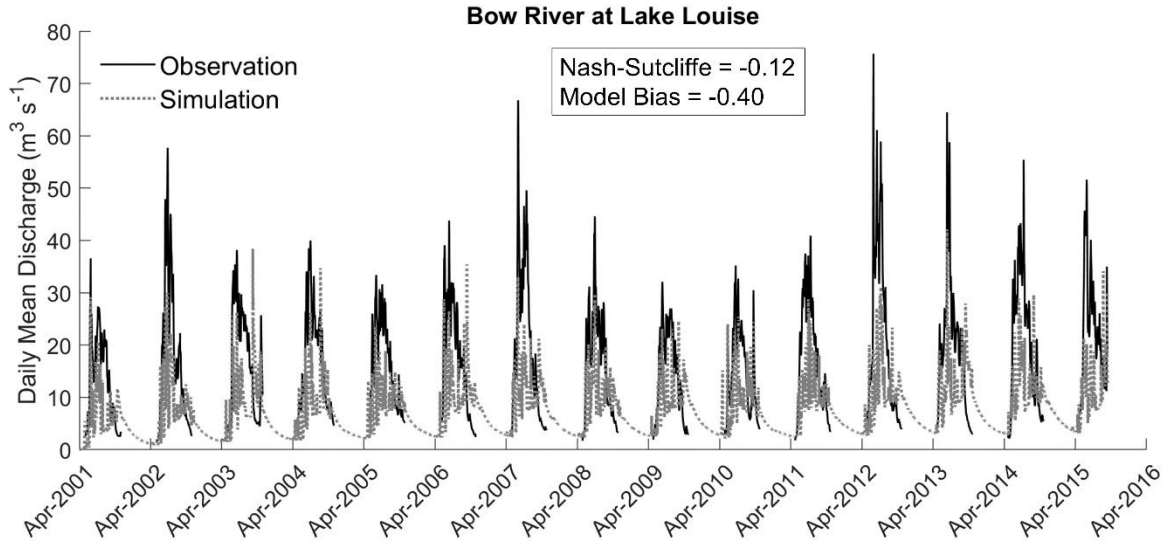


Figure 47. Comparison of the observed and simulated daily streamflow during 1 April 2001-25 September 2015 for Bow River at Lake Louise (i.e. gauge 05BA001).

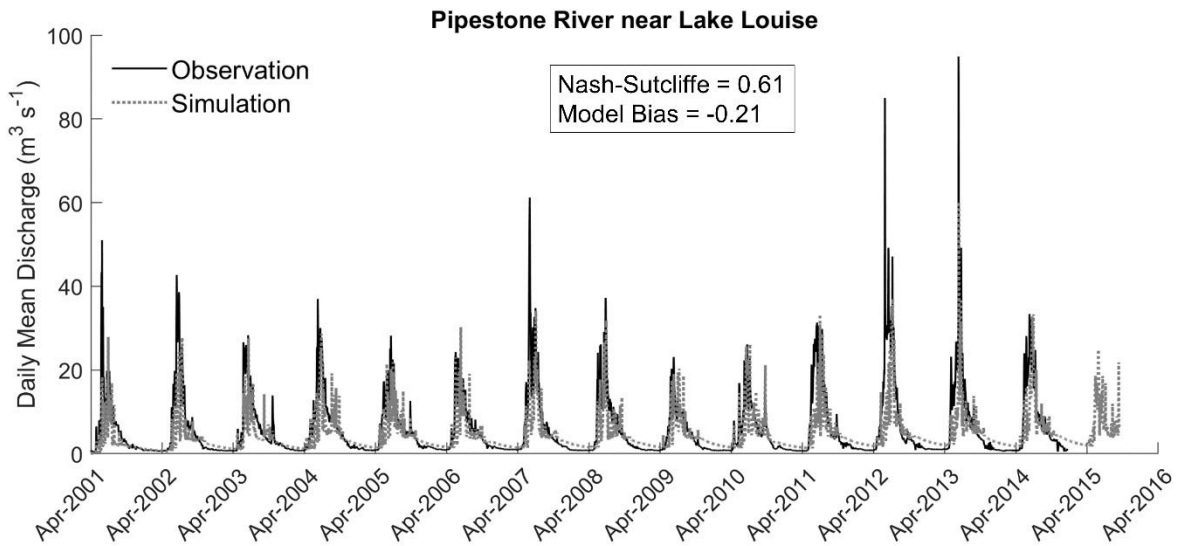


Figure 48. Comparison of the observed and simulated daily streamflow during 1 April 2001-25 September 2015 for Pipestone River near Lake Louise (i.e. gauge 05BA002).

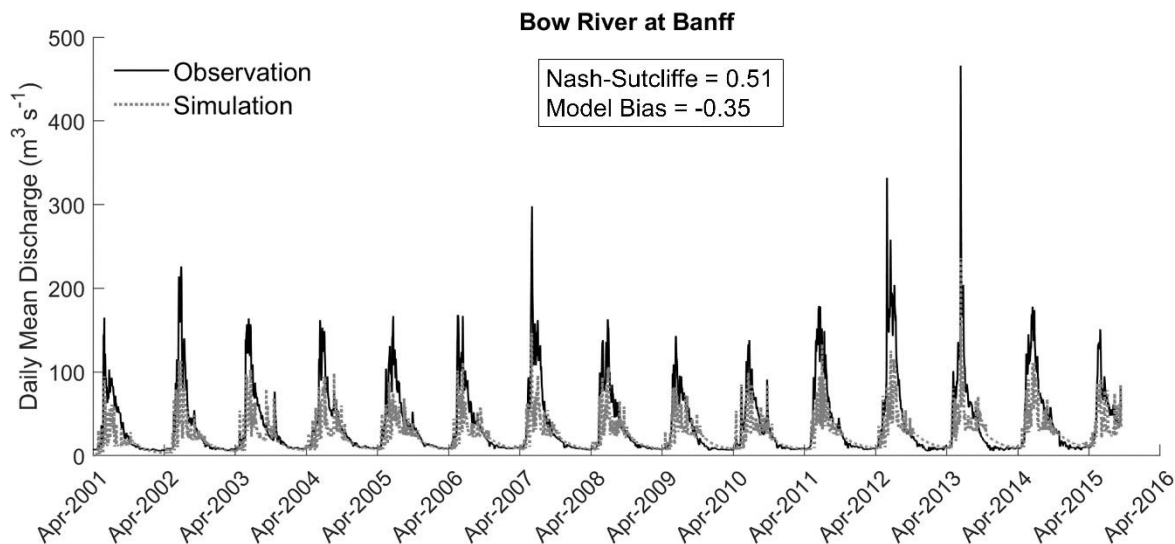


Figure 49. Comparison of the observed and simulated daily streamflow during 1 April 2001-25 September 2015 for Bow River at Banff (i.e. gauge 05BB001).

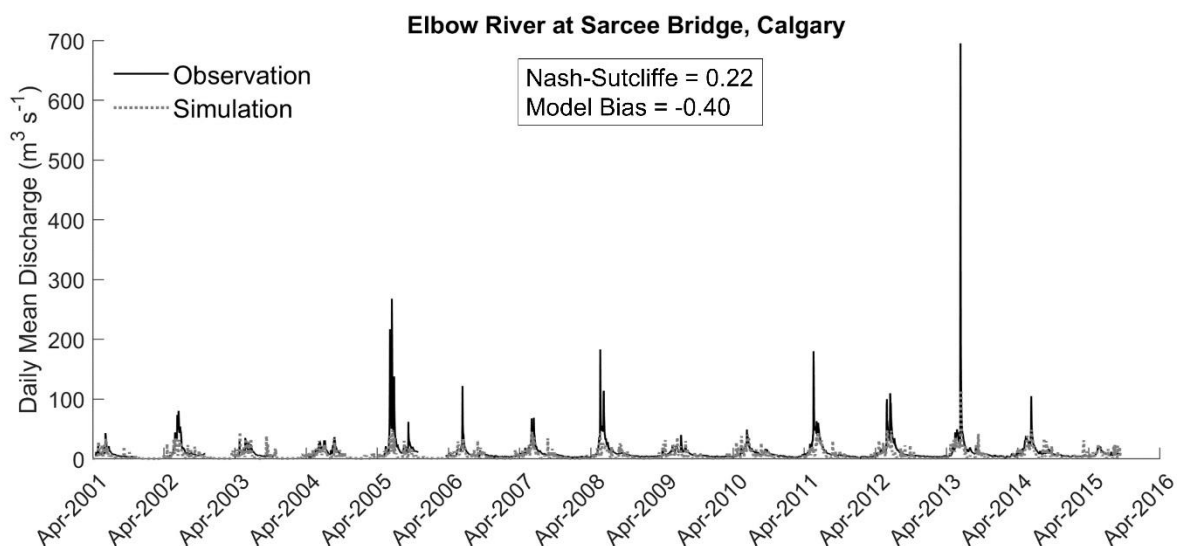


Figure 50. Comparison of the observed and simulated daily streamflow during 1 April 2001-25 September 2015 for Elbow River at Sarcee Bridge, Calgary (i.e. gauge 05BJ010).

One of main factors causing the consistent underestimation of discharge is the underestimation of precipitation in the 10-km bias corrected WRF, despite its bias correction using the 10-km GEM-CaPA model precipitation. Mountain basins in Bow River and Elbow River have high elevation relief, which presents challenges for estimate precipitation at a 10-km spatial resolution. The sparse distribution of precipitation stations at high elevations in the mountains also degrades the usefulness of the GEM-CaPA product for bias correction in mountains. Thus, an additional “double mass curve of discharge” analysis was used to correct some of biases in the 10-km bias corrected WRF precipitation.

Double mass curve discharge correction

Based on the observed and the simulated streamflow discharge using the 10-km bias corrected WRF forcing, cumulative streamflow discharge was computed, which was used to develop double mass curve of discharge for four gauges: 05BA001, 05BA002, 05BB001, and 05BJ010 (Fig. 51). Regression equations were derived for corresponding double mass curve of discharge, and the 10-km bias corrected WRF precipitation was multiplied by the slope values from the regression equations to correct the underestimation bias, referring the following multiplying values (MV):

- For Upper Bow River at Banff model domain,
 - MV = 1.66 for sub-basins 1 to 9, MV = 1.31 for sub-basins 10 to 15, MV = 1.57 for sub-basins 16 to 50,
- MV = 1.69 for all sub-basins in Elbow River at Calgary model domain and Upper Bow River between Banff and Calgary model domain.

Streamflow test using the adjusted WRF forcing

Model simulations of streamflow using the 10-km bias corrected WRF forcing with the adjusted precipitation from “double mass curve of discharge” analysis were conducted for the same 15 water years and were compared to the observed discharge from the same four Water Survey of Canada natural flow streamflow gauges (Figures 16 to 19). Results show that both 15-water year NSE and MB values improved for the streamflow simulations using the adjusted WRF precipitation. The 15-water year NSE values were positive for all testing gauges, ranging from 0.25 for Elbow River at Calgary to 0.72 for Bow River at Banff, suggesting that model could adequately simulate the time evolution of streamflow. In addition, the 15-water year MB values ranged from -0.16 for Bow River at Lake Louise to 0.22 for Elbow River at Calgary, showing improvements compared to the consistent underestimation of total flow volume from the previous simulations, especially for Bow River at Banff with improvement from previous 35% underestimation to only 0.06% overestimation. With these improvements, the 10-km bias corrected WRF forcing with the adjusted precipitation was used to force the model simulations of the forest disturbance scenarios.

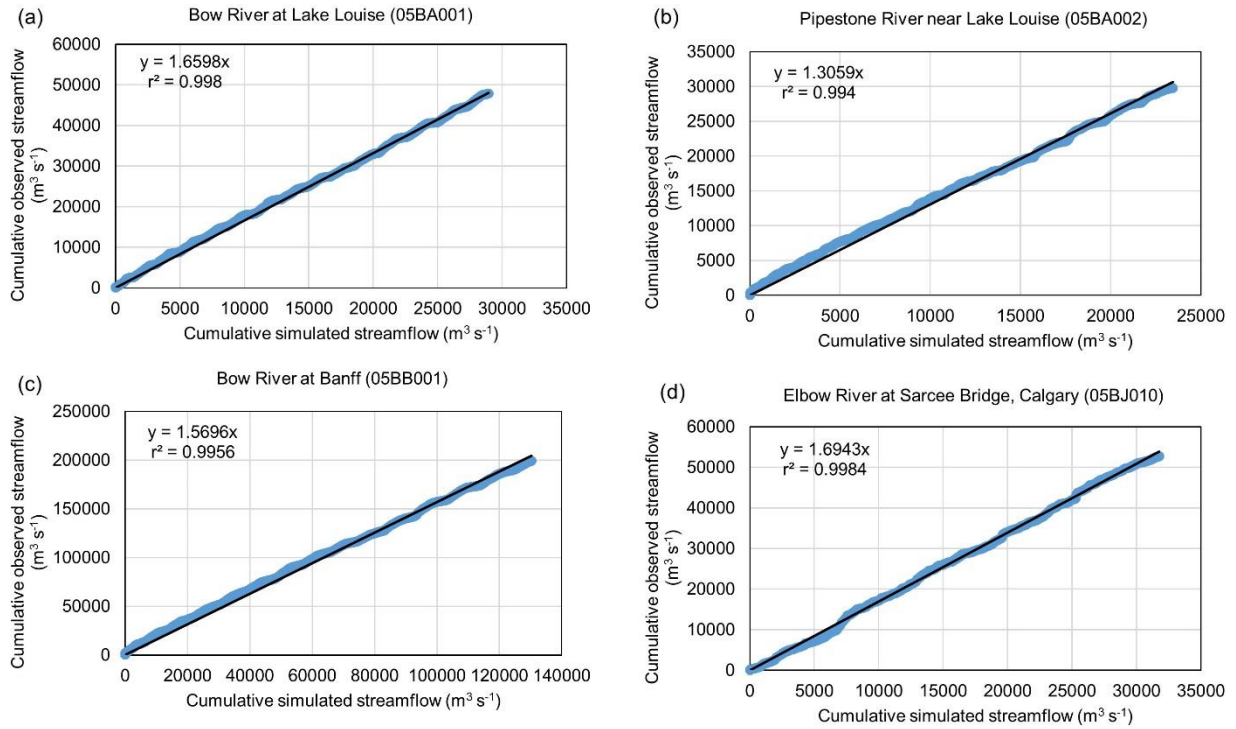


Figure 51. Double mass curve of discharge for (a) Bow River at Lake Louise, (b) Pipestone River near Lake Louise, (c) Bow River at Banff, and (d) Elbow River at Sarcee Bridge, Calgary.

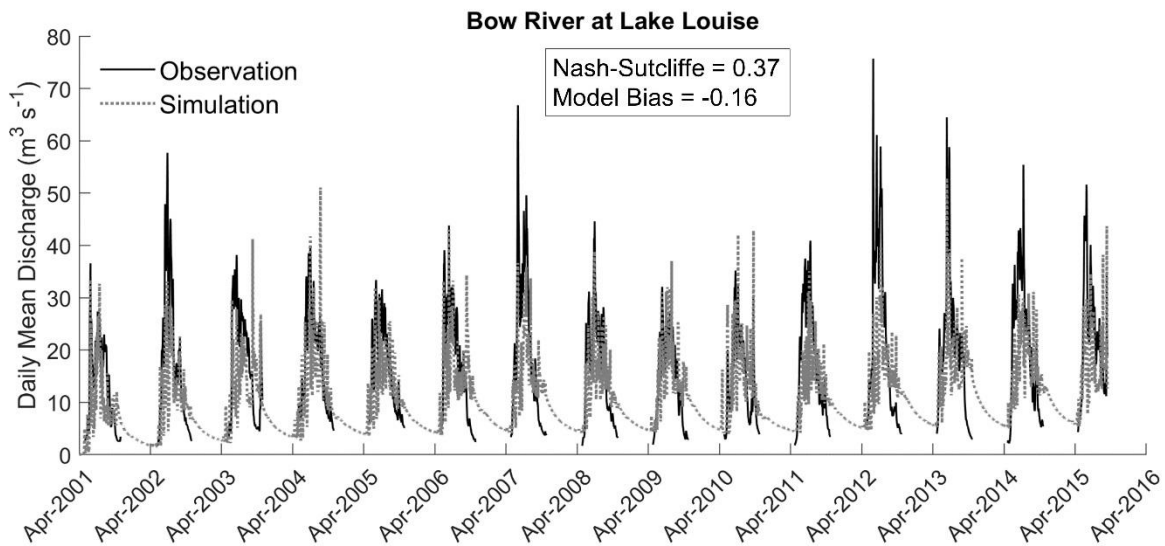


Figure 52. Comparison of the observed and simulated daily streamflow using the adjusted WRF precipitation during 1 April 2001-25 September 2015 for Bow River at Lake Louise.

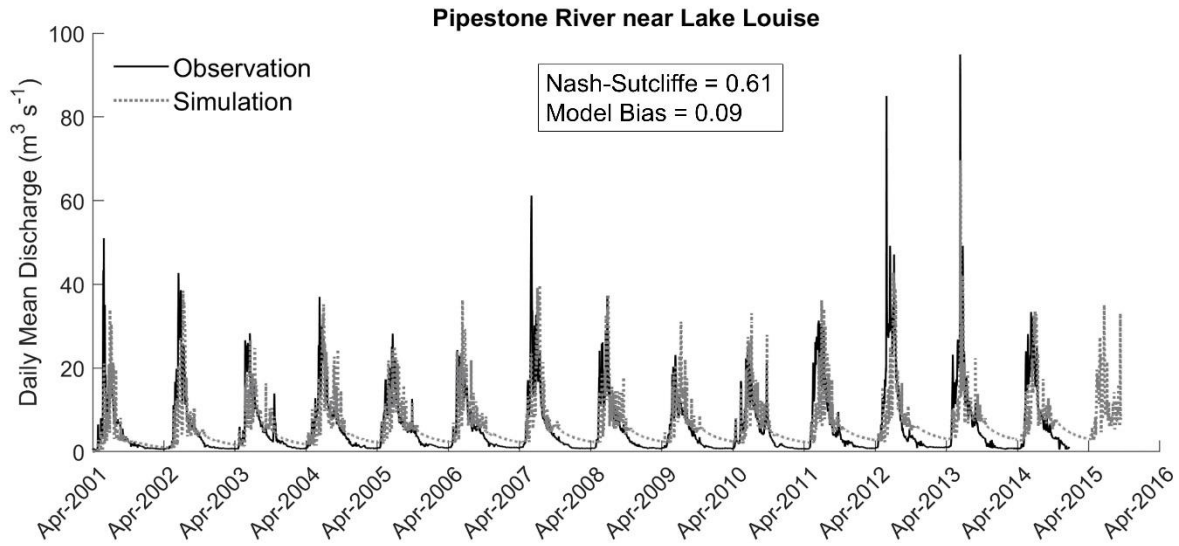


Figure 53. Comparison of the observed and simulated daily streamflow using the adjusted WRF precipitation during 1 April 2001-25 September 2015 for Pipestone River near Lake Louise.

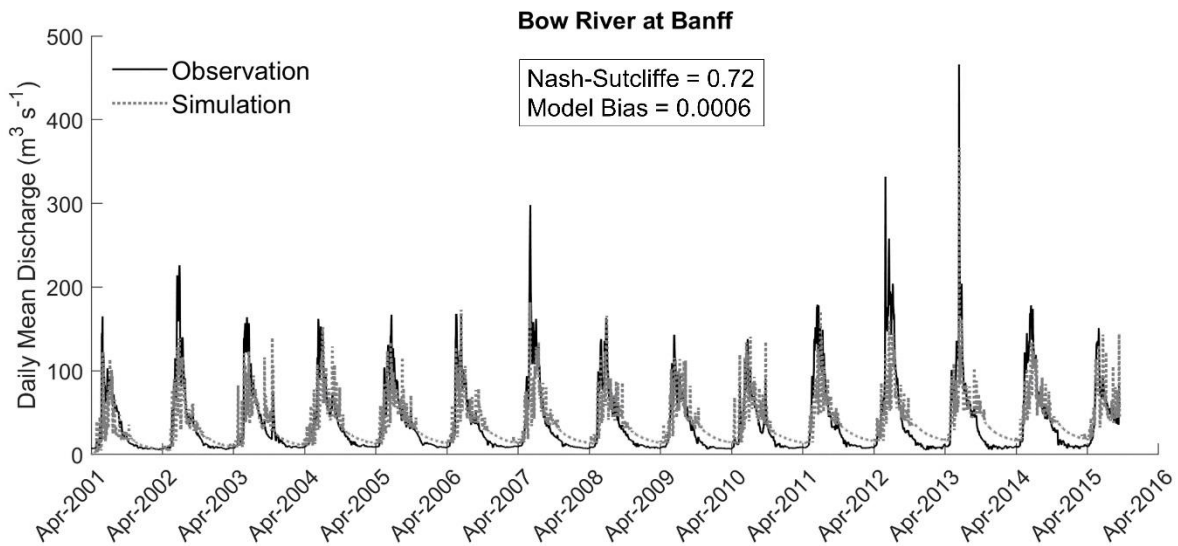


Figure 54. Comparison of the observed and simulated daily streamflow using the adjusted WRF precipitation during 1 April 2001-25 September 2015 for Bow River at Banff.

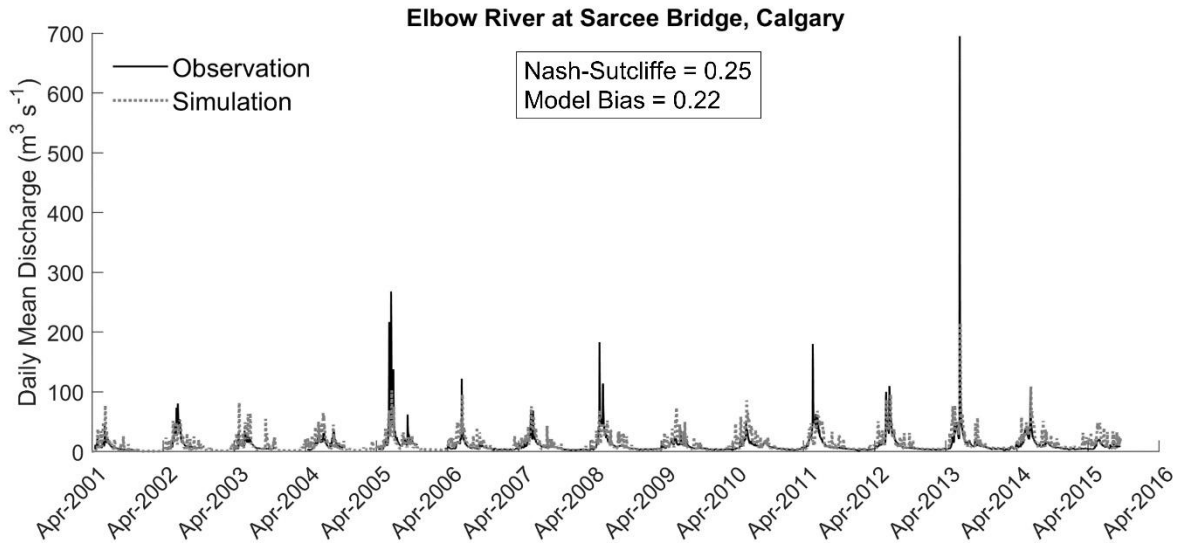


Figure 55. Comparison of the observed and simulated daily streamflow using the adjusted WRF during 1 April 2001-25 September 2015 for Elbow River at Sarcee Bridge, Calgary.

In addition, the streamflow gauge 05BB001 (i.e. Bow River at Banff) has continuous year round observation for 15 water years (from 1 October 2000 to 25 September 2015), and comparison of the 15-water year mean time-series of daily discharge between observation and simulation using the adjusted WRF precipitation is shown in Figure 56. The figure includes shaded areas for simulation and observation based on standard deviations of 15-water year daily discharge. This is another way to examine the confidence of simulation with respect to observation on the basis on 15-water year mean daily discharge. Unfortunately, missed precipitation estimation and possible slow snowmelt calculations due to forcing data or model errors early in the melt season mean that there are substantial differences between bulk simulation and prediction of streamflow regimes for the Bow River at Banff despite the NS statistic of 0.72 and small bias. Poor precipitation forcing in spring resulted in a substantial bias and an attempt to correct this bias with streamflow volumes then degraded winter baseflow simulations, making them roughly double those observed. It is believed that using the 4-km WRF outputs without the GEM-CaPA bias corrections and the resulting degradation of model resolution to 10-km would improve these results. The limited reliability of these model results means that only annual flow volume changes are analysed further for the Bow and Elbow river basins. This can be done with greater confidence as the annual biases between model and observation are very small.

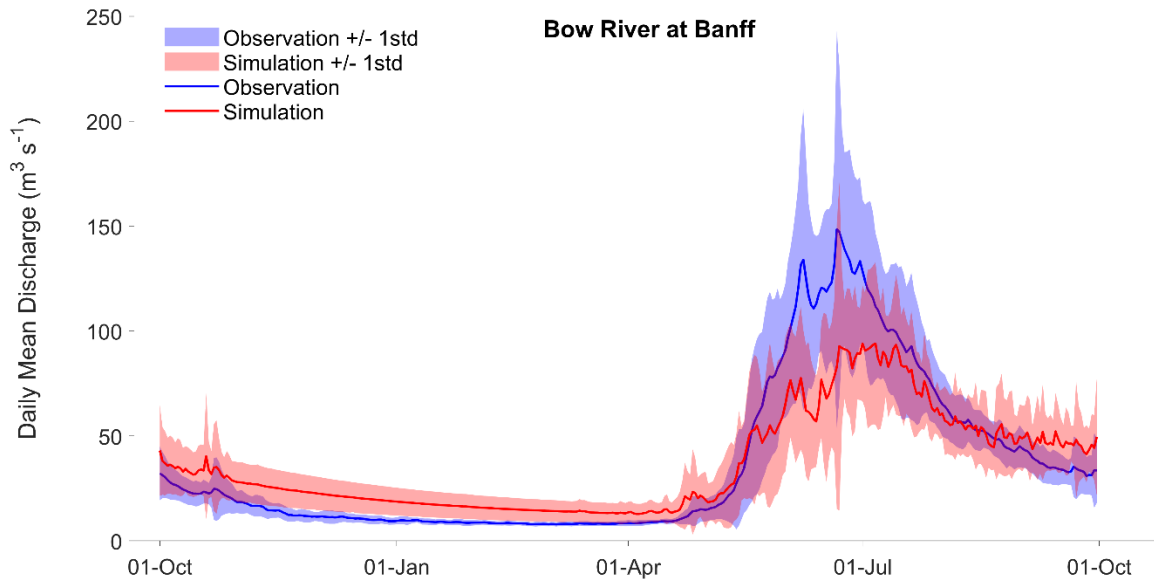


Figure 56. Comparison of the observed and simulated daily streamflow using the adjusted WRF precipitation for Bow River at Banff. The coloured lines represent the annual means and the shadows represent the standard deviations of the 15-water year daily streamflow discharge model outputs and observations.

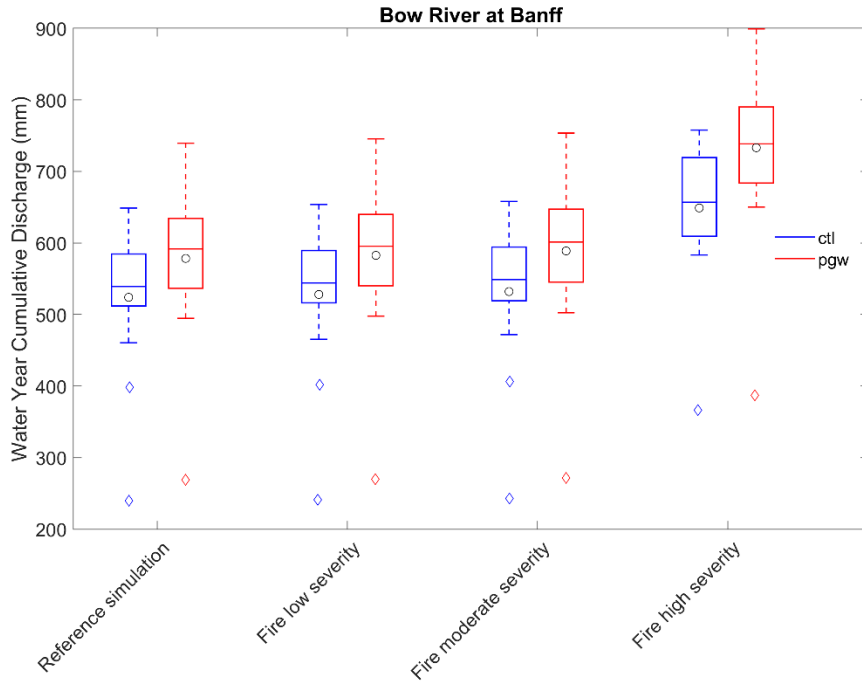
Climate change and Forest disturbance simulations

The impacts of climate change and forest disturbance scenarios on streamflow were examined for the Bow River at Banff, Bow River at Calgary, and Elbow River at Calgary. These streamflow simulations were conducted for both a retrospective period (ctl), 1 October 2000 to 25 September 2015) and under pseudo-global warming (pgw) using a “business as usual” forcing scenario, representative concentration pathway 8.5 (RCP8.5) bias corrected from WRF as described earlier, and were used to analyze the impacts of individual and combined impacts of climate change and forest disturbances on streamflow.

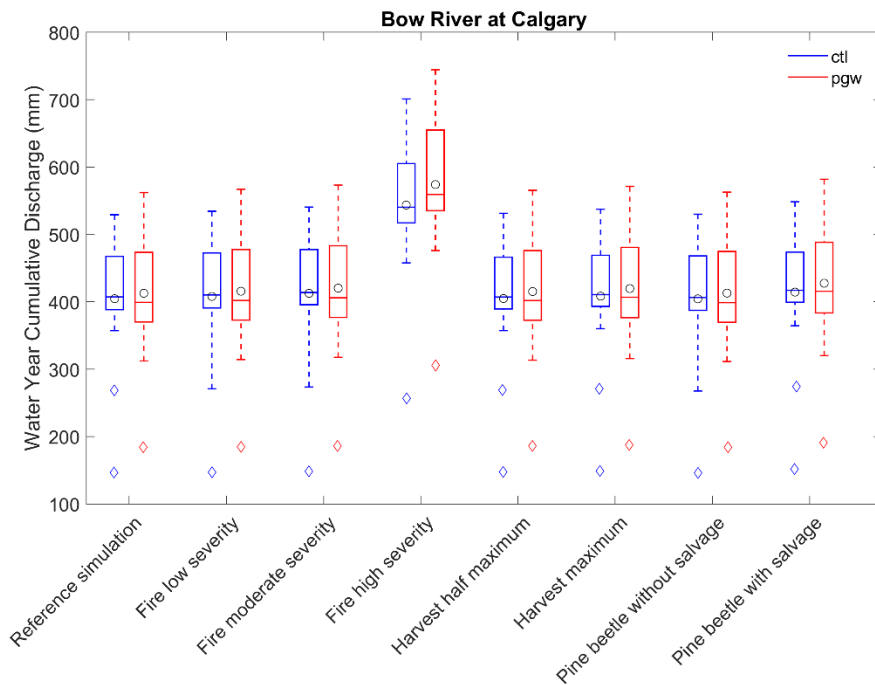
Boxplots of the simulated annual cumulative discharge in both ctl and pgw are shown in Figure 57 for Bow River at Banff, Bow River at Calgary, and Elbow River at Calgary for the 15 water years to assess impacts of climate change and forest disturbance scenarios on annual streamflow discharge volumes. The reference simulation in the figures refers to the streamflow simulation with intact forest conditions, with (pgw) and without (ctl) climate change. For all basins, there was more annual flow volume for the climate change reference simulation (pgw) compared to that in ctl (Tables 6 to 8). The 15-water year mean annual flow volumes proportional increases (%) under climate change increased to 578 mm (10%), 413 mm (2%), and 347 mm (7%) for Bow River at Banff, Bow River at Calgary, and Elbow River basins at Calgary, respectively. Increases in streamflow discharge for the Bow River at Banff were greater for the second lowest flow year (2001-2002) at 24.2% than for the highest flow year (2012-2013) where increases were only 14%, but increases for the lowest flow year (2000-2001) were only 12%. Increases in discharge for the Elbow River and Bow River at Calgary due to climate change were 32.9% and 26% respectively

for the lowest flow year (2000-2001) and only 13.9% and 6.2% respectively for the highest flow year (2012-2013). In general, increases in streamflow discharge volume due to climate change were larger for low flow years than for high flow, including flood, years.

(a)



(b)



(c)

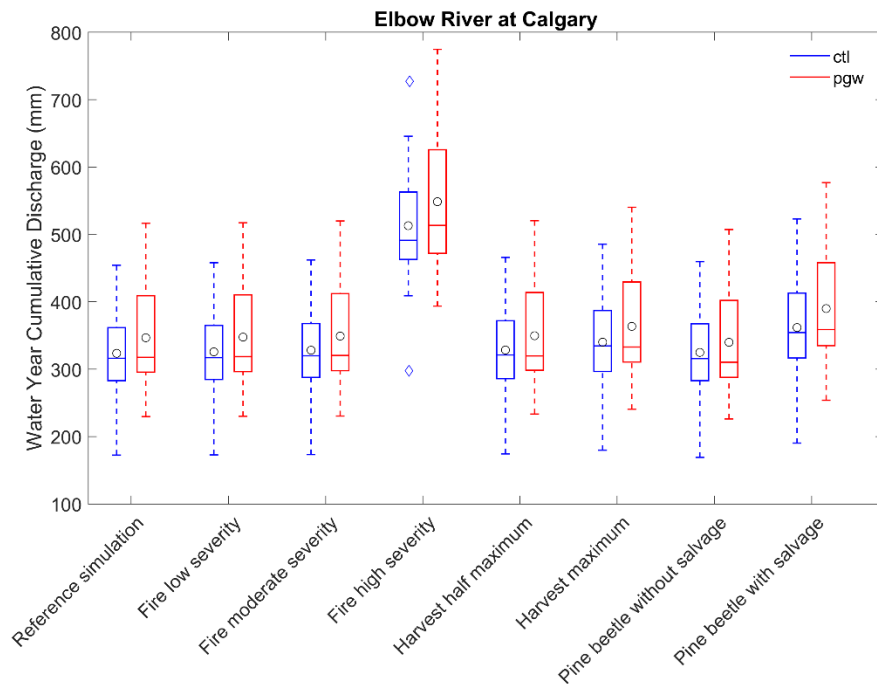


Figure 57. Boxplots of the simulated annual discharge for (a) Bow River at Banff, (b) Bow River at Calgary, and (c) Elbow River at Calgary for 15 water years. The horizontal lines within the boxes are the median values of the 15-water year data, the boxes are the interquartile ranges (IQR = Q1: 25% to Q3: 75%) of the 15-water year data, the whiskers are the Q1 – (1.5 times the IQR) and Q3 + (1.5 times the IQR), the diamonds are the outliers beyond 1.5 times the IQR, the circles are the mean values of the 15-water year data.

For all basins, the annual flow volume had highest increase for the high fire severity scenario. The 15-water year mean annual flow volume increased from 524 mm in the reference simulation (ctl) to 649 mm for the high fire severity scenario (ctl), a 24% increase for Bow River at Banff, and that increased even higher to 733 mm, a 40% increase in high fire severity scenario with pgw (climate change and high fire) for the Bow River at Banff (Table 6). For the Bow River at Calgary, the 15-water year mean annual flow volume rose from 405 mm in the reference simulation (ctl) to 544 mm (34% increase) and 574 mm (42% increase) for the high fire severity scenario in ctl and pgw (climate change and high fire) respectively (Table 7). The 15-water year mean annual flow volume for the Elbow River at Calgary increased from 324 mm in the reference simulation (ctl) to 513 mm in the high fire severity scenario (ctl), a 59% increase, and even higher to 549 mm (70% increase) in high fire severity scenario with pgw (climate change and high fire) (Table 8). For the Bow River at Banff, there were moderate increases in the 15-water year mean annual flow volume from 524 mm in the reference simulation (ctl) to 583 mm (11% increase) and 589 mm (12% increase) for low and moderate fire scenarios with pgw, respectively.

For the Bow River at Calgary, there were small increases in the 15-water year mean annual flow volume, from 405 mm in reference simulation in ctl to 414 mm in pine beetle with salvage scenario in ctl and from 405 mm to 413 mm in moderate fire severity scenario (ctl) - about a 2% increase for both scenarios (Table 7). In other disturbance scenarios (ctl) for the Bow River at Calgary, the increase in the 15-water year mean annual flow volume was smaller than 1%. For harvest and pine beetle scenarios under climate change (pgw) for the Bow River at Calgary, the 15-water year mean annual flow volume ranged from 413 mm (2% increase) for the pine beetle without salvage logging scenario to 420 mm (4% increase) for both moderate fire severity and pine beetle with salvage scenarios compared to the reference simulation (ctl) (Table 7). For the Elbow River at Calgary, the 15-water year mean annual flow volume increased from 324 mm in the reference simulation (ctl) to 362 mm, an 11% increase, for the pine beetle with salvage logging scenario (ctl) and increased from 324 mm to 340 mm, a 5% increase, for the harvest maximum scenario (ctl) (Table 8). Increases in the 15-water year mean annual flow volumes were within 1.5% for the other disturbance scenarios (ctl) for the Elbow River. For future climate harvest and pine beetle scenarios (pgw) for the Elbow River, the 15-water year mean annual flow volumes ranged from 340 mm (5% increase) for pine beetle without salvage logging scenario to 390 mm (21% increase) for pine beetle with salvage logging scenario compared to the reference simulation (ctl) (Table 8).

Table 6. Simulated annual total discharge (mm) in forest disturbance scenarios in ctl and pgw for Bow River at Banff.

	ctl				pgw			
	Reference simulation	Fire low severity	Fire moderate severity	Fire high severity	Reference simulation	Fire low severity	Fire moderate severity	Fire high severity
2000-2001	240	241	243	366	269	270	272	387
2001-2002	398	402	406	618	495	498	503	690
2002-2003	461	465	472	608	523	527	533	672
2003-2004	547	551	556	723	603	607	612	795
2004-2005	524	530	535	622	592	595	601	729
2005-2006	531	533	532	608	536	539	544	650
2006-2007	561	563	565	703	592	596	602	766
2007-2008	537	541	543	654	541	545	551	683
2008-2009	510	514	517	583	550	555	561	696
2009-2010	549	552	554	698	600	604	610	768
2010-2011	541	548	556	664	605	610	617	767
2011-2012	598	601	606	723	703	709	718	898
2012-2013	649	654	658	758	740	745	754	899
2013-2014	628	633	639	746	688	695	703	848
2014-2015	589	595	600	660	640	646	653	748
15-water year mean	524	528	532	649	578	583	589	733

Table 7. Simulated annual total discharge (mm) in forest disturbance scenarios in ctl and pgw for Bow River at Calgary.

	ctl								pgw							
	Reference simulation	Fire low severity	Fire moderate severity	Fire high severity	Harvest half maximum	Harvest maximum	Pine beetle without salvage	Pine beetle with salvage	Reference simulation	Fire low severity	Fire moderate severity	Fire high severity	Harvest half maximum	Harvest maximum	Pine beetle without salvage	Pine beetle with salvage
2000-2001	146	147	148	257	148	149	146	152	184	185	186	306	186	188	184	191
2001-2002	269	271	274	458	269	271	268	275	312	314	318	476	314	316	311	320
2002-2003	357	359	362	533	357	360	356	365	368	370	375	549	370	374	367	381
2003-2004	387	389	394	549	388	391	386	397	406	408	413	582	410	415	406	424
2004-2005	396	400	405	545	398	403	395	413	398	401	405	561	402	408	397	419
2005-2006	411	414	417	514	412	416	411	421	357	359	363	483	359	364	357	372
2006-2007	416	418	422	556	416	419	415	425	401	403	407	558	402	406	400	412
2007-2008	403	406	411	532	402	406	402	412	382	385	389	533	385	389	382	398
2008-2009	402	405	410	501	400	404	401	410	395	397	401	548	397	401	395	409
2009-2010	424	428	433	608	424	429	424	437	436	439	445	635	440	446	437	457
2010-2011	457	462	469	603	457	460	458	466	475	479	484	659	478	482	476	491
2011-2012	481	484	490	606	481	484	482	490	510	515	521	694	513	519	511	528
2012-2013	529	534	541	701	531	538	530	549	562	567	573	744	565	571	563	582
2013-2014	522	527	535	656	522	526	523	532	538	540	547	716	540	545	539	554
2014-2015	470	475	479	535	468	471	470	475	468	473	479	568	469	472	470	477
15-water year mean	405	408	413	544	405	408	404	414	413	416	420	574	415	420	413	428

Table 8. Simulated annual total discharge (mm) in forest disturbance scenarios in ctl and pgw for Elbow River at Calgary.

	ctl								pgw							
	Reference simulation	Fire low severity	Fire moderate severity	Fire high severity	Harvest half maximum	Harvest maximum	Pine beetle without salvage	Pine beetle with salvage	Reference simulation	Fire low severity	Fire moderate severity	Fire high severity	Harvest half maximum	Harvest maximum	Pine beetle without salvage	Pine beetle with salvage
2000-2001	173	173	173	298	174	180	169	190	230	230	231	394	233	241	226	254
2001-2002	229	230	233	409	230	238	224	253	261	262	262	423	264	273	257	289
2002-2003	272	271	274	483	276	285	270	303	309	310	310	521	309	322	300	346
2003-2004	298	299	302	480	299	309	293	329	296	297	298	487	298	313	287	342
2004-2005	310	312	313	565	319	336	308	370	340	341	341	589	343	363	327	403
2005-2006	309	312	315	482	314	326	310	347	283	283	284	444	285	300	275	328
2006-2007	323	325	325	502	327	338	323	359	296	296	298	469	298	310	290	334
2007-2008	322	322	325	500	323	333	322	350	322	323	325	532	325	340	313	372
2008-2009	280	282	285	429	283	294	281	314	313	314	316	506	315	325	308	346
2009-2010	362	365	368	627	373	389	365	420	410	411	413	679	416	434	402	469
2010-2011	362	365	367	551	368	379	368	399	406	407	409	629	413	427	402	454
2011-2012	379	383	387	537	385	397	385	416	411	413	415	612	414	430	403	459
2012-2013	454	458	462	727	466	486	460	523	517	517	520	775	520	540	507	577
2013-2014	427	431	435	646	436	450	436	475	457	459	461	684	460	475	452	503
2014-2015	355	358	360	459	354	363	359	381	351	352	354	487	352	360	350	375
15-water year mean	324	326	328	513	329	340	325	362	347	348	349	549	350	364	340	390

1.3 Key Findings and Conclusions

Canadian Rockies Hydrological Observatory (CRHO)

- The CRHO, operated during and by this study, provided an unprecedented range of mountain multiscale hydrological, meteorological, ecological, cryospheric and subsurface field data for improving our understanding of mountain hydrology and for driving and testing novel hydrological models. The co-location of modelling and process hydrology studies led to rapid uptake of new scientific information into models.

Mountain forest evapotranspiration

- Evapotranspiration and tree transpiration in a sub-alpine forest were quantified for two hydrologically varying study years (wet and dry)
- The drier summer resulted in higher transpiration and evapotranspiration levels, with no recharge to groundwater from surface water inputs during the growing season
- Successive years of summer droughts could impact successional growth of subalpine forests as juvenile trees rely on soil moisture which was low in a drought year
- Windblown snow trapped by vegetation is an important input to summer growth and water supply of sub-alpine forests, both at treeline and lower elevations

Storm runoff celerity as a function of soils and topography

- Warmer winters will result in shallower winter snowpacks and colder soils due to reduced insulation from the winter snowpack.
- Deep learning of streamflow regimes from hydrometric stations throughout the Mountain West of North America has outlined a way to classify regimes and also changes to regime with climate change. This will aid in regionalizing hydrological model application to river basins.

Snowmelt dynamics at forest edges

- A combination of LiDAR measurements from UAVs and remote sensing from satellites is proving useful in quantifying snowpacks in the alpine-subalpine transition. UAV-borne LiDAR can measure snowdepth accurately even under forest canopies and so can be used to inform and evaluate snow models.
- An improved understanding of blowing snow and turbulence interactions has pointed the way for new alpine blowing snow model development that takes into account sweep and ejection motions of the atmosphere rather than relying solely on time-averaged wind flows. This will improve alpine-subalpine snow modelling accuracy.
- An improved understanding and ability to simulate water flow through heterogeneous snowpacks is providing the basis to reformulate operational hydrological models so that they are more accurate in simulating runoff timing during rain-on-snow floods. The water entry pressure to dry snow is a crucial parameter for these improved models.

Wetland storage and drainage

- Together, studies of wetlands in alpine, subalpine, and foothill locations highlight the differences in hydrological functions of wetland, such as evapotranspiration, contributing flow, recharging and transmitting flow, and how this relates to topographic position and hydrographic position. Not all wetlands have equal function and those in foothill locations can be particularly important, but changing, throughout the summer whereas high elevations wetlands have seasonal importance.
- Mountain wetlands supply important baseflow during drought conditions
- Beaver-dammed wetlands provide important reduction in flood streamflow peaks, even in the highest flow conditions on record (June 2013)

Groundwater storage, flow paths and hydraulic response time

- An improved understanding of groundwater flowpaths has been developed based on intensive field studies
- Contributions to streamflow, baseflow and wetlands characterized
- Complex systems of coarse sediments in mountain headwaters (talus slopes, moraines, rock glaciers) are expected to play an important role in temporary storage of glacier melt, snowmelt and rain
- These results help inform regional hydrological model storage components

Marmot Creek Research Basin under Climate Change

- Under a “business as usual” climate change scenario, the basin warms up by 4.7 °C and receives 16% more precipitation, which leads to a 40 mm decline in seasonal peak snowpack, 84 mm decrease in snowmelt volume, and 49 days shorter snowcover duration.
- This will lead to earlier runoff of from 12% to 27% in most ecozones, whereas the treeline ecozone has a small (3%) decrease in runoff volume due to decreased melt volumes from smaller snowdrifts. Higher streamflows will occur in spring and fall and lower streamflows in late summer. Marmot Creek annual streamflow discharge will increase by 18%.

High Mountain Hydrological Prediction

- GEM weather model outputs at 2.5 km have insufficient accuracy for reliable hydrological modelling of high mountain basins.
- High mountain hydrology is dominated by snowmelt in the Canadian Rockies and so a full representation of snow redistribution by wind and gravity, snow interception and the impact of slope and aspect on energy availability for melt is crucial for accurate hydrological modelling.

Glacier Hydrology Modelling

- Detailed modelling of Peyto Glacier Research Basin indicate an increase in runoff from the 1960s to recent years. This increasing trend suggest the glacier is still able to provide a significant contribution to streamflow and buffer low water years. However, the melt patterns are changing; snowmelt peak is now a month earlier than historical values and glacier melt extends further into the fall.
- Diagnosis of model runs shows that high flow years have 34% more annual streamflow than low flow years, the source of extra streamflow in high flow years is from: + 13% snowmelt, + 80% icemelt, + 280% firmelt, + 106% rainfall-runoff and visible changes in the transition season, with earlier spring melt and increased fall rainfall-runoff.

Modelling the Bow and Elbow River Basin under Climate Change and Forest Disturbances

- The Cold Regions Hydrological Model (CRHM) was setup with almost 3000 HRU for the Bow and Elbow river basins above Calgary. CRHM was driven with bias-corrected WRF model outputs at 10-km resolution and found to predict annual streamflows adequately.
- CRHM was driven by WRF perturbed under pseudo-global warming for a business as usual climate scenario to produce a likely climate of the late 21st C for comparison to the early 21st C.
- CRHM was perturbed to simulate land cover disturbances from wildfire, pine beetle and forest harvesting for the recent and future climate of the basins.
- Annual streamflow volumetric changes for climate change were modest, being increases of 2% for the Bow River and 7% for the Elbow River at Calgary, with higher increases in low flow years.
- The low and moderate severity wildfire, forest harvesting and pine beetle scenarios had little impact on streamflow volumes. The largest impact was on the Elbow River at Calgary where the pine beetle with salvage logging scenario resulted in an 11% increase in streamflow volumes.
- The severe wildfire scenario increased flows on the Bow by 34% and the Elbow by 59% at Calgary. With the combination of severe wildfire and climate change flows on the Bow and Elbow at Calgary increased by 42% and 70% respectively.

The Future

These results will form the basis for future student training and will be presented at conferences in Canada and around the world over the next few years. A follow-on study with AI will further extrapolate and improve modelling from this initial study.

1.4 Scientific Achievements

Highly Qualified Personal

Name	Institution	Level	Period	Thesis Title/Project	Status
HQP name	Name of institution	PhD, Masters, etc.	Insert years	If applicable	Complete, in progress, etc.
Morgan Braaten (Pomeroy)	University of Saskatchewan	Undergrad research assistant	2017-2017	n/a	complete
Uswah Aziz (Westbrook)	University of Saskatchewan	Undergrad research assistant	2017-2017	n/a	complete
Amanda Ronnquist (Westbrook)	University of Saskatchewan	Undergrad	2017-2018	n/a	complete
Emmy Phillips (Pomeroy)	University of Saskatchewan	Undergraduate Student Assistant	2018-present	Canadian Rockies Hydrological Observatory	in progress
Julia Hathaway (Petrone)	University of Waterloo	MSc	2019-present	TBD	in progress
Sheryl Chau (Petrone)	University of Waterloo	MSc	2019-present	TBD	in progress
Jacob Staines (Pomeroy)	University of Saskatchewan	MSc	2018-present	Mountain forest snow interception measurement and modelling	in progress
Hailey Robichaud (Pomeroy/Helgason)	University of Saskatchewan	MSc	2016-present	Climate change and sensitivity in a high alpine catchment	in progress
Stephanie Streich (Westbrook)	University of Saskatchewan	MSc	2016-2019	The hydrological functions of a mountain valley-bottom peatland	in progress
Hongye Wu (Westbrook)	University of Saskatchewan	MSc	2016-present	Contribution of avalanches to an alpine lake-wetland complex	in progress
Jason Mercer (Westbrook)	University of Saskatchewan	MSc	2013-2018	Insights into mountain wetland resilience to climate change: an evaluation of the hydrologic processes contributing to the hydrodynamics of alpine wetlands in the	complete

				Canadian Rocky Mountains	
Greg Hoenmans (Pomeroy/Diiwu)	University of Saskatchewan	MSc thesis	Non-2017-2018	The Effect of Soil Compaction and Runoff Generation on the Eastern Slopes of the Rocky Mountains	complete
Jesse He (Hayashi)	University of Calgary	MSc	2017-present	Hydrogeological characterization and model	in progress
Benjamin Roesky (Hayashi)	University of Calgary	MSc	2017-present	Groundwater-stream interaction in alpine catchments	in progress
Dylan Hrach (Petrone)	University of Waterloo	MSc	2017-present	Quantifying seasonal evapotranspiration of a sub-alpine wetland, Kananaskis, Alberta	in progress
Jessica Williamson (Petrone)	University of Waterloo	MSc	2017-present	Assessing the role of tree growth patterns on the spatial variability of evapotranspiration on a subalpine hill-slope in Kananaskis, Alberta	in progress
Lindsey Langs (Petrone)	University of Waterloo	MSc	2016-2019	Quantifying coniferous subalpine tree transpiration and source water in the Canadian Rocky Mountains	complete
Evan Siemens (Pomeroy)	University of Saskatchewan	MSc	2011-2016	The effects of climate variability on hydrological processes in a Canadian Rocky Mountain headwater catchment	complete
Craig Christensen (Hayashi)	University of Calgary	MSc	5/2016-7/2017	A geophysical study of alpine groundwater processes and their geologic controls in the southeastern Canadian Rocky Mountains	complete
Abby Wang (Petrone)	University of Waterloo	PhD	2019-present	TBD	in progress
Victor Tang (Carey)	McMaster University	PhD	2016-present	Characterizing hydrological change in mountain river basins	in progress

Nikolas Aksamit (Pomeroy)	University of Saskatchewan	PhD	2016-2017	Alpine Turbulence and Blowing Snow	complete
Nicolas Leroux (Pomeroy)	University of Saskatchewan	PhD	2016-2018	Mass and Heat Flow through Snowpacks	complete
Zhibang Lv (Pomeroy)	University of Saskatchewan	PhD	2016-present	Assimilation of snow information into a cold regions hydrological model	in progress
Chris Marsh (Pomeroy/Wheater)	University of Saskatchewan	PhD	2016-present	Multi-Scale Modelling of Cold Regions Hydrology	in progress
Dhiraj Pradhananga (Pomeroy)	University of Saskatchewan	PhD	2016-present	Response of Canadian Rockies Glacier Hydrology to Changing Climate	in progress
Caroline Aubry-Wake (Pomeroy)	University of Saskatchewan	PhD	2017-present	Modelling climate change impacts on glacier hydrology	in progress
André Bertonicini (Pomeroy)	University of Saskatchewan	PhD	2017-present	Snow hydrology, remote sensing, data assimilation and prediction	in progress
Mina Rohanzadegan (Petrone/Pomeroy)	University of Waterloo	PhD	2017-present	High Resolution Large-Eddy Simulations of Flow in Complex Terrain of	in progress
Kabir Rasouli (Pomeroy/Hayashi)	University of Saskatchewan	PDF	2017-present	Climate change and vegetation change impacts on mountain hydrology	in progress
Nikolas Aksamit (Pomeroy)	University of Saskatchewan	PDF	2018-2018	Unsteady flow of mountain blowing snow	complete
Nicolas Leroux (Pomeroy)	University of Saskatchewan	PDF	2018-present	Mass and Heat Flow through Snowpacks	in progress
Phillip Harder (Pomeroy)	University of Saskatchewan	PDF	2018-present	UAV applications to measure mountain snow and hydrometeorology	in progress
Nicholas Wayand (Pomeroy)	University of Saskatchewan	PDF	2016-2018	n/a	completed
Greg Galloway (Pomeroy)	University of Saskatchewan	Technician	4/2016-present	Canadian Rockies Hydrological Observatory	in progress

Eric Courtin (Pomeroy)	University of Saskatchewan	Technician	2017-2018	Canadian Hydrological Observatory	Rockies	complete
Angus Duncan (Pomeroy)	University of Saskatchewan	Technician	2012-2016	Canadian Hydrological Observatory	Rockies	complete
Robin Heavens (Pomeroy)	University of Saskatchewan	Technician	2018-present	Canadian Hydrological Observatory	Rockies	in progress
Mike Mokievsky-Zubok (Pomeroy)	University of Saskatchewan	Research Assistant	2017-present	Canadian Hydrological Observatory	Rockies	in progress
Kirsten Reid (Pomeroy)	University of Saskatchewan	Research Assistant	2017-2017	n/a		complete
Tom Brown (Pomeroy)	University of Saskatchewan	Research Engineer	2016-present	Cold Hydrological development	Regions Model	in progress
Paul Whitfield (Pomeroy)	University of Saskatchewan	Research Fellow	2016-present	Impacts of climate and land cover change on river regime		in progress
Xing Fang (Pomeroy)	University of Saskatchewan	Research Officer	2016-present	Hydrological modelling of climate and land use impacts on the Bow River Basin		in progress
Vincent Vionnet (Pomeroy)	University of Saskatchewan	Visiting Professor	2017-present	Mountain hydrology	snow	in progress
Alistair Wallace (Pomeroy)	University of Saskatchewan	Lab Manager	2018-present	UAV applications to measure mountain snow and hydrometeorology		in progress
Dong Zhao (Pomeroy)	University of Saskatchewan	Research Scientist	2018-present	UAV applications to measure mountain snow and hydrometeorology		in progress
Joseph Shea (Pomeroy)	University of Saskatchewan	Research Scientist	2016-2017	n/a		complete

Publications

*HQP

▪ Contributions – John Pomeroy-led

Rasouli K*, **Pomeroy JW**, Whitfield PH*, (2019). Hydrological Responses of Headwater Basins to Monthly Perturbed Climate in the North American Cordillera, *Journal of Hydrometeorology*, 20(5): 863 - 882.

Fang X*, **Pomeroy JW**, DeBeer C.*, Harder P.*, Siemens E*, (2019). Hydrometeorological data from Marmot Creek Research Basin, Canadian Rockies. *Earth Syst. Sci. Data*, 11, 455-471.

Aksamit, NO*, Whitfield, PH*, (2019). Examining the pluvial to nival river regime spectrum using nonlinear methods: minimum delay embedding dimension. *Journal of Hydrology*, 572, 851-868.

Leroux NR*, **Pomeroy JW**, (2018). Simulation of Capillary Pressure Overshoot in Snow Combining Trapping of the Wetting Phase With a Nonequilibrium Richards Equation Model, *Water Resources Research*, 55(1): 236 - 248.

Krinner G, Derksen C, Essery R, Flanner M, Hagemann S, Clark M, Hall A, Rott H, Brutel-Vuilmet C, Kim H, Ménard CB, Mudryk L, Thacheray C, Wang L, Arduini G, Balsamo G, Bartlett P, Boike J, Boone A, Chéruy F, Colin J, Cuntz M, Dai Y, Decharme B, Derry J, Ducharne A, Dutra E, Fang X*, Fierz C, Ghattas J, Gusev Y, Haverd V, Kontu A, Lafaysse M, Law R, Lawrence D, Li W, Marke T, Marks D, Ménégos M, Nasonova O, Nitta T, Niwano M, **Pomeroy J**, Raleigh MS, Schaedler G, Semenov V, Smirnova TG, Stacke T, Strasser U, Svenson S, Turkov D, Wang T, Wever N, Yuan H, Zhou W, Zhu D, (2018). ESM-Snow MIP: assessing snow models and quantifying snow-related climate feedbacks, *Geoscientific Model Development*, 11(-): 5027 - 5049.

Conway JP*, **Pomeroy JW**, Helgason WD, Kinar NJ*, (2018). Challenges in modelling turbulent heat fluxes to snowpacks in forest clearings, *Journal of Hydrometeorology*, 19(-): 1599 - 1616.

Thériault JM, Hung I, Vaquer P, Stewart RE, **Pomeroy JW**, (2018). Precipitation characteristics and associated weather conditions on the eastern slopes of the Rocky Mountains during March-April 2015, *Hydrology and Earth System Sciences*, 22(8): 4491 - 4512.

Marsh CB*, Spiteri RJ, **Pomeroy JW**, Wheeler HS, (2018). Multi-objective unstructured triangular mesh generation for use in hydrological and land surface models, *Computers and Geosciences*, 119(-): 49 - 67.

Wayand NE*, Marsh CB*, Shea JM*, **Pomeroy JW**, (2018). Globally Scalable Alpine Snow Metrics, *Remote Sensing of Environment*, 213(-): 61 - 72.

Leroux N*, **Pomeroy JW**, (Submitted). Simulation of Capillary Overshoot in Snow Combining Trapping of the Wetting Phase with a Non-Equilibrium Richards Equation Model, *Water Resources Research*

Aksamit NO*, **Pomeroy JW**, (2018). Scale Interactions in Turbulence for Mountain Blowing Snow, *Journal of Hydrometeorology*, 19(-): 305 - 320. DOI: 10.1175/JHM-D-17-0179.1

Pomeroy J, (Feb 15, 2018). As a water crisis looms in Cape Town, could it happen in Canada? In *The Conversation and Maclean's*

MacDonald M, **Pomeroy J**, Essery R, (2018). Water and energy fluxes over northern prairies as affected by chinook winds and winter precipitation, *Agricultural and Forest Meteorology*, 248(-): 372 - 385. DOI: 10.1016/j.agrformet.2017.10.025

Aksamit NO*, **Pomeroy JW**, (2017). The Effect of Coherent Structures in the Atmospheric Surface Layer on Blowing-Snow Transport, *Boundary-Layer Meteorology*, 167 (2): 211 - 233. DOI: 10.1007/s10546-017-0318-2

Whitfield PH*, **Pomeroy JW**, (2017). Assessing the quality of the streamflow record for a long-term reference hydrometric station: Bow River at Banff, *Canadian Water Resources Journal*, 42(4): 391 - 415. DOI: 10.1080/07011784.2017.1399086

DeBeer C M, **Pomeroy JW**, (2017). Influence of snowpack and melt energy heterogeneity on snow cover depletion and snowmelt runoff simulation in a cold mountain environment, *Journal of Hydrology*, 553(1): 199 - 213. DOI: 10.1016/j.jhydrol.2017.07.051

Leroux NR*, **Pomeroy JW**, (2017). Modelling capillary hysteresis effects on preferential flow through melting and cold layered snowpacks, *Advances in Water Resources*, 107(-): 250 - 264. DOI: 10.1016/j.advwatres.2017.06.024

Pomeroy J.W., M. MacDonald, P. Dornes, R. Armstrong. 2016. Chapter 4 "Water Budgets in Ecosystems". In, *A Biogeoscience Approach to Ecosystems*. Eds. Edward A. Johnson and Yvonne E. Martin. Cambridge University Press, Cambridge, UK. 88-132.

Musselman, K.N* and **J.W. Pomeroy**. Estimation of needleleaf canopy and trunk temperatures and longwave contribution to melting snow. 2017. *Journal of Hydrometeorology*, 18, pp. 555-572. DOI: 10.1175/JHM-D-16-0111.1.

Smith, C.D., A. Kontu, R. Laffin and **J.W. Pomeroy**. 2017. An assessment of two automated snow water equivalent instruments during the WMO Solid Precipitation intercomparison Experiment. *The Cryosphere*, 11, pp. 101-116. DOI: 10.5194/tc-11-101-2017.

Aksamit, N.O.* and **J.W. Pomeroy**. 2016. Near-Surface Snow Particle Dynamics from Particle Tracking Velocimetry and Turbulence Measurements during Alpine Blowing Snow Storms. *The Cryosphere*, 10, pp. 3043-3062. DOI: 10.5194/tc-10-3043-2016.

Harder P*, M. Schirmer, **J.W Pomeroy** and W. Helgason. 2016. Accuracy of snow depth estimation in mountain and prairie environments by an unmanned aerial vehicle. *The Cryosphere*, 10, pp. 2559-2571. DOI: 10.5194/tc-10-2559-2016.

Pomeroy J.W., R.L.H. Essery and W.D. Helgason. 2016. Aerodynamic and Radiative Controls on the Snow Surface Temperature. *Journal of Hydrometeorology*, 17, 2175-2189. 2016. DOI: 10.1175/JHM-D-15-0226.1.

Whitfield P.H. and **J. W. Pomeroy**. 2016. Changes to flood peaks of a mountain river: implications for analysis of the 2013 flood in the Upper Bow River, Canada. *Hydrological Processes*, 30(25), 4657-4673. DOI: 10.1002/hyp.10957.

Pomeroy J.W., Xing F*, and Marks D. 2016. The Cold Rain-on-Snow Event of June 2013 in the Canadian Rockies – Characteristics and Diagnosis. *Hydrological Processes*, 30(17), 2899-2914. DOI:10.1002/hyp.10905.

Fang X* and **Pomeroy J.** 2016. Impact of antecedent conditions on simulations of a flood in a mountain headwater basin. *Hydrological Processes*, 30(16), 2754-2772. DOI: 10.1002/hyp.10910.
Liu A., Mooney C., Szeto K., Thériault J.M., Kochtubajda B., Stewart R.E., Boodoo S., Goodson R., Li Y., and **Pomeroy J.** 2016. The June 2013 Alberta Catastrophic Flooding Event: Part 1 – Climatological aspects and hydrometeorological features. *Hydrological Processes*. DOI: 10.1002/hyp.10906.

Rothwell R., Hillman G., and **Pomeroy J.W.** 2016. Marmot Creek Experimental Watershed Study. *The Forestry Chronicle*, 92 (1): p. 32-36. DOI: 10.5558/tfc2016-010.

▪ Contributions – Masaki Hayashi-led

Christensen, C.W.* , **Hayashi, M.** and Bentley, L.R. Hydrogeological characterization of an alpine aquifer system in the Canadian Rocky Mountains. *Hydrogeology Journal* (to be submitted in May 2019).

He, J.* and **Hayashi, M.** 2019. Lake O'Hara alpine hydrological observatory: Hydrological and meteorological dataset, 2004-2017. *Earth System Science Data*, 11: 111-117.

Harrington, J.S., Mozil, A., **Hayashi, M.** and Bentley, L.R. 2018. Groundwater flow and storage processes in an inactive rock glacier. *Hydrological Processes*, 32: 3070-3088.

Christensen, C.W.* , Hayashi, M. and Bentley, L.R. (2017) Scanning Calgary's 'water towers': Applications of hydrogeophysics in challenging mountain terrain. *CSEG Recorder* (in press).

▪ Contributions – Rich Petrone-led

Langs, L*, **Petrone, R.** Quantifying subalpine forest water use during two hydrologically variable growing seasons in the Canadian Rocky Mountain. *Hydrological Processes* (To be submitted in June, 2019).

Langs, L*, **Petrone, R.** A $\delta^{18}\text{O}$ and $\delta^2\text{H}$ stable isotope analysis of subalpine forest water sources under seasonal and hydrological stress. *Ecohydrology* (To be submitted in June, 2019).

▪ Contributions – Cherie Westbrook-led

Mercer J*, **Westbrook CJ.** The impact of soil hydrophysical and microtopographic patterns on ecosystem specific yield in Canadian alpine wetlands. *Journal of Hydrology* (to be submitted in July 2019).

Mercer J*, **Westbrook CJ.** Hydrological processes regulating water table dynamics of an alpine peatland in the Canadian Rockies. *Journal of Hydrology* (to be submitted in August 2019).

Westbrook CJ, Ronnquist A*, Bedard-Haughn A. Transient floodwater storage provided by beaver ponds. *Ecohydrology* (to be submitted in July 2019).

Streich SC*, **Westbrook CJ.** Hydrological function of a mountain fen at low elevation under dry conditions. *Hydrological Processes* (under review).

Westbrook, CJ. Hydrological lessons learned from studying Rocky Mountain peatlands drained by streams. *Wetlands in Yukon: A Science-Based Discussion*. Whitehorse, Yukon, March 2, 2017.

Mercer J.*, **Westbrook CJ.** 2016. Ultrahigh resolution mapping of peatland microform with ground-based structure from motion with multi-view stereo. *Journal of Geophysical Research – Biogeosciences* 121: 2901-2916.

▪ Contributions – Sean Carey-led

Wang, H.*, Tetzlaff, D., Buttle, J., **Carey, S.**, Laudon, H., McNamara, J.P., Spence, C., Soulsby, C. (2019). Climate-phenology-hydrology interactions in northern high latitudes: Assessing the value of remote sensing data in catchment ecohydrological studies. *Science of the Total Environment*, 656, 19-28.

▪ Contributions – Warren Helgason-led

Conway JP*, Pomeroy JW, **Helgason WD**, Kinar NJ*, (2018). Challenges in modelling turbulent heat fluxes to snowpacks in forest clearings, *Journal of Hydrometeorology*, 19(-): 1599 - 1616.

Important Meetings, Events, Presentation and Distinctions

*HQP

▪ Contributions – John Pomeroy-led

Invited

Pomeroy J, Pietroniro A, Davison B, Princz D, (2019). Global Water Futures and the MESH Modelling System for Water Forecasting & Prediction. Regional Environmental Centre for Central Asia (CAREC) Regional Round Table, Almaty, Kazakhstan, May 27, 2019

Pomeroy J, (2019). Rocky Mountain Water Supply Resilience and Vulnerability Evaluation. Alberta Innovates Water Innovation Program (WIP) Forum, Edmonton, Canada, May 22, 2019

Leroux NR*, **Pomeroy JW**, (2018). Improving the simulation of capillary pressure in snow with a non-equilibrium Richards equation model. International Symposium on Snow and Avalanche, Niseko, Japan, December 7, 2018

Pomeroy J, (2018). Impact of meteorological forcing data on snowpack and streamflow simulations in the Canadian Rockies. Fourth Annual International Network for Alpine Research Catchment Hydrology (INARCH) Workshop, Portillo, Chile, October 25, 2018

Pomeroy J, (2018). How interactions between climate and vegetation impact hydrological processes in mountain headwater basins. Fourth Annual International Network for Alpine Research Catchment Hydrology (INARCH) Workshop, Portillo, Chile, October 25, 2018

Pomeroy J, (2018). International Network for Alpine Research Catchment Hydrology (INARCH). Fourth Annual International Network for Alpine Research Catchment Hydrology (INARCH) Workshop, Santiago and Portillo, Chile, October 24, 2018

Pomeroy J, (2018). Global Water Futures (GWF) RHP. GEWEX Hydroclimatology Panel (GHP) Meeting, Santiago, Chile, October 24, 2018

Pomeroy J, (2018). Global Water Futures for Alberta. Agri-Environmental Partnership of Alberta (AEPA) Advisory Committee Meeting, Edmonton, Canada, October 17, 2018

Pomeroy J, (2018). International Conference Plenary session: Agricultural Water Futures in an era of Changing Agriculture and Climate. International Conference and 69th International Executive Council Meeting of the International Commission on Irrigation and Drainage, Saskatoon, Canada, August 12, 2018

Pomeroy J, (2018). Improving hydrologic process representations. Integrated Modelling Program for Canada (IMPC) First Annual Meeting, Saskatoon, Canada, July 18, 2018

Pomeroy J, (2018). Global Water Futures: Year One Progress. Integrated Modelling Program for Canada (IMPC) First Annual Meeting, Saskatoon, Canada, July 18, 2018

Pomeroy J, (2018). The Global Water Futures Program and its National Water Forecasting and Prediction System for Canada. 3rd Kazakhstan-Canada Business Council Meeting, Ottawa, Canada, June 11, 2018

Pomeroy J, (2018). Rocky Mountain Water Supply Resilience and Vulnerability Evaluation. Alberta Innovates Water Innovation Program Forum, Edmonton, Canada, May 23, 2018

Pomeroy J, (2018). Extreme Hydrology, Climate Change and Water Futures in Canada. Insurance Brokers Association of Alberta (IBAA), Banff, Canada, May 6, 2018

Pomeroy J, (2018). Opening Plenary: Global Water Futures Program and its Science Contributions to GEWEX. 8th Global Energy and Water Exchanges (GEWEX) Open Science Conference: Extremes and Water on the Edge, Canmore, Canada, May 6, 2018

Pomeroy J, (2018). The role of integrating observation and prediction systems in generating data and learning from models - a hydrological and weather extremes perspective. Joint Young Earth System Scientists (YESS) and Young Hydrologic Society (YHS) Early Career Researcher (ECR) Workshop at the 8th Global Energy and Water Exchanges (GEWEX) Conference, Canmore, Canada, May 3, 2018

Pomeroy J, (2018). Upcoming projects and work by Global Water Futures. Government of Alberta Workshop on Floodplain Mapping and Climate Change, Edmonton, March 20, 2018

Short documentary film - *Changing Climate and Environment of Western Canada*, March 6, 2018

Pomeroy J, Helgason W, (2018). Theme B overview and synthesis: CCRN Special Observation and Analysis Period (SOAP). Changing Cold Regions Network Annual General Meeting "The CCRN Finale", Saskatoon, March 5, 2018

DeBeer C, Wheeler H, **Pomeroy J**, (2018). CCRN status and future directions as a GEWEX RHP. Changing Cold Regions Network Annual General Meeting "The CCRN Finale", Saskatoon, March 5, 2018

Pomeroy J, (2018). Cold regions process and modelling studies. Changing Cold Regions Network Annual General Meeting "The CCRN Finale", Saskatoon, March 5, 2018

Pomeroy J, Rasouli K*, Fang X*, Whitfield P*, Marks D, Janowicz R, (2017). Water Futures for Cold Mountain Ecohydrology under Climate Change - Results from the North American Cordilleran Transect. AGU Fall Meeting, New Orleans, December 11, 2017

Pomeroy J, Pradhananga D*, Brown T*, Anderson E*, Demuth M, (2017). Modelling Changing Glacier Hydrological Processes using an Object Oriented Cold Regions Hydrological Model and Long-term In-situ and Remote Sensing Information. AGU Fall Meeting, New Orleans, December 11, 2017

Marsh C*, **Pomeroy J, Wheeler H, (2017).** Simulating Complex, Cold-region Process Interactions Using a Multi-scale, Variable-complexity Hydrological Model. American Geophysical Union Fall Meeting, New Orleans, December 11, 2017

InterAction Council, High-Level Expert Group (HLEG), Canadian international policy on water, peace and security, Ottawa, November 28, 2017

Pomeroy J, (2017). Plenary presentation. Rocky Mountain Water Supply Resilience and Vulnerability Evaluation. 2017 Alberta Irrigation Projects Association Water Conference, Lethbridge, November 20, 2017.

External Review Panel Member for the Integrated Network Design Project conducted by the Meteorological Service of Canada (MSC), November 2017 to January 2018.

Pomeroy J, Shook K*, Fang X*, Annand H*, Krogh S*, (2017). Overview of CRHM development and application at the observatories, including long term diagnostic CRHM runs using WRF PGW, station downscaled RCM and statistically downscaled RCM, including transient change impacts. Discussion on insights from fine-scale results for large-scale modelling and next steps. Changing Cold Regions Network Modelling and Theme D Workshop, Canmore, November 2, 2017

Blue Ribbon Panel Review of Environment and Climate Change Canada's National Hydrological Service Workshop, National Hydrological Service, Ottawa, October 2017 to November 2017

Pomeroy J, (2017). Guest speaker. The big thaw, Canada and the Global Water Futures Programme. Grantham Institute Seminar, Imperial College, London, October 27, 2017

Pomeroy J and INARCH members, (2017). Climate Change and Mountain Hydrology: Results from the Global Energy and Water Exchange Project's International Network for Alpine Research Catchment Hydrology. Knowledge Forum on Water Security and Climate Change: Innovative Solutions for Sustainable Water Resources Management, UNESCO, Paris, October 18, 2017

Pomeroy J, (2017). The Global Water Futures Programme and its Science Contributions to the UN's Sustainable Development Goals and the Paris Climate Agreement. Knowledge Forum on Water Security and Climate Change: Innovative Solutions for Sustainable Water Resources Management, UNESCO, Paris, October 18, 2017

DeBeer C, **Pomeroy J, (2017).** International Network for Alpine Research Catchment Hydrology (INARCH). 2017 GEWEX Hydroclimate Program – Third Pole Environment, Joint Meeting, Kathmandu, Nepal, October 17, 2017

Pomeroy J, (2017). **Keynote presentation**. The Global Water Futures Programme and the National Water Prediction and Forecasting System. Canadian Dam Association Conference & Exhibition, Kelowna, October 14, 2017.

Pomeroy J, (2017). Cold regions hydrology in mountain and northern river basins: measurements, processes and modelling. High Altitudes meet High Latitudes: Globalizing Polar Issues Conference, Crans-Montana, Switzerland, September 11, 2017

Pomeroy J, Westbrook C, McDonnell J, Helgason W, Ireson A, Bedard-Haughn A, (2017). Canadian Rockies Hydrological Observatory. Global Institute for Water Security Annual Progress and Plans Workshop, Saskatoon, June 12, 2017

Pomeroy J, (2017). Rocky Mountain Water Supply Resilience and Vulnerability Evaluation. Alberta Innovates - Water Innovation Program Forum, Edmonton, May 24, 2017

Pomeroy J, (2017). Global Water Futures. Bow River Basin Council 2017 Science Forum, Calgary, May 3, 2017

Non-invited

Whitfield P*, **Pomeroy J**, (2019). Examining the Pluvial to Nival River Regime Spectrum across North America Using Nonlinear Methods. 2019 Canadian Water Resources Association (CWRA) National Conference, Blue Mountain Resort, Canada, May 26, 2019

Rasouli K*, **Pomeroy J**, (2019). Impacts of Climate, Vegetation, and Soil Changes on Hydrological Processes in Wolf Creek Research Basin, Yukon Territory, Canada. Arctic Science Summit Week 2019 Climate Change and Development of the Arctic Population, Arkhangelsk, Russia, May 22, 2019

Thériault J, Déry S, **Pomeroy J**, Stewart R, Almonte J, (2019). Storms and Precipitation Across the Continental Divide Experiment (SPADE): Overview of the current field project. Global Water Futures Second Annual Open Science Meeting, Saskatoon, Canada, May 15, 2019

Loukili Y*, **Pomeroy J**, (2019). Forensic glacial hydrology of the Slims River piracy and the fate of Yukon's Kluane Lake levels. Global Water Futures Second Annual Open Science Meeting, Saskatoon, Canada, May 15, 2019

Vionnet V*, Marsh C*, Menounos B, Shea J, **Pomeroy JW**, (2019). Multi-scale snowdrift-resolving modelling of mountain snowpack evolution. Global Water Futures Second Annual Open Science Meeting, Saskatoon, Canada, May 15, 2019

Asong ZE, Wheeler HS, **Pomeroy JW**, Pietroniro A, Elshamy M, (2018). Regional scenarios of change over western Canada: future climate projections. American Geophysical Union (AGU) Annual Meeting, Washington, United States, December 10, 2018

Pradhananga D*, **Pomeroy JW**, (2018). Hydrological Response of Two Mountain Glaciers in the Canadian Rockies to Warming Climate and Change in Glacier Configurations. American Geophysical Union (AGU) Annual Meeting, Washington, United States, December 10, 2018

Aubry-Wake C*, **Pomeroy JW**, (2018). Influences of glacier retreat, summer weather and winter snowpack on the increased variability in runoff composition in a quickly changing glacierized catchment. American Geophysical Union (AGU) Annual Meeting, Washington, United States, December 10, 2018

Rohanizadegan M*, Kosovic B, **Pomeroy JW**, Petrone RM, Helgason WD, (2018). Evaluating evaporative fluxes in complex mountain terrain. Joint Meeting of the Canadian Geophysical Union (CGU), Canadian Soil Science Society, Computational Infrastructure in Geodynamics, Eastern Section of Seismological Society of America and Canadian Society for Agricultural and Forest Meteorology, Niagara Falls, Canada, June 10, 2018

Kinar NJ*, **Pomeroy JW**, (2018). Internet of Things (IoT) Systems and Measurement of Snowpacks. Joint Meeting of the Canadian Geophysical Union (CGU), Canadian Soil Science Society, Computational Infrastructure in Geodynamics, Eastern Section of Seismological Society of America and Canadian Society for Agricultural and Forest Meteorology, Niagara Falls, Canada, June 10, 2018

Shea J*, Whitfield P*, **Pomeroy J**, (2018). The role of basin geometry on snow sensitivity in mountain basins. Joint Meeting of the Canadian Geophysical Union (CGU), Canadian Soil Science Society, Computational Infrastructure in Geodynamics, Eastern Section of Seismological Society of America and Canadian Society for Agricultural and Forest Meteorology, Niagara Falls, Canada, June 10, 2018

Leroux N*, **Pomeroy J**, Helgason W, (2018). Impact of heat advection induced by topography-driven air ventilation on snow surface temperature. 75th Annual Eastern Snow Conference (ESC): SNOW PAST PRESENT and FUTURE, College Park, Maryland, USA, June 5, 2018

Whitfield PH*, Shook KR*, Kraaijenbrink P, **Pomeroy JW**, (2018). Changing cold regions in western Canada: hydrology and hydrological and landscape change east of the Cordillera. The 71st Canadian Water Resources Association (CWRA) National Conference, Victoria, Canada, May 28, 2018

DeBeer C, Wheeler H, **Pomeroy J**, Stewart R, Carey S, (2018). Climatic, Cryospheric, Ecological, and Hydrological Change in the Interior of Western Canada: The Changing Cold Regions Network and its activities as a GEWEX RHP. 8th Global Energy and Water Exchanges (GEWEX) Open Science Conference: Extremes and Water on the Edge, Canmore, Canada, May 6, 2018

Aubry-Wake C*, **Pomeroy JW**, (2018). Impacts of snowpack accumulation and summer weather extremes on alpine glacier hydrology. 8th Global Energy and Water Exchanges (GEWEX) Open Science Conference: Extremes and Water on the Edge, Canmore, Canada, May 6, 2018

Leroux N*, **Pomeroy J**, (2018). Simulation of capillary overshoot in snow with a non-equilibrium Richards equation model combined with a trapping model for the water phase. European Geosciences Union (EGU) General Assembly, Vienna, Austria, April 8, 2018

***Pomeroy J**, Pietroniro A, Shook K*, (2018). Using Science and Enlightened Modelling to Fight Hydromthology, Zombie Models and Hydrological Indifference in Prediction of Ungauged Basins. European Geosciences Union (EGU) General Assembly, Vienna, Austria, April 8, 2018

Shook K*, **Pomeroy J**, (2018). The cold regions hydrological modelling paradox: why complex models can be run successfully with uncalibrated parameterisations. European Geosciences Union (EGU) General Assembly, Vienna, Austria, April 8, 2018

Vionnet V, Wayand N, Marsh C*, Fortin V, **Pomeroy JW**, Snowdrift-resolving atmospheric downscaling for snow hydrological forecasting in alpine regions. 3rd Annual INARCH Workshop, Schneefernerhaus Zugspitze, Germany, February 8, 2018

Marsh CB*, Spiteri RJ, **Pomeroy JW**, Wheeler HS, PBSM3D: A complex terrain blowing snow model for use with variable resolution meshes. 3rd Annual INARCH Workshop, Schneefernerhaus Zugspitze, Germany, February 8, 2018

Wayand N*, Marsh C*, Shea J*, **Pomeroy J**, (2017). Remotely Sensed Snow Redistribution Indices. American Geophysical Union Fall Meeting, New Orleans, December 11, 2017

Fortin V, Vionnet V, Dimitrijevic M, Abrahamowicz M, Gauthier N, Garneau C, Belair S, Milbrandt J, **Pomeroy J**, Forecasting of rain-on-snow events in alpine region using a fully coupled atmosphere/snowpack/hydrology model. American Geophysical Union Fall Meeting, New Orleans, December 11, 2017

Shea J*, Harder P*, **Pomeroy J**, Kraaijenbrink P, Improved quantification of mountain snowpack properties using observations from Unmanned Air Vehicles (UAVs). American Geophysical Union Fall Meeting, New Orleans, December 11, 2017

Marsh C*, Wayand N*, **Pomeroy J**, Wheeler H, Spiteri R, (2017). A finite volume, scalar-transport blowing snow model for use with variable resolution meshes. American Geophysical Union Fall Meeting, New Orleans, December 11, 2017

Rasouli K*, **Pomeroy J**, (2017). Permafrost Response to Transient Vegetation and Climate Changes in a Northern Mountain Basin, Canada. The 2nd Asian Conference on Permafrost, Sapporo, Japan, July 2, 2017

Aksamit N*, **Pomeroy J W**, (2017). Coherent structures in the alpine atmospheric surface layer coupled with blowing snow response. International Conference on Alpine Meteorology, Reykjavik, Iceland June 18, 2017

Pradhananga D*, **Pomeroy J**, (2017). Hydrological response of Peyto Glacier to climate change and glacier recession. Canadian Geophysical Union and Canadian Society of Agricultural and Forest Meteorology Joint Annual Scientific Meeting, Vancouver, May 28, 2017

Lv Z*, **Pomeroy J W**, Detecting intercepted snow on mountain needleleaf forest canopies using satellite remote sensing. Canadian Geophysical Union and Canadian Society of Agricultural and Forest Meteorology Joint Annual Scientific Meeting, Vancouver, May 28, 2017

Rasouli K*, Whitfield P H*, Martz L W, Ireson A M, Janowicz J R, Marks D, **Pomeroy J W**, (2017). Are effects of transient vegetation and soil changes as important as climate change impacts on hydrological processes? Canadian Geophysical Union and Canadian Society of Agricultural and Forest Meteorology Joint Annual Scientific Meeting, Vancouver, May 28, 2017

Marsh C*, **Pomeroy J W**, Wheeler H S, Spiteri R, (2017). The Canadian Hydrological Model: A multiscale, multiphysics, variable-complexity hydrological model. Canadian Geophysical Union and Canadian Society of Agricultural and Forest Meteorology Joint Annual Scientific Meeting, Vancouver, May 28, 2017

Wayand N E*, Marsh C*, **Pomeroy J**, (2017). Evaluating blowing snow and avalanche models over the Canadian Rockies. Canadian Geophysical Union and Canadian Society of Agricultural and Forest Meteorology Joint Annual Scientific Meeting, Vancouver, May 28, 2017

Kinar N J*, **Pomeroy J W**, Shea J*, Schirmer M, Harder P*, (2017). 2D Frequency Analysis of Irregularly Sampled Snowpack Properties. Canadian Geophysical Union and Canadian Society of Agricultural and Forest Meteorology Joint Annual Scientific Meeting, Vancouver, May 28, 2017

Shea J M*, Harder P*, **Pomeroy J W**, (2017). Improving quantification of mountain snowpack properties using observations from Unmanned Air Vehicles (UAVs). Canadian Geophysical Union and Canadian Society of Agricultural and Forest Meteorology Joint Annual Scientific Meeting, Vancouver, May 28, 2017

Fang X*, **Pomeroy J**, Wayand N*, (2017). Evaluating meteorological forcing sources for simulation of snowpack and streamflow in the Canadian Rockies. Canadian Geophysical Union and Canadian Society of Agricultural and Forest Meteorology Joint Annual Scientific Meeting, Vancouver, May 28, 2017

Wayand NE*, Marsh C*, and **Pomeroy J**. Evaluating the impact of blowing snow and avalanche redistribution on modelling alpine snowpack and snowcovered area over the Canadian Rockies. Western Snow Conference, Boise, Idaho, April 17, 2017

▪ **Contributions – Masaki Hayashi-led**

Hayashi was selected by the US National Groundwater Association to serve as the Henry Darcy Distinguished Lecturer in 2018. This is one of the highest international honors in groundwater science. He gave the Darcy Lecture titled “Alpine hydrogeology: The critical role of groundwater in sourcing the headwaters of the world” at 79 locations in 19 countries around the world highlighting the importance of groundwater processes in controlling the hydrology of headwater catchments.

Rasouli, K.*, Pomeroy, J.W., **Hayashi, M.**, Fang, X.*, Gutmann, E.D., Li, Y. Assessment of the suitability of high resolution numerical weather model outputs for hydrological modelling in mountainous cold regions. Fall Meeting of the American Geophysical Union. New Orleans, Louisiana, December 11-15, 2017.

Surface water – groundwater interaction: From watershed processes to hyporheic exchange (GLGY 699.01). Six-day short course attended by 29 students including 12 staff of Alberta Government. University of Calgary, July 17-22, 2017. This course included a field trip to Fortress Ski Area.

Rasouli, K*, Krogh, S., Pavlovskii, I., **Hayashi, M.** and **Pomeroy, J.W.** The role of soil freezing and thawing in hydrological processes: Canadian case studies. The 2nd Asian Conference of Permafrost, Sapporo, Japan, July 2-6, 2017.

Hayashi, M., Christensen, C. and Bentley, L.R. Groundwater studies in the Canadian Rockies. Seminar presented at the Spring Naturalist Weekend, Biogeoscience Institute, University of Calgary, June 10, 2017.

Christensen, C.W., **Hayashi, M.** and Bentley, L.R. A hydrogeophysical survey of groundwater flow pathways in an alpine headwater basin. 22nd European Meeting of Environmental and Engineering Geophysics, Barcelona, Spain, September 4-8, 2016 (invited presentation).

▪ **Contributions – Rich Petrone-led**

Langs, L*., **Petrone, R.** A mixed methods approach to quantifying and understand subalpine forest water use in the Canadian Rocky Mountains, Kananaskis, Alberta. Global Water Futures Annual Science Meeting May 2019, oral presentation.

Williamson, J*., **Petrone, R.** Assessing the role of tree growth patterns on the spatial variability of evapotranspiration on a subalpine hill slope in Kananaskis, Alberta. McMaster Water Week 2018, poster presentation.

Hrach, D*., **Petrone, R.** Quantifying seasonal evapotranspiration of a sub-alpine wetland, Kananaskis, Alberta. McMaster Water Week 2018, poster presentation. Award winner of the GWF Young Professionals Best Student Post Award.

Langs, L*., **Petrone, R.** Investigating alpine forest water use during variable growing season and climate conditions in the Canadian Rocky Mountains, Kananaskis, Alberta. Canadian Geophysical Union Annual Meeting Niagara Falls 2018, oral presentation.

Langs, L*., **Petrone, R.** A $\delta^{18}\text{O}$ and $\delta^2\text{H}$ stable water isotope analysis of subalpine forest water sources under seasonal and hydrological stress in the Canadian Rocky Mountains, Kananaskis, Alberta. Canadian Geophysical Union Annual Meeting Niagara Falls 2018, poster presentation.

Hrach, D*., **Petrone, R.** Quantifying seasonality and role of shading dynamics on a subalpine wetland, Kananaskis, Alberta. CGU Eastern Student Section Meeting 2018, poster presentation.

Williamson, J*., **Petrone, R.** Assessing the role of tree growth patterns on the spatial variability of evapotranspiration on a subalpine hill slope in Kananaskis, Alberta. CGU Eastern Student Section Meeting 2018, poster presentation.

Langs, L*., **Petrone, R.** Investigating alpine forest water use during variable growing season and climate conditions in the Canadian Rocky Mountains, Kananaskis, Alberta. CGU Eastern Student Section Meeting 2018, poster presentation.

Hrach, D., **Petrone, R.** Quantifying seasonality and role of shading dynamics on a subalpine wetland, Kananaskis, Alberta. CGU Eastern Student Section Meeting 2018, poster presentation.

Williamson, J*., **Petrone, R.** Assessing the role of tree growth patterns on the spatial variability of evapotranspiration on a subalpine hill slope in Kananaskis, Alberta. CGU Eastern Student Section Meeting 2018, poster presentation.

Rohanizadegan, M*., **Petrone, R.**, Pomeroy, J., Warren, H. Improving meteorological forcing of mountain evapotranspiration calculations. Canadian Geophysical Union Annual Meeting 2017, poster presentation.

Langs, L*., **Petrone, R.** Methods investigating alpine forest water use under varying environmental conditions in the Canadian Rocky Mountains. Canadian Geophysical Union Annual Meeting Vancouver 2017, poster presentation.

Rohanizadegan, M*., **Petrone, R.**, **Pomeroy, J.**, **Helgason, W.** Improving meteorological forcing of mountain evapotranspiration calculations. 18th Annual WRF User's Workshop, Boulder, Colorado, June 12-16, 2017.

▪ Contributions – Cherie Westbrook-led

Westbrook was invited to be a *scientific advisor* to the development of both the City of Calgary's Watershed Health plan (in 2019) and the Government of Yukon's wetlands policy (in 2018-present) as a result of her research on wetland and groundwater-surface water exchange in the Rocky Mountains.

Mercer JJ*, **Westbrook CJ**. Hydrological processes regulating alpine wetland water table dynamics. Society of Wetland Science Annual Meeting, Denver, Colorado, USA, May 29 – June 1, 2018.

Streich S*, **Westbrook C**. The hydrological functions of a mountain valley-bottom wetland. Canadian Water Resources Association annual meeting, Victoria, BC, May 28 – June 1, 2018.

Westbrook CJ, Ronnquist A*, Bedard-Haughn A. Dynamic beaver pond levels in mountain peatlands provide transient floodwater storage. Society of Wetland Science Annual Meeting, Denver, Colorado, USA, May 29 – June 1, 2018.

Westbrook CJ, Ronnquist A*, Bedard-Haughn A. Dynamic beaver pond levels in mountain peatlands provide transient floodwater storage. International Beaver Symposium, Denmark, September 17 – 20, 2018.

Westbrook CJ, Mercer JJ*, Streich SC*. Comparison of alpine and foothill peatland hydrodynamics. 27th IUGG General Assembly, Montreal, Canada, 8-18 July 2019.

Westbrook, CJ. Hydrological lessons learned from studying Rocky Mountain peatlands drained by streams. Wetlands in Yukon: A Science-Based Discussion. Whitehorse, Yukon, March 2, 2017.

1.5 Selected References

Armstrong RN. 2011. Spatial variability of actual evaporation in a prairie landscape, Ph.D. thesis, Department of Geography and Planning, University of Saskatchewan, Saskatoon, Saskatchewan, Canada, 194 pp.

Ayers HD. 1959. Influence of soil profile and vegetation characteristics on net rainfall supply to runoff. Proceedings of Hydrology Symposium No.1: Spillway Design Floods, NRCC, Ottawa, 198-205.

Beke GJ. 1969. Soils of three experimental watersheds in Alberta and their hydrological significance. Ph.D. thesis, Department of Soil Science, University of Alberta, Edmonton, 456.

Bernhardt M, Schulz K. 2010. SnowSlide: A simple routine for calculating gravitational snow transport. Geophysical Research Letters 37: L11502. DOI:10.1029/2010GL043086.

Brooks RH, Corey AT. 1964. Hydraulic Properties of Porous Media, Hydrology Paper 3. Colorado State University: Fort Collins, Colorado; 27.

Cannon AJ. 2018. Multivariate quantile mapping bias correction: an N-dimensional probability density function transform for climate model simulations of multiple variables. Climate Dynamics 50: 31-49. DOI:10.1007/s00382-017-3580-6.

Chow VT. 1959. Open Channel Hydraulics. McGraw-Hill: New York; 680.

Chow VT. 1964. Handbook of Applied Hydrology. McGraw-Hill: New York; 1495.

Clark CO. 1945. Storage and the unit hydrograph. In Proceedings of the American Society of Civil Engineering, 69: 1419-1447.

DeBeer CM, Pomeroy JW. 2017. Influence of snowpack and melt energy heterogeneity on snow cover depletion and snowmelt runoff simulation in a cold mountain environment. Journal of Hydrology 553: 199-213. DOI:10.1016/j.jhydrol.2017.07.051.

Dornes PF, Pomeroy JW, Pietroniro A, Carey SK, Quinton WL. 2008. Influence of landscape aggregation in modelling snow-cover ablation and snowmelt runoff in a sub-arctic mountainous environment. Hydrological Sciences Journal 53(4): 725-740.

Ellis CR, Pomeroy JW, Brown T, MacDonald J. 2010. Simulation of snow accumulation and melt in needleleaf forest environments. Hydrology and Earth System Sciences 14: 925-940. DOI:10.5194/hess-14-925-2010.

Fang X, Pomeroy JW, Westbrook CJ, Guo X, Minke AG, Brown T. 2010. Prediction of snowmelt derived streamflow in a wetland dominated prairie basin. Hydrology and Earth System Sciences 14: 991-1006. DOI:10.5194/hess-14-991-2010.

Fang X, Pomeroy JW, Ellis CR, MacDonald MK, DeBeer CM, Brown T. 2013. Multi-variable evaluation of hydrological model predictions for a headwater basin in the Canadian Rocky Mountains. Hydrology and Earth System Sciences 17: 1635-1659. DOI:10.5194/hess-17-1635-2013.

Garnier BJ, Ohmura, A. 1970. The evaluation of surface variations in solar radiation income. Solar Energy 13: 21-34.

Granger RJ, Gray DM. 1989. Evaporation from natural non-saturated surfaces. Journal of Hydrology 111: 21-29.

Granger RJ, Pomeroy JW. 1997. Sustainability of the western Canadian boreal forest under changing hydrological conditions - 2-summer energy and water use, in: Sustainability of Water Resources under Increasing Uncertainty,

edited by: Rosjberg D, Boutayeb N, Gustard A, Kundzewicz Z, Rasmussen P. IAHS Publication No. 240, IAHS Press, Wallingford, United Kingdom, 243-250.

Hack JT. 1957. Studies of longitudinal stream profiles in Virginia and Maryland. US Geological Survey Professional Paper, 294-B.

Harder P, Pomeroy JW, Westbrook CJ. 2015. Hydrological resilience of a Canadian Rockies headwaters basin subject to changing climate, extreme weather, and forest management. *Hydrological Processes* 29: 3905-3924. DOI:10.1002/hyp.10596.

Hedstrom NR, Pomeroy JW. 1998. Measurements and modelling of snow interception in the boreal forest. *Hydrological Processes* 12: 1611-1625.

Keith DM, Johnson EA, Valeo C. 2010. A hillslope forest floor (duff) water budget and the transition to local control. *Hydrological Processes* 24: 2738-2751. DOI:10.1002/hyp.7697

Krinner G, Derksen C, Essery R, Flanner M, Hagemann S, Clark M, Hall A, Rott H, Brutel-Vuilmet C, Kim H, Ménard CB, Mudryk L, Thackeray C, Wang L, Arduini G, Balsamo G, Bartlett P, Boike J, Boone A, Chéruey F, Colin J, Cuntz M, Dai Y, Decharme B, Derry J, Ducharne A, Dutra E, Fang X, Fierz C, Ghattas J, Gusev Y, Haverd V, Kontu A, Lafaysse M, Law R, Lawrence D, Li W, Marke T, Marks D, Ménégos M, Nasonova O, Nitta T, Niwano M, Pomeroy J, Raleigh MS, Schaedler G, Semenov V, Smirnova TG, Stacke T, Strasser U, Svenson S, Turkov D, Wang T, Wever N, Yuan H, Zhou W, Zhu D. 2018. ESM-SnowMIP: assessing snow models and quantifying snow-related climate feedbacks. *Geoscientific Model Development* 11: 5027-5049. DOI:10.5194/gmd-11-5027-2018.

Krogh SA, Pomeroy JW, McPhee J. 2015. Physically based mountain hydrological modeling using reanalysis data in Patagonia. *Journal of Hydrometeorology* 16: 172-193. DOI:10.1175/jhm-d-13-0178.1.

Lal, R., & Shukla, M. (2004). *Principles of soil physics*. New York: M. Dekker

Lapen DR, Martz LW. 1993. The measurement of two simple topographic indices of wind sheltering exposure from raster digital elevation models. *Computers and Geosciences* 19: 769-779. DOI:10.1016/0098-3004(93)90049-B.

Leavesley GH, Lichty RW, Troutman BM, Saindon LG. 1983. *Precipitation-runoff modelling system: user's manual*. Report 83-4238 US Geological Survey Water Resources Investigations; 207.

López-Moreno JI, Pomeroy JW, Revuelto J, Vicente-Serrano SM. 2013. Response of snow processes to climate change: spatial variability in a small basin in the Spanish Pyrenees. *Hydrological Processes* 27: 2637-2650. DOI:10.1002/hyp.9408.

Luce CH, Tarboton DG. 2010. Evaluation of alternative formulae for calculation of surface temperature in snowmelt models using frequency analysis of temperature observations. *Hydrology and Earth System Sciences* 14: 535-543.

MacDonald MK, Pomeroy JW, Pietroniro A. 2010. On the importance of sublimation to an alpine snow mass balance in the Canadian Rocky Mountains. *Hydrology and Earth System Sciences* 14: 1401-1415. DOI:10.5194/hess-14-1401-2010.

Male DH, Gray DM. 1981. Snowcover ablation and runoff. In Gray DM and Male DH (Eds.), *Handbook of Snow: Principles, Processes, Management & Use*. Toronto, Ontario: Pergamon Press Canada Ltd., pp. 360-436.

Marks D, Kimball J, Tingey D, Link T. 1998. The sensitivity of snowmelt processes to climate conditions and forest cover during rain-on-snow: a case study of the 1996 Pacific Northwest flood. *Hydrological Processes* 12: 1569-1587.

Mays LW. 2001. *Water Resources Engineering*. John Wiley & Sons, Inc., New York.

Monteith JL. 1965. Evaporation and environment. In *State and Movement of Water in Living Organisms*. 19th Symposium of the Society for Experimental Biology. Cambridge University Press: Cambridge; 205-234.

Nash JE, Sutcliffe JV. 1970. River flow forecasting through conceptual models. Part I—A discussion of principles. *Journal of Hydrology* 10: 282–290.

Pomeroy JW, Granger R, Pietroniro A, Elliott J, Toth B, Hedstrom N. 1999. Classification of the boreal forest for hydrological processes. In, (ed. Severin Woxholt) *Proceedings, the Ninth International Boreal Forest Research Association Conference, Oslo, September 21-23, 1998*. *Aktuelt fra skogforskningen*, 4/99, Norsk institutt for skogforskning, Norwegian Forest Research Institute, Oslo. 49-59.

Pomeroy JW, Li L. 2000. Prairie and Arctic areal snow cover mass balance using a blowing snow model. *Journal of Geophysical Research* 105: 26619-26634.

Pomeroy JW, Gray DM, Hedstrom NR, Janowicz JR. 2002. Prediction of seasonal snow accumulation in cold climate forests. *Hydrological Processes* 16: 3543-3558.

Pomeroy JW, Gray DM, Brown T, Hedstrom NR, Quinton W, Granger RJ, Carey S. 2007. The Cold Regions Hydrological Model, a platform for basing process representation and model structure on physical evidence. *Hydrological Processes* 21: 2650-2667. DOI:10.1002/hyp.6787.

Pomeroy JW, Marks D, Link T, Ellis C, Hardy J, Rowlands A, Granger R. 2009. The impact of coniferous forest temperature on incoming longwave radiation to melting snow. *Hydrological Processes* 23: 2513-2525. DOI:10.1002/hyp.7325.

Pomeroy JW, Fang X, Shook K, Whitfield PH. 2013. Predicting in ungauged basins using physical principles obtained using the deductive, inductive, and abductive reasoning approach. In *Putting Prediction in Ungauged Basins into Practice*, Pomeroy JW, Whitfield PH, Spence C (eds). Canadian Water Resources Association: Canmore, Alberta; 41-62.

Pomeroy JW, Fang X, Marks D. 2016. A cold rain on snow event in the Canadian Rockies –characteristics and diagnosis. *Hydrological Processes* 30: 2899-2914. DOI:10.1002/hyp.10905.

Priestley CHB, Taylor RJ. 1972. On the assessment of surface heat flux and evaporation using large-scale parameters. *Monthly Weather Review* 100: 81-92.

Rasouli K, Pomeroy JW, Whitfield PH. 2019. Hydrological responses of headwater basins to monthly perturbed climate in the North American Cordillera. *Journal of Hydrometeorology*. DOI:10.1175/JHM-D-18-0166.1.

Schmidt RA, Gluns DR. 1991. Snowfall interception on branches of three conifer species. *Canadian Journal of Forest Research* 21: 1262-1269.

Sicart JE, Pomeroy JW, Essery RLH, Bewley D. 2006. Incoming longwave radiation to melting snow: observations, sensitivity and estimation in northern environments. *Hydrological Processes* 20: 3697-3708. DOI:10.1002/hyp.6383.

Soil Landscapes of Canada Working Group. 2011. *Soil Landscapes of Canada version 3.2*. Agriculture and Agri-Food Canada.

Verseghy DL. 1991. CLASS-A Canadian land surface scheme for GCMs. I. soil model. *International Journal of Climatology* 11: 111-133.

Weber M, Bernhardt M, Pomeroy JW, Fang X, Härer S, Schulz K. 2016. Description of current and future snow processes in a small basin in the Bavarian Alps. *Environmental Earth Sciences* 75: 1223. DOI:10.1007/s12665-016-6027-1.

Williams TJ, Pomeroy JW, Janowicz JR, Carey SK, Rasouli K, Quinton WL. 2015. A radiative–conductive–convective approach to calculate thaw season ground surface temperatures for modelling frost table dynamics. *Hydrological Processes* 29: 3954-3965.

Xie C, Gough WA. 2013. A simple thaw-freeze algorithm for multi-layered soil using the Stefan equation. *Permafrost and Periglacial Processes*, 24: 252-260. DOI:10.1002/ppp.1770.

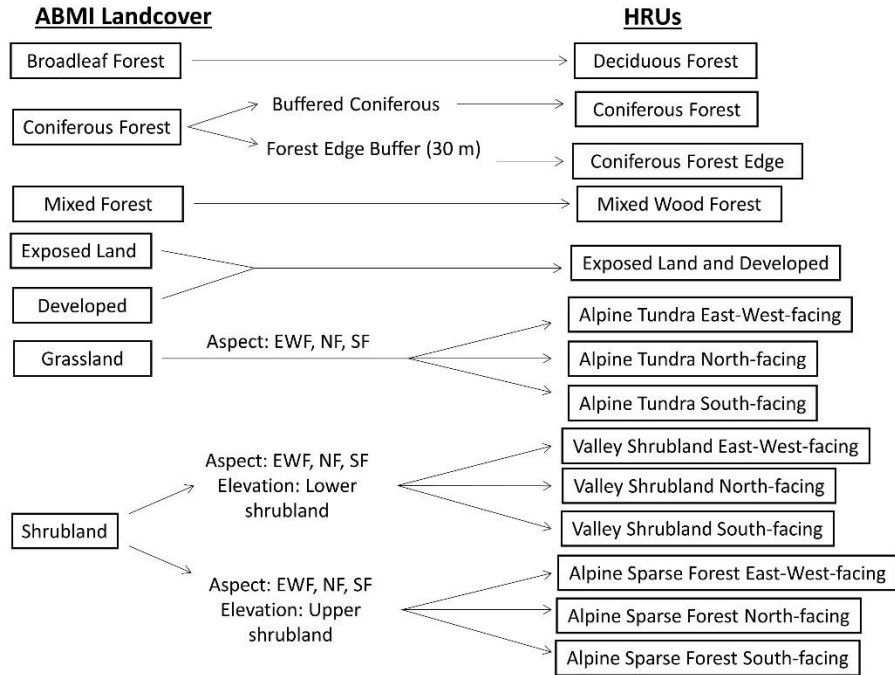
Zhang Y, Carey SK, Quinton W L, Janowicz JR, Pomeroy JW, Flerchinger GN. 2010. Comparison of algorithms and parameterisations for infiltration into organic-covered permafrost soils. *Hydrology and Earth System Sciences* 14: 729-750. DOI:10.5194/hess-14-729-2010.

Zhao L, Gray DM. 1999. Estimating snowmelt infiltration into frozen soils. *Hydrological Processes* 13: 1827-1842.

Zhou J, Pomeroy JW, Zhang W, Cheng G, Wang G, Chen C. 2014. Simulating cold regions hydrological processes using a modular model in the west of China. *Journal of Hydrology* 509: 13–24.

Appendix 2: HRU determination flowcharts for Bow River and Elbow River basins above Calgary

Upper Bow River at Banff – HRU determination



Upper Bow River at Banff – HRU determination

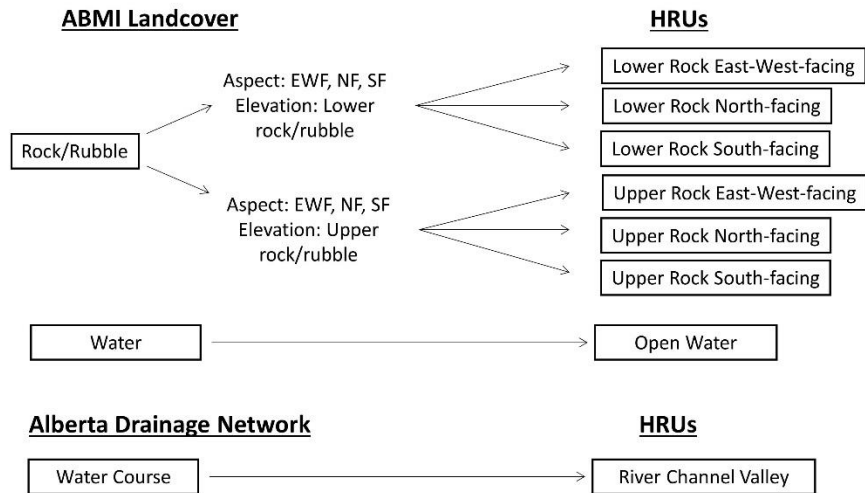


Figure A2. Flowchart of HRU determination for Upper Bow River at Banff model domain.

Upper Bow River at Banff – HRU determination

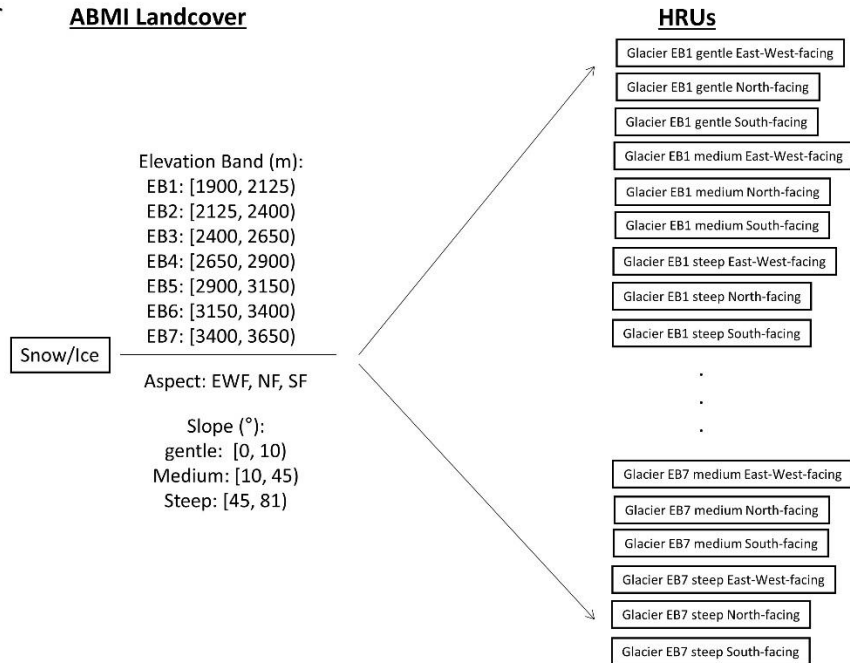


Figure A2. Concluded.

Upper Bow River between Banff and Calgary, Elbow River at Calgary – HRU determination

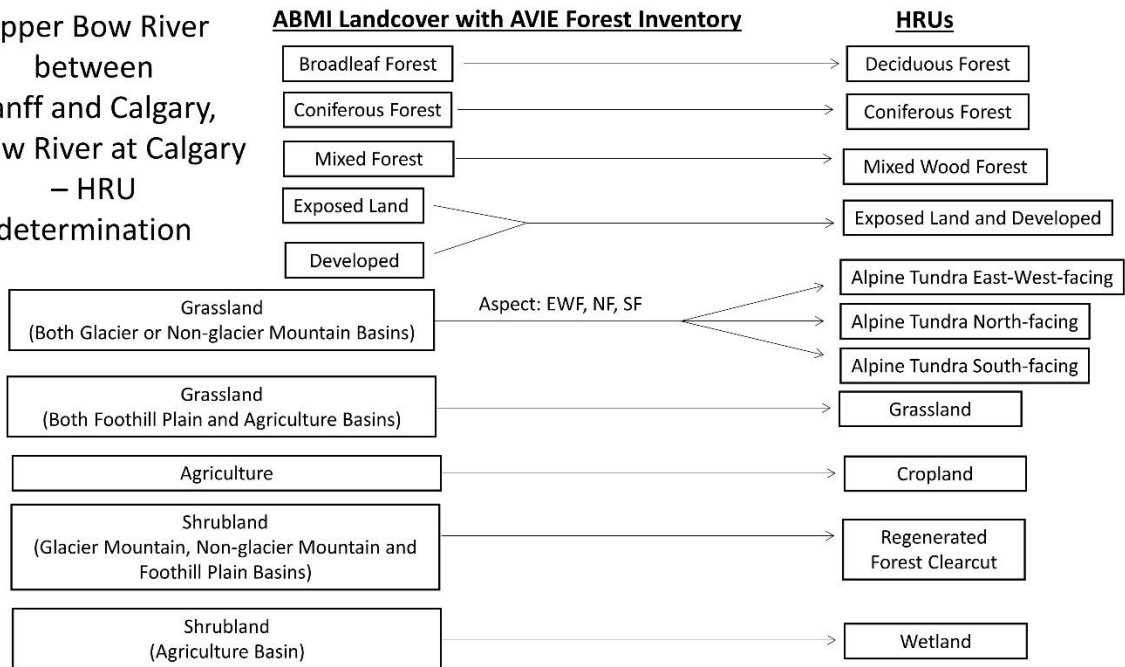


Figure A3. Flowchart of HRU determination for Upper Bow River between Banff and Calgary and Elbow River at Calgary model domains.

Upper Bow River
between
Banff and Calgary,
Elbow River at Calgary
– HRU
determination

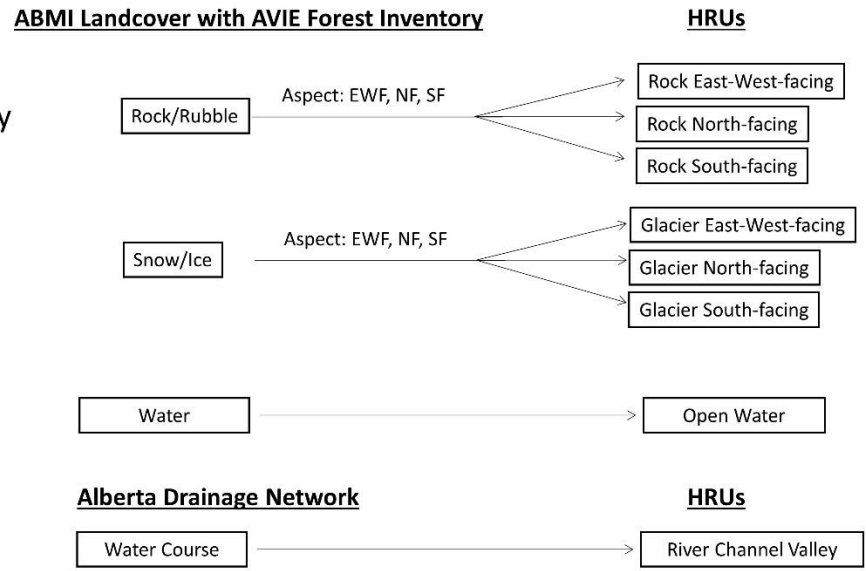


Figure A3. Concluded.

Appendix 3: Sub-basins information for Bow River and Elbow River basins above Calgary

Table A1. Sub-basin number, sub-basin name, sub-basin HRU number, sub-basin group (Grp) number, sub-basin type and area for Upper Bow River at Banff model domain in CRHM.

Sub-basin number	Sub-basin name	HRU number	Grp number	Type	Area (km ²)
1	05BA001_1	54	A	Glacier Mountain Basin	25.93
2	05BA001_2	41	B	Glacier Mountain Basin	27.59
3	05BA001_3	33	C	Glacier Mountain Basin	51.22
4	05BA001_4	47	D	Glacier Mountain Basin	52.67
5	05BA001_5	35	E	Glacier Mountain Basin	33.42
6	05BA001_6	62	F	Glacier Mountain Basin	67.53
7	05BA001_7	35	G	Glacier Mountain Basin	84.46
8	05BA001_8	50	H	Glacier Mountain Basin	66.06
9	05BA001_9	11	I	Glacier Mountain Basin	11.81
10	05BA002_1	35	J	Glacier Mountain Basin	64.79
11	05BA002_2	38	K	Glacier Mountain Basin	24.63
12	05BA002_3	33	L	Glacier Mountain Basin	25.96
13	05BA002_4	57	M	Glacier Mountain Basin	56.55
14	05BA002_5	30	N	Glacier Mountain Basin	43.92
15	05BA002_6	24	O	Glacier Mountain Basin	88.30
16	05BB001_1	30	P	Glacier Mountain Basin	34.01
17	05BB001_2	69	Q	Glacier Mountain Basin	29.74
18	05BB001_3	20	R	Non-glacier Mountain Basin	7.28
19	05BB001_4	62	S	Glacier Mountain Basin	37.09
20	05BB001_5	20	T	Non-glacier Mountain Basin	40.24
21	05BB001_6	57	U	Glacier Mountain Basin	56.93
22	05BB001_7	20	V	Non-glacier Mountain Basin	23.53
23	05BB001_8	29	W	Glacier Mountain Basin	64.64
24	05BB001_9	30	X	Glacier Mountain Basin	27.80
25	05BB001_10	24	Y	Glacier Mountain Basin	33.18
26	05BB001_11	20	Z	Non-glacier Mountain Basin	116.38
27	05BB001_12	46	AA	Glacier Mountain Basin	51.73
28	05BB001_13	24	AB	Glacier Mountain Basin	24.19
29	05BB001_14	21	AC	Non-glacier Mountain Basin	75.15
30	05BB001_15	30	AD	Glacier Mountain Basin	76.88
31	05BB001_16	19	AE	Non-glacier Mountain Basin	24.36
32	05BB001_17	20	AF	Non-glacier Mountain Basin	20.54
33	05BB001_18	65	AG	Glacier Mountain Basin	51.44
34	05BB001_19	19	AH	Non-glacier Mountain Basin	36.99
35	05BB001_20	14	AI	Non-glacier Mountain Basin	16.38
36	05BB001_21	19	AJ	Non-glacier Mountain Basin	27.26
37	05BB001_22	19	AK	Non-glacier Mountain Basin	19.31
38	05BB001_23	22	AL	Non-glacier Mountain Basin	118.13
39	05BB001_24	20	AM	Non-glacier Mountain Basin	72.07
40	05BB001_25	19	AN	Non-glacier Mountain Basin	31.92
41	05BB001_26	21	AO	Non-glacier Mountain Basin	36.06
42	05BB001_27	17	AP	Non-glacier Mountain Basin	23.53
43	05BB001_28	19	AQ	Non-glacier Mountain Basin	64.25
44	05BB001_29	15	AR	Non-glacier Mountain Basin	7.92
45	05BB001_30	21	AS	Non-glacier Mountain Basin	11.18
46	05BB001_31	19	AT	Non-glacier Mountain Basin	44.66
47	05BB001_32	20	AU	Non-glacier Mountain Basin	91.90
48	05BB001_33	15	AV	Non-glacier Mountain Basin	31.13
49	05BB001_34	21	AW	Non-glacier Mountain Basin	16.37
50	05BB001_35	21	AX	Non-glacier Mountain Basin	23.01

Table A2. Sub-basin number, sub-basin name, sub-basin HRU number, sub-basin group (Grp) number, sub-basin type and area for Upper Bow River between Banff and Calgary model domain in CRHM.

Sub-basin number	Sub-basin name	HRU number	Grp number	Type	Area (km ²)
51	05BC_001_1	15	A	Glacier Mountain Basin	58.64
52	05BC_001_2	12	B	Glacier Mountain Basin	45.03
53	05BC_001_3	9	C	Non-glacier Mountain Basin	24.39
54	05BC_001_4	15	D	Glacier Mountain Basin	38.77
55	05BC_001_5	12	E	Glacier Mountain Basin	41.14
56	05BC_001_6	16	F	Glacier Mountain Basin	36.83
57	05BC_001_7	13	G	Glacier Mountain Basin	30.58
58	05BC_001_8	13	H	Glacier Mountain Basin	25.91
59	05BC_001_9	14	I	Non-glacier Mountain Basin	61.75
60	05BC_001_10	12	J	Non-glacier Mountain Basin	111.26
61	05BC_001_11	13	K	Non-glacier Mountain Basin	171.55
62	05BC_001_12	13	L	Non-glacier Mountain Basin	70.60
63	05BC_001_13	11	M	Non-glacier Mountain Basin	33.19
64	05BD_001_1	13	N	Glacier Mountain Basin	57.28
65	05BD_001_2	13	O	Glacier Mountain Basin	47.32
66	05BD_001_3	11	P	Non-glacier Mountain Basin	36.58
67	05BD_001_4	11	Q	Non-glacier Mountain Basin	37.22
68	05BD_001_5	10	R	Non-glacier Mountain Basin	78.57
69	05BD_001_6	10	S	Non-glacier Mountain Basin	44.28
70	05BD_001_7	11	T	Non-glacier Mountain Basin	93.54
71	05BD_001_8	11	U	Non-glacier Mountain Basin	89.86
72	05BD_001_9	13	V	Non-glacier Mountain Basin	155.58
73	05BD_001_10	11	W	Non-glacier Mountain Basin	87.02
74	05BE_001_1	6	X	Foothill Plain Basin	4.68
75	05BE_001_2	12	Y	Non-glacier Mountain Basin	35.14
76	05BE_001_3	12	Z	Non-glacier Mountain Basin	52.15
77	05BE_001_4	13	AA	Non-glacier Mountain Basin	87.53
78	05BE_001_5	11	AB	Non-glacier Mountain Basin	43.45
79	05BE_001_6	14	AC	Non-glacier Mountain Basin	57.80
80	05BE_001_7	14	AD	Non-glacier Mountain Basin	78.73
81	05BE_001_8	13	AE	Non-glacier Mountain Basin	45.16
82	05BE_001_9	12	AF	Non-glacier Mountain Basin	32.80
83	05BE_001_10	14	AG	Non-glacier Mountain Basin	57.78
84	05BE_001_11	14	AH	Non-glacier Mountain Basin	54.98
85	05BE_001_12	9	AI	Foothill Plain Basin	75.46
86	05BE_001_13	9	AJ	Foothill Plain Basin	31.12
87	05BE_001_14	10	AK	Agriculture Basin	49.90
88	05BE_001_15	10	AL	Agriculture Basin	45.84
89	05BE_001_16	10	AM	Agriculture Basin	90.93
90	05BE_001_17	10	AN	Agriculture Basin	54.25
91	05BE_001_18	9	AO	Agriculture Basin	93.98
92	05BF_001_1	17	AP	Glacier Mountain Basin	131.17
93	05BF_001_2	13	AQ	Glacier Mountain Basin	39.64
94	05BF_001_3	12	AR	Glacier Mountain Basin	22.53
95	05BF_001_4	12	AS	Glacier Mountain Basin	33.67
96	05BF_001_5	17	AT	Glacier Mountain Basin	30.23
97	05BF_001_6	9	AU	Non-glacier Mountain Basin	23.45
98	05BF_001_7	16	AV	Glacier Mountain Basin	59.84
99	05BF_001_8	14	AW	Non-glacier Mountain Basin	58.71
100	05BF_001_9	14	AX	Non-glacier Mountain Basin	108.49

Table A2. Concluded.

Sub-basin number	Sub-basin name	HRU number	Grp number	Type	Area (km ²)
101	05BF_001_10	13	AY	Non-glacier Mountain Basin	24.78
102	05BF_001_11	14	AZ	Non-glacier Mountain Basin	77.54
103	05BF_001_12	13	BA	Non-glacier Mountain Basin	38.43
104	05BF_001_13	14	BB	Non-glacier Mountain Basin	42.65
105	05BF_001_14	13	BC	Non-glacier Mountain Basin	49.49
106	05BF_001_15	13	BD	Non-glacier Mountain Basin	23.51
107	05BF_001_16	14	BE	Non-glacier Mountain Basin	54.70
108	05BF_001_17	11	BF	Non-glacier Mountain Basin	28.70
109	05BF_001_18	14	BG	Non-glacier Mountain Basin	45.69
110	05BF_001_19	12	BH	Non-glacier Mountain Basin	32.79
111	05BF_001_20	10	BI	Agriculture Basin	32.52
112	05BG_001_1	10	BJ	Non-glacier Mountain Basin	57.42
113	05BG_001_2	10	BK	Non-glacier Mountain Basin	24.39
114	05BG_001_3	14	BL	Non-glacier Mountain Basin	176.58
115	05BG_001_4	13	BM	Non-glacier Mountain Basin	74.06
116	05BG_001_5	12	BN	Non-glacier Mountain Basin	41.18
117	05BG_001_6	7	BO	Foothill Plain Basin	55.93
118	05BG_001_7	13	BP	Non-glacier Mountain Basin	42.90
119	05BG_001_8	9	BQ	Foothill Plain Basin	104.63
120	05BG_001_9	9	BR	Foothill Plain Basin	60.53
121	05BG_001_10	12	BS	Non-glacier Mountain Basin	100.82
122	05BG_001_11	14	BT	Non-glacier Mountain Basin	46.18
123	05BG_001_12	10	BU	Agriculture Basin	56.42
124	05BG_001_13	10	BV	Agriculture Basin	22.41
125	05BG_001_14	10	BW	Agriculture Basin	38.22
126	05BG_001_15	9	BX	Agriculture Basin	24.76
127	05BG_001_16	7	BY	Agriculture Basin	10.98
128	05BH_001_1	13	BZ	Non-glacier Mountain Basin	61.60
129	05BH_001_2	13	CA	Non-glacier Mountain Basin	38.66
130	05BH_001_3	13	CB	Non-glacier Mountain Basin	21.45
131	05BH_001_4	9	CC	Foothill Plain Basin	24.17
132	05BH_001_5	9	CD	Foothill Plain Basin	28.29
133	05BH_001_6	9	CE	Agriculture Basin	68.60
134	05BH_001_7	10	CF	Agriculture Basin	59.10
135	05BH_001_8	10	CG	Agriculture Basin	173.76
136	05BH_001_9	9	CH	Agriculture Basin	66.85
137	05BH_001_10	8	CI	Agriculture Basin	42.79
138	05BH_001_11	10	CJ	Agriculture Basin	34.25
139	05BH_001_12	10	CK	Agriculture Basin	87.75
140	05BH_001_13	9	CL	Agriculture Basin	112.88
141	05BH_001_14	9	CM	Agriculture Basin	170.44
142	05BH_001_15	9	CN	Agriculture Basin	276.31

Table A3. Sub-basin number, sub-basin name, sub-basin HRU number, sub-basin group (Grp) number, sub-basin type and area for Elbow River at Calgary model domain in CRHM.

Sub-basin number	Sub-basin name	HRU number	Grp number	Type	Area (km ²)
1	05BJ_001_1	7	A	Non-glacier Mountain Basin	29.57
2	05BJ_001_2	15	B	Glacier Mountain Basin	70.55
3	05BJ_001_3	12	C	Non-glacier Mountain Basin	27.52
4	05BJ_001_4	13	D	Non-glacier Mountain Basin	53.69
5	05BJ_001_5	9	E	Non-glacier Mountain Basin	25.47
6	05BJ_001_6	8	F	Non-glacier Mountain Basin	23.29
7	05BJ_001_7	11	G	Non-glacier Mountain Basin	28.45
8	05BJ_001_8	14	H	Non-glacier Mountain Basin	20.45
9	05BJ_001_9	13	I	Non-glacier Mountain Basin	59.50
10	05BJ_001_10	14	J	Non-glacier Mountain Basin	40.26
11	05BJ_001_11	14	K	Non-glacier Mountain Basin	47.62
12	05BJ_001_12	9	L	Foothill Plain Basin	13.22
13	05BJ_001_13	14	M	Non-glacier Mountain Basin	50.34
14	05BJ_001_14	14	N	Non-glacier Mountain Basin	120.80
15	05BJ_001_15	12	O	Non-glacier Mountain Basin	63.30
16	05BJ_001_16	9	P	Foothill Plain Basin	26.37
17	05BJ_001_17	8	Q	Foothill Plain Basin	41.72
18	05BJ_001_18	10	R	Agriculture Basin	161.54
19	05BJ_001_19	7	S	Agriculture Basin	35.89
20	05BJ_001_20	8	T	Agriculture Basin	36.10
21	05BJ_001_21	7	U	Agriculture Basin	30.44
22	05BJ_001_22	6	V	Agriculture Basin	34.99
23	05BJ_001_23	6	W	Agriculture Basin	23.13
24	05BJ_001_24	9	X	Agriculture Basin	90.58
25	05BJ_001_25	8	Y	Agriculture Basin	37.13

Appendix 4: 10-km bias corrected WRF grids used to force hydrological models for Bow River and Elbow River basins above Calgary

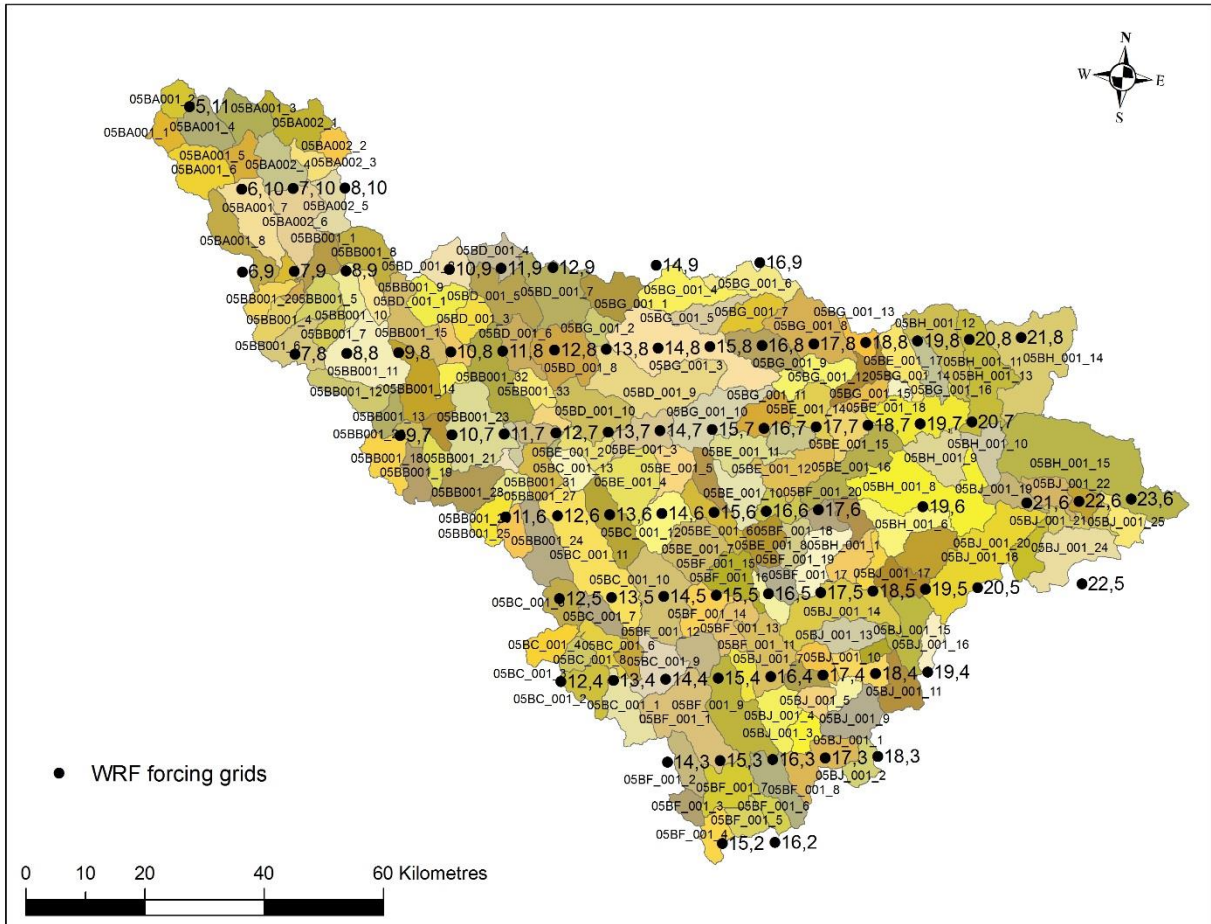


Figure A4. 10-km bias corrected WRF forcing grids for hydrological models for Bow River and Elbow River basins above Calgary. Note the numbers show the longitude and latitude indexes of the WRF grids, e.g. grid of 5, 11 is WRF grid at longitude index 5 and latitude index 11. More information of these WRF grids is provided in Tables A4 to A6.

Table A4. 10-km bias corrected WRF grids for forcing sub-basins in Upper Bow River at Banff model domain. Note that HRU_OBS is the index in CRHM to allocate forcing for each sub-basin.

Sub-basin number	Sub-basin name	Longitude (°)	Latitude (°)	Longitude index	Latitude index	Elevation (m)	HRU_OBS
1	05BA001_1	-116.4375	51.6875	5	11	2152	1
2	05BA001_2	-116.4375	51.6875	5	11	2152	1
3	05BA001_3	-116.3125	51.5625	6	10	1898	2
4	05BA001_4	-116.4375	51.6875	5	11	2152	1
5	05BA001_5	-116.3125	51.5625	6	10	1898	2
6	05BA001_6	-116.4375	51.6875	5	11	2152	1
7	05BA001_7	-116.3125	51.5625	6	10	1898	2
8	05BA001_8	-116.3125	51.4375	6	9	2230	3
9	05BA001_9	-116.1875	51.4375	7	9	2145	4
10	05BA002_1	-116.1875	51.5625	7	10	1927	5
11	05BA002_2	-116.0625	51.5625	8	10	2202	7
12	05BA002_3	-116.1875	51.5625	7	10	1927	5
13	05BA002_4	-116.1875	51.5625	7	10	1927	5
14	05BA002_5	-116.0625	51.5625	8	10	2202	7
15	05BA002_6	-116.1875	51.5625	7	10	1927	5
16	05BB001_1	-116.0625	51.4375	8	9	1946	8
17	05BB001_2	-116.3125	51.4375	6	9	2230	3
18	05BB001_3	-116.1875	51.4375	7	9	2145	4
19	05BB001_4	-116.1875	51.3125	7	8	2019	6
20	05BB001_5	-116.0625	51.4375	8	9	1946	8
21	05BB001_6	-116.1875	51.3125	7	8	2019	6
22	05BB001_7	-116.0625	51.3125	8	8	2011	9
23	05BB001_8	-116.0625	51.4375	8	9	1946	8
24	05BB001_9	-116.0625	51.4375	8	9	1946	8
25	05BB001_10	-116.0625	51.4375	8	9	1946	8
26	05BB001_11	-116.0625	51.3125	8	8	2011	9
27	05BB001_12	-116.0625	51.3125	8	8	2011	9
28	05BB001_13	-115.9375	51.1875	9	7	2044	10
29	05BB001_14	-115.9375	51.3125	9	8	2129	11
30	05BB001_15	-115.9375	51.3125	9	8	2129	11
31	05BB001_16	-115.8125	51.3125	10	8	2041	12
32	05BB001_17	-115.8125	51.3125	10	8	2041	12
33	05BB001_18	-115.9375	51.1875	9	7	2044	10
34	05BB001_19	-115.9375	51.1875	9	7	2044	10
35	05BB001_20	-115.9375	51.1875	9	7	2044	10
36	05BB001_21	-115.8125	51.1875	10	7	2157	13
37	05BB001_22	-115.8125	51.1875	10	7	2157	13
38	05BB001_23	-115.8125	51.1875	10	7	2157	13
39	05BB001_24	-115.5625	51.0625	12	6	2272	16
40	05BB001_25	-115.6875	51.0625	11	6	2300	14
41	05BB001_26	-115.6875	51.0625	11	6	2300	14
42	05BB001_27	-115.6875	51.0625	11	6	2300	14
43	05BB001_28	-115.8125	51.1875	10	7	2157	13
44	05BB001_29	-115.6875	51.1875	11	7	2134	15
45	05BB001_30	-115.6875	51.1875	11	7	2134	15
46	05BB001_31	-115.5625	51.1875	12	7	2052	17
47	05BB001_32	-115.6875	51.1875	11	7	2134	15
48	05BB001_33	-115.5625	51.1875	12	7	2052	17
49	05BB001_34	-115.5625	51.1875	12	7	2052	17
50	05BB001_35	-115.5625	51.1875	12	7	2052	17

Table A5. 10-km bias corrected WRF grids for forcing sub-basins in Upper Bow River between Banff and Calgary model domain. Note that HRU_OBS is the index in CRHM to allocate forcing for each sub-basin.

Sub-basin number	Sub-basin name	Longitude (°)	Latitude (°)	Longitude index	Latitude index	Elevation (m)	HRU_OBS
51	05BC_001_1	-115.4375	50.8125	13	4	2187	10
52	05BC_001_2	-115.4375	50.8125	13	4	2187	10
53	05BC_001_3	-115.5625	50.8125	12	4	2026	4
54	05BC_001_4	-115.5625	50.8125	12	4	2026	4
55	05BC_001_5	-115.5625	50.9375	12	5	2224	5
56	05BC_001_6	-115.4375	50.8125	13	4	2187	10
57	05BC_001_7	-115.4375	50.9375	13	5	2204	11
58	05BC_001_8	-115.4375	50.8125	13	4	2187	10
59	05BC_001_9	-115.3125	50.8125	14	4	2286	16
60	05BC_001_10	-115.3125	50.9375	14	5	2208	17
61	05BC_001_11	-115.4375	51.0625	13	6	2120	12
62	05BC_001_12	-115.4375	51.0625	13	6	2120	12
63	05BC_001_13	-115.5625	51.1875	12	7	2052	6
64	05BD_001_1	-115.8125	51.4375	10	9	2111	1
65	05BD_001_2	-115.8125	51.4375	10	9	2111	1
66	05BD_001_3	-115.8125	51.4375	10	9	2111	1
67	05BD_001_4	-115.6875	51.4375	11	9	2130	2
68	05BD_001_5	-115.6875	51.4375	11	9	2130	2
69	05BD_001_6	-115.6875	51.3125	11	8	1861	3
70	05BD_001_7	-115.5625	51.4375	12	9	2133	7
71	05BD_001_8	-115.5625	51.3125	12	8	1705	8
72	05BD_001_9	-115.3125	51.3125	14	8	2027	14
73	05BD_001_10	-115.4375	51.1875	13	7	1858	13
74	05BE_001_1	-115.5625	51.1875	12	7	2052	6
75	05BE_001_2	-115.4375	51.1875	13	7	1858	13
76	05BE_001_3	-115.3125	51.1875	14	7	1764	18
77	05BE_001_4	-115.4375	51.0625	13	6	2120	12
78	05BE_001_5	-115.3125	51.0625	14	6	2088	19
79	05BE_001_6	-115.3125	51.0625	14	6	2088	19
80	05BE_001_7	-115.1875	51.0625	15	6	2057	25
81	05BE_001_8	-115.1875	51.0625	15	6	2057	25
82	05BE_001_9	-115.1875	51.0625	15	6	2057	25
83	05BE_001_10	-115.0625	51.0625	16	6	1868	30
84	05BE_001_11	-115.0625	51.1875	16	7	1522	33
85	05BE_001_12	-114.9375	51.0625	17	6	1939	38
86	05BE_001_13	-114.9375	51.1875	17	7	1550	39
87	05BE_001_14	-114.9375	51.1875	17	7	1550	39
88	05BE_001_15	-114.8125	51.1875	18	7	1502	41
89	05BE_001_16	-114.8125	51.1875	18	7	1502	41
90	05BE_001_17	-114.6875	51.3125	19	8	1289	46
91	05BE_001_18	-114.6875	51.1875	19	7	1372	43
92	05BF_001_1	-115.3125	50.6875	14	3	2150	20
93	05BF_001_2	-115.3125	50.6875	14	3	2150	20
94	05BF_001_3	-115.3125	50.6875	14	3	2150	20
95	05BF_001_4	-115.1875	50.5625	15	2	2193	26
96	05BF_001_5	-115.1875	50.5625	15	2	2193	26
97	05BF_001_6	-115.0625	50.5625	16	2	2199	34
98	05BF_001_7	-115.1875	50.6875	15	3	2296	27
99	05BF_001_8	-115.0625	50.6875	16	3	2209	35
100	05BF_001_9	-115.1875	50.8125	15	4	2213	21

Table A5. Concluded.

Sub-basin number	Sub-basin name	Longitude (°)	Latitude (°)	Longitude index	Latitude index	Elevation (m)	HRU_OBS
101	05BF_001_10	-115.0625	50.8125	16	4	2125	28
102	05BF_001_11	-115.0625	50.8125	16	4	2125	28
103	05BF_001_12	-115.1875	50.8125	15	4	2213	21
104	05BF_001_13	-115.1875	50.9375	15	5	2242	22
105	05BF_001_14	-115.1875	50.9375	15	5	2242	22
106	05BF_001_16	-115.1875	50.9375	15	5	2242	22
107	05BF_001_15	-115.0625	50.9375	16	5	2172	29
108	05BF_001_17	-115.0625	50.9375	16	5	2172	29
109	05BF_001_18	-115.0625	51.0625	16	6	1868	30
110	05BF_001_19	-115.0625	51.0625	16	6	1868	30
111	05BF_001_20	-115.0625	51.0625	16	6	1868	30
112	05BG_001_1	-115.4375	51.3125	13	8	1807	9
113	05BG_001_2	-115.4375	51.3125	13	8	1807	9
114	05BG_001_3	-115.3125	51.3125	14	8	2027	14
115	05BG_001_4	-115.3125	51.4375	14	9	2072	15
116	05BG_001_5	-115.1875	51.3125	15	8	2006	23
117	05BG_001_6	-115.0625	51.4375	16	9	1591	31
118	05BG_001_7	-115.0625	51.3125	16	8	1598	32
119	05BG_001_8	-114.9375	51.3125	17	8	1342	36
120	05BG_001_9	-115.0625	51.3125	16	8	1598	32
121	05BG_001_10	-115.1875	51.1875	15	7	1725	24
122	05BG_001_11	-115.0625	51.1875	16	7	1522	33
123	05BG_001_12	-114.9375	51.3125	17	8	1342	36
124	05BG_001_13	-114.8125	51.3125	18	8	1308	40
125	05BG_001_14	-114.8125	51.3125	18	8	1308	40
126	05BG_001_15	-114.8125	51.1875	18	7	1502	41
127	05BG_001_16	-114.6875	51.1875	19	7	1372	43
128	05BH_001_1	-114.9375	50.9375	17	5	2127	37
129	05BH_001_2	-114.8125	50.9375	18	5	1795	42
130	05BH_001_3	-114.8125	50.9375	18	5	1795	42
131	05BH_001_4	-114.9375	51.0625	17	6	1939	38
132	05BH_001_5	-114.9375	51.0625	17	6	1939	38
133	05BH_001_6	-114.6875	51.0625	19	6	1485	44
134	05BH_001_7	-114.6875	50.9375	19	5	1639	45
135	05BH_001_8	-114.6875	51.0625	19	6	1485	44
136	05BH_001_9	-114.6875	51.1875	19	7	1372	43
137	05BH_001_10	-114.5625	51.1875	20	7	1279	47
138	05BH_001_11	-114.6875	51.3125	19	8	1289	46
139	05BH_001_12	-114.6875	51.3125	19	8	1289	46
140	05BH_001_13	-114.5625	51.3125	20	8	1237	48
141	05BH_001_14	-114.4375	51.3125	21	8	1206	49
142	05BH_001_15	-114.4375	51.0625	22	6	1199	50

Table A6. 10-km bias corrected WRF grids for forcing sub-basins in Elbow River at Calgary model domain. Note that HRU_OBS is the index in CRHM to allocate forcing for each sub-basin.

Sub-basin number	Sub-basin name	Longitude (°)	Latitude (°)	Longitude index	Latitude index	Elevation (m)	HRU_OBS
1	05BJ_001_1	-114.8125	50.6875	18	3	2161	4
2	05BJ_001_2	-114.9375	50.6875	17	3	2239	1
3	05BJ_001_3	-114.9375	50.6875	17	3	2239	1
4	05BJ_001_4	-114.9375	50.6875	17	3	2239	1
5	05BJ_001_5	-114.9375	50.8125	17	4	2263	2
6	05BJ_001_6	-114.9375	50.8125	17	4	2263	2
7	05BJ_001_7	-114.9375	50.8125	17	4	2263	2
8	05BJ_001_8	-114.9375	50.8125	17	4	2263	2
9	05BJ_001_9	-114.8125	50.6875	18	3	2161	4
10	05BJ_001_10	-114.8125	50.8125	18	4	2059	5
11	05BJ_001_11	-114.8125	50.8125	18	4	2059	5
12	05BJ_001_12	-114.8125	50.8125	18	4	2059	5
13	05BJ_001_13	-114.9375	50.8125	17	4	2263	2
14	05BJ_001_14	-114.9375	50.9375	17	5	2127	3
15	05BJ_001_15	-114.6875	50.9375	19	5	1639	6
16	05BJ_001_16	-114.6875	50.8125	19	4	1743	7
17	05BJ_001_17	-114.6875	50.9375	19	5	1639	6
18	05BJ_001_18	-114.5625	50.9375	20	5	1461	8
19	05BJ_001_19	-114.4375	51.0625	21	6	1275	9
20	05BJ_001_20	-114.4375	51.0625	21	6	1275	9
21	05BJ_001_21	-114.3125	51.0625	22	6	1199	10
22	05BJ_001_22	-114.4375	51.0625	21	6	1275	9
23	05BJ_001_23	-114.3125	51.0625	22	6	1199	10
24	05BJ_001_24	-114.3125	50.9375	22	5	1250	11
25	05BJ_001_25	-114.1875	51.0625	23	6	1132	12